LIGHT SENSING IN BACTERIA

Albertus Jan Vermeulen

Submitted to the faculty of the University Graduate School

in partial fulfillment of the requirements for the degree

Doctor of Philosophy

in the Department of Molecular and Cellular Biochemistry, Indiana University

February 2015

Accepted by the Graduate Faculty, Indiana University, in partial fulfillment of the requirements for the degree of Doctor of Philosophy.

Doctoral Committee

……..

Carl Bauer, Ph.D.

……..

Lingling Chen, Ph.D.

……..

David Kehoe, Ph.D.

…….

Roger Hangarter, Ph.D.

January 14, 2015

Acknowledgements

Like many things I did this dissertation wouldn't have been possible without the help of a great number of people. First and foremost I would like to thank Carl for giving me the opportunity to grind my teeth on this project, and for giving me the space to learn from successes and mistakes alike. I would also like to thank my committee, Drs. Lingling Chen, David Kehoe and Roger Hangarter for their support and advice when my project hit some road bumps.

And then there are the people of the Bauer lab past and present. On the practical side: thank you, Vladimira, for teaching me protein purification and crystallography. And thank you, Sebastien, for teaching me about cloning. Zhuo for paving the way for the cobalamin story, and Max for helping me getting started with working with *Rhodobacter sphaeroides*. And all of you for being friends, funny coworkers, coffee buddies, beer drink buddies, fellow Europeans, and 蛋撻 appreciators.

Finally I'd like to thank Peiwei Li for being the best supporter I could wish for. I'm sure nobody knows more about the struggles and victories that went into this work. Thank you for helping me carry this through.

Albertus Jan Vermeulen

Light Sensing in Bacteria

Light reception plays an important role in regulating lifestyle changes in bacteria. My research focused on a number of different light-sensing systems in different bacteria: PpaA in *Rhodobacter sphaeroides*, PixD-PixE in *Synechocystis* sp. PCC, and the known light-receptors in *Rhodospirillum centenum*.

PpaA from *R. sphaeroides* had previously been shown to be a heme-binding protein, despite its sequence similarity to cobalamin-binding proteins. My research showed that PpaA is in fact a bona fide cobalamin-binding protein. PpaA binds specifically hydroxy-cobalamin, but not other forms of cobalamin. PpaA does have some ability to bind heme, but a mutant form of PpaA that showed better heme-binding was inactive in vivo. This suggests that PpaA functional cofactor is cobalamin, rather than heme.

We also tested cobalamin-binding in a number of homologs of PpaA and found that almost all are indeed cobalamin-binding proteins.

The genome of *Rhodospirillum centenum* contains four reading frames that encode light sensing proteins. We identified possible role for each of these light-receptors by making deletion mutants, and testing the impact of these deletion on the transcription levels. Our results suggest that the PYP-phytochrome hybrid Ppr plays a role as a global regulator of transcription. A BLUF and a bacteriophytochrome on the other hand showed changes in expression levels of a number of genes involved in motility. Lastly, deletion of a LOV domain containing protein did not result in any significant changes in gene

expression levels. This suggests that the LOV protein does not regulate life-style changes, but rather controls immediate responses.

PixD is a short BLUF protein that has been shown to play a role in regulating phototaxis in *Synechocystis* sp. PCC6803. We were able to show that Slr1692, encoded by an ORF upstream of pixE-pixD might play a role in regulating phototaxis.

……..

Carl Bauer, Ph.D.

……..

Lingling Chen, Ph.D.

……..

David Kehoe, Ph.D.

…….

Roger Hangarter, Ph.D.

Table of contents

List of figures and tables

Figures

Tables

Chapter 1 - Light perception in bacteria

Light is a ubiquitous environmental factor that plays an important role in the life of bacteria. Light not only plays a role in regulating processes in photosynthetic prokaryotes, but also in non-photosynthetic bacteria. An early example of light perception in bacteria is the formation of fruiting bodies in the non-photosynthetic myxobacterium *Stigmatella aurantica*. Starved *S. aurantica* forms aggregates, which then may develop into fruiting bodies. The formation of stalks that support fruiting bodies only takes place after aggregates are exposed to light (*1*). How *S. aurantica* senses light and transforms a light signal into a cellular response is still unknown. With increasing numbers of genomes sequenced, more bacteria have been found to contain genes encoding light receptors, or indeed cell processes that are affected by light. The importance of light sensing has been shown in a wide range of prokaryotes.

The past 15 years has shown rapid growth of knowledge of light receptors and their function in bacteria. This review covers the different classes of light receptors that are found in prokaryotes and recent advances that have been made in understanding their roles in regulating bacterial physiology. In this overview I will pay special attention to cobalamin-dependent light receptors that have only recently been discovered.

Overview of different light receptor families

Traditionally light receptors were considered to be either blue or red/far-red light sensitive. Recent findings however have expanded the region of light that can be sensed

to also include wavelengths in green and orange region. Moreover, some variants of phytochromes show a remarkable blue shift in their action spectra (see below).

Almost all light receptor proteins contain a cofactor that undergoes a change upon light excitation. The only known exception is the plant light receptor UVR8. Instead of a light sensitive cofactor UVR8 contains a triad of tryptophans that transmit a light signal to the protein (*2*). Since UVR8 is only found in plants and not in bacteria it will not be discussed here. All other light receptors contain either retinal, p-coumaric acid, flavins or tetrapyrroles as light absorbing chromophores . These cofactors differ in how they respond to light and what reaction they trigger.

Sensory rhodopsins

Rhodopsins are membrane embedded proteins that were first described as light activated ion channels in Archea. Later rhodopsins were found that did not function as ion channels but instead functioned as light sensors that control motility (phototaxis) (*3*). These sensory rhodopsins interact with cytoplasmic effector proteins that in turn relay the signal to the cytosol. For example, the well-studied SRI and SRII sensory rhodopsins in *Halobacterium salinarum* regulate phototaxis through a cytoplasmic MCP domain fused to the membrane-embedded rhodospsin (*4*).

Sensory rhodopsins contain a retinal cofactor that is covalently attached to a lysine residue. This retinal cofactor absorbs light in the blue and green light region. Once excited by a photon, the retinal cofactor will undergo isomerization of a carbon-carbon double bond from 13-*cis* to all-*trans*. Under dark conditions, the retinal reverts back to its 13-*cis* state. The protein moiety of rhodopsins can have a strong influence on the spectrum and properties of the retinal cofactor.

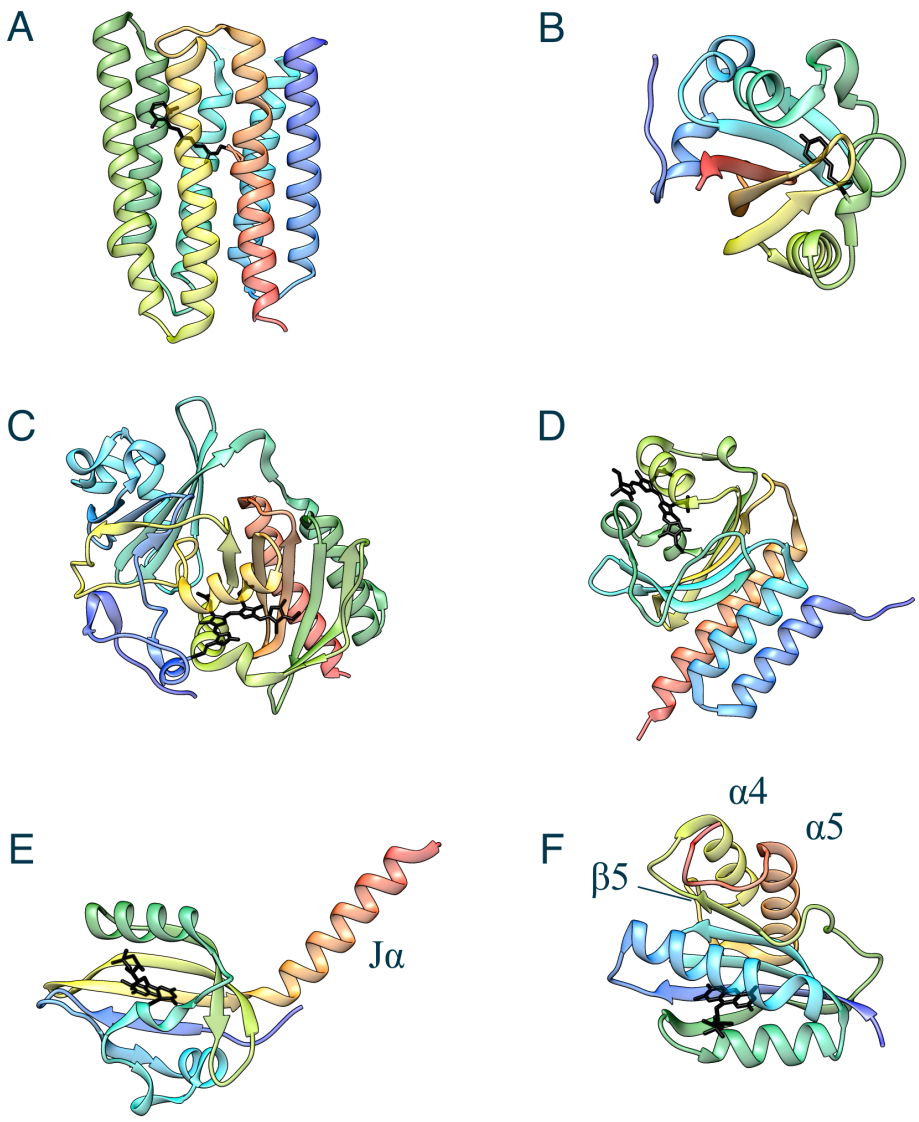

Figure 1.1 Examples of light receptors found in bacteria. The protein is shown in rainbow coloring (N-terminus: blue; C-terminus: red) and the cofactor in black. Multimeric proteins are shown as monomers. (A) Sensory rhodopsin ARS from Anabaena PCC7120. ARS contains a mixture of retinal conformers, only one of the two is shown here. (PDB file 1XIO); (B) PYP of Halorhodospira halophila (PDB file 2ZOH); (C) bacteriophytochrome BphB from Deinococcus radiodurans (PDB file 2O9C); (D) cyanobacteriochrome AnPixJ from Anabaena PCC7120 (PDB file 3W2Z); (E) LOV domain of YtvA (Bacillus subtilis) shown in light excited form (PDB file 2PR6); (F) PixD of Synechocystis sp. PCC6803 (PDB file 2HFO)

The first eubacterial sensory rhodopsin discovered was ARS from *Anabaena* PCC7120 (*5*). This rhodopsin has a few unusual features, such as the presence of all-*trans* retinal in its dark state instead of a 13-*cis* retinal and a photoinducible conversion of the lit state to the dark state (*6*). ARS interacts with the small cytosolic protein ARST, which greatly increases the rate of dark reversion of light excited ARS (*7*). ARST is also a DNA-binding protein that is able to bind to the *pec* and *pcp* promoters (*5, 7*). In response to green light, ARS-ARST upregulates the biosynthesis of phycoerythrins. Thus, ARS and ARST are believed to play a role in chromactic adaption of *Anabaena*.

Photoactive yellow protein

Photoactive yellow protein (PYP) shares some similarities with the (sensory) rhodopsins. To further emphasize these similarities the name xanthopsins was proposed, however that name is rarely used in the literature (*8*). PYP contains a blue light sensing *p*-coumaric acid cofactor bound by a PAS domain (*9*). The *p*-coumaric acid cofactor is covalently attached to a strongly conserved cysteine residue in the β-sheet of the PAS domain. Similar to rhodopsins, PYP light receptors contain a linear cofactor that undergoes *cis* to *trans* isomerization of an ethylene bond upon light excitation. As a result of this isomerization, a hydrogen-bond is lost between a conserved glutamate and the hydroxyl group on the phenyl ring of *p*-coumaric acid. The loss of this hydrogen-bond in turn allows for large scale conformational changes (*10*). In addition, the chromophore folds out of the binding pocket, thereby increasing the exposed hydrophobic area (*11*).

To date a number of PYP domain containing proteins have been found, yet most of these are not functionally characterized. Although a number of functions have been proposed, most of these functions are predicted based on genetic context and have not

been confirmed experimentally (*12*). In *Rhodobacter capsulatus*, for example, a PYP encoding gene is located in a gene cluster encoding components involved in the formation of gas vesicle that play a role in buoyancy (*13*). Gas vesicles have not been observed in *R. capsulatus* and are not common among purple non-sulfur bacteria. To date only the Antarctic purple non-sulfur bacterium *Rhodoferax antarticus* strain Fryx1 has been shown to form gas vesicles (*14*). Whether or not PYP in *R. capsulatus* does in fact regulate the formation of gas vesicles therefore needs to be confirmed experimentally. Several purple bacterial species also contain a PYP domain bound to a GAF containing bacteriophytochrome (*15*). As is the case of stand alone PYP proteins, the function of these hybrid PYP-bacteriophytochromes remain largely uncharacterized.

Light sensors using flavin as a cofactor

Flavin as a light-sensing cofactor is a widely occurring theme. Three families of flavoprotein light-receptors are cryptochromes, LOV proteins, and BLUF proteins. All three use flavin as a cofactor, but they differ in what kind of flavin is used and how the protein interacts with the flavin cofactor.

Cryptochromes are found throughout all kingdoms of life (*16*). Cryptochromes are often discussed in conjunction with the photolyases, from which the cryptochromes are thought to have descended. Photolyases are light-activated DNA repair enzymes and also use a flavin cofactor. Cryptochromes share many structural and mechanistic features, but lack photolyase activity and instead function as a light receptor (*17*). Cryptochromes can be divided in roughly three families: the plant cryptochromes, the animal cryptochromes and the DASH cryptochromes. Plant cryptochromes have been shown to be involved in a number of different processes, from chloroplast movement to hormone

production. In animals, cryptochromes are involved in regulating the circadian clock. CRY-DASH proteins are more widely found. One of the first CRY-DASH proteins identified (Sll1629 from *Synechocystis*) is thought to act as a transcriptional repressor. Light excitation of the flavin cofactor of cryptochromes leads to the formation of a neutral $FADH^{o}$ radical. This $FADH^{o}$ radical is then reduced by a nearby tryptophan. In photolyases $FADH^{-}$ is a required cofactor for DNA repair (*16*).

LOV (Light Oxygen Voltage) proteins preferentially bind flavin mononucleotide (FMN) as a light absorbing cofactor (*18*). The LOV domain itself is a subgroup of the PAS family and contains an α/β fold. The signature motif for LOV domains is a GXNCRFLQ motif located in the Eα helix (*19*). The strongly conserved cysteine in this motif forms a Cys-C(4) covalent bond as part of the LOV photocycle. The formation of a covalent bond is a crucial step in the light cycle of LOV proteins: mutation of the cysteine to an alanine renders the LOV domain photochemically inactive. Light excitation of the FMN cofactor triggers the formation of an FMN singlet state that in turn develops into a triplet state, which then reacts with the conserved cysteine to form a covalent bond. This covalent bond decays upon FMNH oxidation by water (*20*). In the LOV2 domain of Phot1, a phototropin from *Avena sativa* an α-helix at the C-terminus of the LOV domain unfolds partially upon light excitation (*21*). On the other hand, crystal structures of the *Bs*YtvA LOV domain in dark or light excited condition shows little structural changes in this helix (*22*). In a separate study, the *Bs*YtvA_LOV domain was fused to the Jα-helix and histidine kinase domains of FixL from *Bradhyrhizobium japonicum* (*23*). The resulting engineered light-dependent histidine kinase, YF1, shows loss of autophosphorylation activity when exposed to light. The structure of full-length

YF1 suggests a rotational movement of the Jα helix. This movement is further enhanced by the N-terminal coiled-coil formed by the two A'α helices (*24*).

Blue light using flavin (BLUF) light receptors are mostly found in prokaryotes, although some BLUF proteins have been found in algae. Compared to cryptochromes and LOV proteins, BLUF domains have a very subtle light response where light excitation merely leads to a change in the hydrogen bond network around the flavin cofactor. During light excitation, the flavin accepts an electron from the strongly conserved tyrosine, yet how this radical formation leads to changes in the hydrogen bond network is not fully understood (*25*). Reorganization of the hydrogen-bond network ultimately leads to conformational changes in the C-terminal β-sheet (β5) and 2 α-helices (α4, α5) (*26-28*). NMR studies showed that chemical shifts are most pronounced in the C-terminal β5, α4 and α5 (*26-29*), suggesting that signals are ultimately transmitted through the C-terminal α-helices.

One well-studied example of a BLUF protein is the BLUF-EAL protein BlrP1 from *Klebsiella pneumoniae*. In this light receptor the EAL mediated phosphodiesterase activity increased upon light excitation of the BLUF domain (*30*). A crystal structure of the full-length protein showed a dimerized conformation, which is also found in solution (*30*). Based on this, and derived structures, a model for signal transduction was proposed that starts with a rearrangement of β5 upon light excitation. This in turn affects α4, which through a compound helix interface between the dimerized EAL domains, is transferred to the EAL domain of the other subunit (*30*). Studies with BlrP1 in solution confirmed the flexibility of this regions in response to light excitation (*31*). The importance of the C-terminal helices was also found in several other systems, suggesting

that this may indeed be a conserved signaling mechanism among BLUF proteins (*26, 29, 31, 32*).

Linear tetrapyrrole containing light receptors

The first phytochromes described were in plants where they affect the timing and development of shoots, leaves and flowers (*33*). About 35 years later phytochromes were also discovered in bacteria (*34-36*). Over the years, the phytochrome family has grown into a diverse group of light receptors that are present in many species of bacteria. These photoreceptors have a conserved GAF domain that binds a linear tetrapyrrole as light-sensitive cofactor. Traditionally phytochromes were thought of as red/far-red light receptors. This is due to the nature of the plant/cyanobacterial chromophore, that switches back and forth between two states, Pr and Pfr. The light activated form (Pfr) can revert back to its red light sensing ground state (Pr) by exposure to light of a longer wavelength, or thermally in the dark. For classic phytochromes light excitation happens after exposure to red light, and reversion by exposure to far-red light. Recently a number of bacterial phytochromes and phytochrome-like proteins have been characterized that expand the palette of these photoreceptors into the orange, green and blue regions of the light spectrum.

The traditional plant phytochromes consist of a photosensory core made of a PAS (Per-ARNT-Sim), a GAF (cGMP phosphodiesterase/adenylate cyclase/FhlA) and a PHY (phytochrome specific) domain. A light-sensitive linear tetrapyrrole, phycocyanobilin (PCB) is covalently attached to a cysteine in the GAF domain. All three domains interact with the tetrapyrrole cofactor, with the PHY domain folding back over the GAF domain and providing a solvent barrier (*37*). Bacteriophytochromes are phytochromes found in

bacteria other than cyanobacteria. Bacteriophytochromes share the same domain architecture, but covalently bind a biliverdin IXα (BV) instead of PCB. Another difference is that the cofactor is not covalently attached to a Cys in the GAF domain, but to a residue N-terminal of the PAS domain. A special class of bacteriophytochromes has a ground state that absorbs at a longer wavelenght than the activated state (*38, 39*). These are called the bathophytochromes and are mainly found in the Rhizobiales order (*40*).

Besides classic phytochromes, two classes of phytochromes with simpler domain architectures have been found; the Cph2 like phytochromes and the cyanobacteriochromes. The former have a photosensory core that consists of a GAF and a PHY domain. Cph2-like phytochromes show normal phytochrome behavior. The cyanobacteriochromes (CBCRs) merely have a GAF domain that binds the linear tetrapyrrole. The CBCRs are only found in cyanobacteria. CBCRs are particularly striking in their spectroscopic diversity with many characterized CBCRs showing a strongly blue-shifted absorption spectrum. Part of the blue shift involves a second cysteine that forms a covalent bond as part of the light cycle. The discovery of CBCR's greatly expands the range of wavelengths sensed by phytochromes. The CBCRs are, however, not the only color-shifted phytochromes. A recent study showed that several algaea also contain phytochromes with sometimes strongly blue-shifted absorption spectra (*41*). It is not fully understood why these algal phytochromes are chromatically shifted. Some of these blue-shifted phytochromes may use a two-cysteine system as found in the CBCRs. It is now clear that the phytochromes are a very diverse family that transcend the traditional red/far-red sensors that they were once thought to be.

A signaling mechanism for bacteriophytochrome BphB from *Deinococcus radiodurans* has been proposed based on cryo-electro microscopic structural studies. This bacteriophytochrome has a histidine kinase domain as output domain (*34*). The cryo-electron microscopy data showed that DrBphB forms a head-to-head dimer in solution (*42*). A similar conformation has also been found for BphP3 from *R. palustris* using small angle x-ray scattering (*43*). Light excitation causes a slight rotation of the histidine kinase domains in relation to each other, thus assuming a position that favors transphosphorylation (*42*). Since phytochromes in general form dimers in solution (*44*) this model may apply to all phytochromes.

Despite the predominance of phytochromes among many diverse species of bacteria there remains few studies as to their physiological function. The best characterized are RcaE in *Fremyella diplosiphon,* which is involved in chromatic adaptation (*36*), and several phytochromes in the purple bacteria *Rhodopseudomonas palustris* that affect synthesis of the photosystem (*38*).

B_{12} as light-sensing cofactor

Cobalamin (also known as vitamin B_{12}, Figure 1.2) has traditionally been studied as a cofactor in enzymatic reactions, such as methylation, adenylation and isomerization reactions (*45*). The use of cobalamin is unevenly distributed across the kingdoms of life: archaea and eubacteria can have multiple cobalamin dependent pathways, whereas mammals have only two cobalamin-dependent enzymes. Cobalamins are absent in higher plants, although some algae do require cobalamin (*46*). Only bacteria are capable of synthesizing cobalamin. Biosynthesis of Cbl is a complicated process and involves about

thirty enzyme-catalyzed reactions (*47*). The final product of this pathway is adenosyl-cobalamin. The Cbl biosynthesis pathway shares some steps with the heme and bacteriochlorophyll biosynthesis pathways, it is the first to branch off.

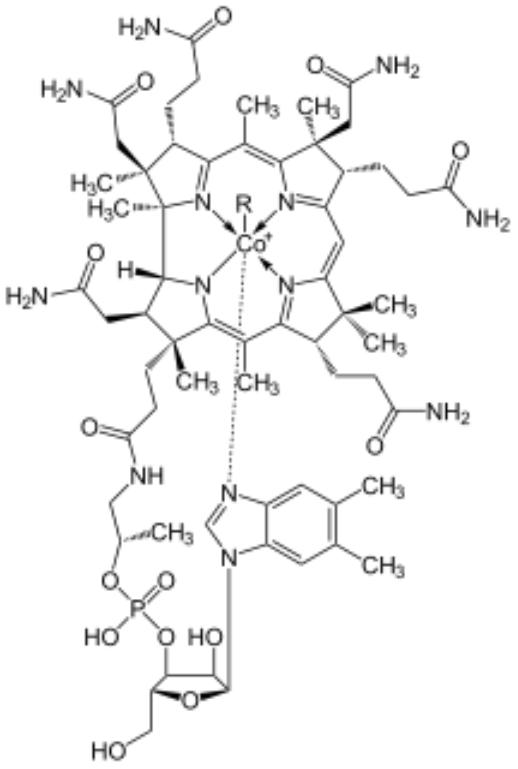

Figure 1.2 Structure of cobalamin. Cobalamin is found in different forms, most importantly methyl-cobalamin (R = -CH_3), adenosyl-cobalamin (R = -5'deoxyadenosyl), hydroxy-cobalamin (R = -OH) and cyano-cobalamin (R = -CN).

Cobalamin is the most complicated non-polymeric biomolecule that cells synthesize. At its core is a tetrapyrrole ring that coordinates cobalt. The tetrapyrrole ring is very similar to that of heme and bacteriochlorophyll, but it is more conjugated with

side groups. The lower side group is a DMBI tail that under physiological conditions folds back and provides an axial ligand to the bound cobalt. The face of this coordination is called the α side. In biological systems cobalamins can be found in two states; base-on, where the DMBI tail interacts with the cobalt group, or base-off. In the base-off state the cobalt ion can be coordinated by water, a histidine or something else. The protein bound forms of cobalamin can be either base-on or base-off.

The upper β side of the cobalt group can be occupied by a number of chemical groups. The biologically active forms are adenosyl-cobalamin and methyl-cobalamin. These cobalamins participate in adenosyl or methyl transfer reactions. The biosynthesis of cobalamin results in adenosyl-cobalamin. The cobalt-carbon bond in these cobalamins is generally weak and can easily be broken.

Recently, cobalamin has gained more attention as a molecule that can also sense or be sensed. To date three proteins have been described that bind cobalamin in a non-enzymatic or transport context. These proteins are CarH in *Myxococcus xanthus*, AerR in *Rhodobacter capsulatus* and HbpS in *Streptomycis reticuli* (*48-50*). CarH regulates the light-dependent pigmentation, AerR controls expression of photosynthetic pigments and HbpS is part of a redox regulated two component signalling system. The CarH and AerR systems will be discussed in detail below.

CarH

Exposure to light induces carotenoid formation in *Myxococcus xanthus* (*51*). With the exception of CrtI, all carotenoid biosynthesis genes are located in one operon under control of the P_B promoter (*52*). The transcriptional repressor CarA binds to the P_B

promoter and down-regulates expression of the carotenoid genes (*53*). CarS in turn removes CarA from the DNA through the interaction between its SH3 domain and the HTH domain of CarA (*54*). In addition a homolog of CarA, CarH was found to act as a cobalamin-dependent repressor of the *carB* operon (*50*). Previous studies had shown that the expression of the *carB* operon is not only light dependent, but also dependent on the presence of cobalamin, but the mechanism was poorly understood (*52*).

CarH, like CarA is a HTH, B_{12}-binding hybrid protein, but unlike CarA it can bind cobalamin (*50*). A homolog from *Thermos thermophilus*, TtCarH, can bind various forms of cobalamin (cyano-, methyl- and adenosyl-cobalamin), but when adenosyl-cobalamin is bound it forms the active tetramer which can bind the P_B DNA. Light-excitation of TtCarH causes photolysis of the cobalamin chromophor and subsequent dissociation of the tetramer to monomers. TtCarH in its monomeric state does not bind DNA, thus relieving repression of the P_B promoter. TtCarH can be light-excited with a broad range of wavelengths: UV, blue and green light, but not red light, all caused photolysis of the cobalamin cofactor. Indeed the UV/vis absorption spectra confirm the formation of hydroxycobalamin.

The B_{12}-binding domain of CarH and TtCarH show good similarity to the signature motifs of B_{12}-binding domains. The CarH homolog CarA also shows good similarity, but is not able to bind cobalamin (*50*). Why this occurs is not known, although a tryptophan may interfere with the insertion of the DMB tail of cobalamin. Mutation of the strongly conserved histidine leads to abrogation of cobalamin-dependent oligomerization of the C-terminal domains of CarH and TtCarH in a bacterial-two-hybrid screen (*50*). *In vivo*, a histidine to alanine mutant CarH failed to repress *carB* expression

under dark conditions in the presence of B_{12}, showing that this mutation does indeed lead to loss of function (*55*). Whether CarH or TtCarH histidine to alanine mutants can bind cobalamin is not reported.

AerR

The CrtJ/PpsR antirepressor AerR was first reported to be a redox-responsive DNA-binding protein (*56*). Later work, however, showed that AerR acts as an antirepressor of CrtJ (*48*). AerR is unique in the sense that it only binds hydroxy-cobalamin, and not other forms of cobalamin. AerR is a member of the PpaA/AerR family of proteins, and as such was thought to bind heme instead of cobalamin through its SCHIC domain (*57*). SCHIC domains share sequence similarity with B_{12}-binding domains, but there are some differences that are conserved within the PpaA/AerR family. Given the involvement of AerR in redox-regulated processes it was expected that AerR acts as a redox-sensor making heme a likely cofactor.

AerR, like CarH, contains a conserved histidine. Mutation of this conserved histidine to an alanine disrupted cobalamin-binding *in vitro*. Yet *in vivo* a histidine to alanine mutation showed an intermediate phenotype. Further work showed that the cobalamin cofactor is covalently bound to a non-conserved histidine located close to the N-terminus of the protein. A double histidine to alanine mutation showed a *ΔaerR* phenotype, indicating that two histidine coordination plays a key role in the function of AerR (*48*).

Whether or not AerR acts as a light-receptor is not known. Photolysis is a likely source of hydroxy-cobalamin, but it might also be possible that the cobalt undergoes a

redox reaction. This, however, is unlikely as reported redox potentials of cobalamin range from -240 to -572 mV (versus NHE), well below the redox potential of the cytosol (around -220 mV) (*58-62*). In addition it was found that an AerR-H145A mutant no longer shows a reduction of pigmentation under high light conditions, suggesting a loss of response to light conditions (*48*).

Typical light receptors are not only able to convert from dark to lit state, but also revert back from lit to dark state. At the moment no such mechanism is known for the cobalamin based light sensors, as activation involves breaking an intermolecular bond. It seems counterintuitive to have 'single use' light receptors, but there are precedents. SyCikA (Slr1969) in *Synechocystis* sp. PCC6803 for example shows normal rate activation by violet light. The reverse reaction by yellow light on the other hand is much slower. A dark reversion as is usually seen in (bacterio)phytochromes and cyanobacteriochromes is virtually absent (*63*). It is not clear if and what role SyCikA plays *in vivo*, let alone how this protein functions as a single use light receptor.

B_{12}-binding riboswitches

By comparison more is known about RNAs binding cobalamin than non-enzymatic proteins binding cobalamin. Cobalamin binding riboswitches are widely spread in the bacterial kingdom, but seem to be absent in Archaea and Eukaryotes (*64*). Sequence analysis of a large number of cobalamin riboswitches showed that these are mostly found in operons encoding component of cobalamin biosynthesis, transport or B_{12}-dependent metabolic pathways (*65*).

Involvement of 5' leaders of mRNA in downregulation of *btuB* (*E. coli*) or *cob* (*S. Typhimurium*) genes expression had been shown before (*66, 67*). Later work showed that presence of ado-Cbl stimulated formation of an RNA hairpin sequestering the ribosomal binding site *in vivo* (*68*). *In vitro* the presence of ado-Cbl resulted in a reduction of ribosome binding, while OH-, CN-Cbl or cobamine did not have this effect (*69*). The 5'-UTR of *btuB* was indeed shown to bind ado-Cbl selectively and not other forms of cobalamin (*70*).

Another well-studied example of a cobalamin riboswitch is the *eutG* riboswitch located in the ethanolamine (EA) utilization operon of *Enterococcus faecalis* (*71, 72*). The enzyme ethanolamine-ammonia lyase, part of the EA degradation pathway, uses cobalamin as a cofactor. The *eutG* riboswitch reduces termination of transcription when Ado-Cbl is bound (*72*). Thus presence of Ado-Cbl leads to upregulation of expression. Like *btuB*, structural changes in the riboswitch are induced by Ado-Cbl, but to a much lesser extent by CN-Cbl (*72*). Sequence analysis shows that in Gram-positive bacteria the B_{12} box is often times followed by a candidate terminator sequence, whereas in Gram-negative bacteria instead of a terminator sequence a ribosome sequestering sequence can be found (*73*). Interestingly, work by Baker and Perego suggested that Ado-Cbl promotes termination (*71*).

Not all riboswitches are specific for AdoCbl: a study by Johnson et al. showed hydroxy-cobalamin binding by two riboswitches deduced from environmental genomes (*74*). These sequences appear to be missing the P6 stem-loop region, a feature shared with some cyanobacterial cobalamin riboswitches (*73, 75*). One explanation for this apparent change in affinity could be that in these environments most available cobalamin

will be in a OH-Cbl form due to photolysis (*74*). A SELEX evolved riboswitch was evolved to bind cyanocobalamin (*76*). Structures of both CN-Cbl and OH-Cbl binding riboswitches show a similar interaction between the RNA and the β-ligand face of the cobalamin (*74, 77*).

Distribution of light receptors

Sequences encoding light sensitive proteins are widely spread among archaea and bacteria. A recent survey of available genome sequences showed that 22% of the prokaryotes contains at least one phytochrome-like GAF domain, a BLUF domain or a LOV domain (*78*). To our knowledge no systematic studies on the phylogenetic distribution of PYP or sensory rhodopsins have been published. However, PYP proteins have been found in α-, β-, γ- and δ-Proteobacteria and Bacteriodetes (*9, 79*). Likewise, sensory rhodopsins have been found in all three domains of life (*4*). The B12-dependent light receptors are still poorly studied and therefore it is hard to estimate their dispersal.

A study of phytochrome, LOV and BLUF proteins revealed a few distribution patterns (*80*). Archaea, Firmicutes and Chloroflexi for example only contain LOV proteins and lack the other two light receptors. Cyanobacteria on the other hand are particularly rich in phytochrome-related proteins and contain relatively few BLUF proteins (*78*). Interestingly, anoxygenic phototrophs and plant-associated or plant-pathogenic bacteria often contain all three light receptors. Perhaps more striking is the absence of bilin-GAF phytochromes, LOV or BLUF proteins in the photosynthetic Heliobacteria (Firmicutes) and many cyanobacteria (*80*).

The B_{12} dependent light receptors are also widely spread among bacteria. A study showed the occurrence of *M. xanthus* CarH homologues across different phyla (*50*). The

same study also found a number of single domain B_{12} binding proteins and B_{12}-binding domains fused with histidine kinases. It should be noted that these studies searched the databases using a classical base-off sequence. B_{12}-binding domains may in fact be more diverse than that. The PpaA/AerR homologs on the other hand are – with a few exceptions - uniquely found in the purple non-sulfur bacteria.

Output domains and functions of light-sensing in prokaryotes

Searches for output domains in the different light receptor proteins showed that phytochromes and LOV domains are mostly associated with histidine kinase domains, while BLUF domains are often the only domain present or linked to c-di-GMP turnover domain (i.e. EAL or GGDEF) (*80*). While this does not demonstrate what role these light receptors play *in vivo*, it does give some indication as to what type of output signal they generate. The second messenger c-di-GMP has been associated with adaptations in life style, such as a switch from free-living to biofilm-associated (*81*). Therefore it has been hypothesized that light sensing, especially by BLUF proteins, is associated with life-style decisions (*82*). This hypothesis has been supported by several examples; however, one has to be careful generalizing the function of output domain. For example, YcgF (also known as BluF) from *E. coli* is a BLUF-EAL fusion protein. The EAL domain however does not show enzymatic activity and instead has been shown to play a role in protein-protein interactions (*83*). YcgF acts as a blue-light controlled antirepressor to the MerR-like transcription repressor YcgE (*83*). YcgF also serves as a cautionary tale about the light-sensing domain. While YcgF does act as a bona fide light receptor, it also shows a temperature-dependent regulation of its regulatory activity (*83*). One also has to be careful not to jump to the conclusion that a polypeptide showing sequence similarity to a

light receptor is in fact going to function as a bona fide light receptor. BphP2 and BphP3, two bacteriophytochromes in *R. palustris*, for example, were found to have some activity despite the absence of a chromophore (*84*). These phytochromes may therefore also function independent of light conditions. Similarly a CBCR, CikA from *Synechococcus elongatus*, was found to act as a sensor of the redox state of the quinone pool (*85*).

The biological function of light reception in bacteria has received relatively little attention. While many light receptors have been studied biochemically, only a few have been studied in an *in vivo* context. An overview of light receptors of which the *in vivo* functions have been studied is given in Table 1.1. While this table may be incomplete it is clear that the majority of the studied light receptors seem to play a role in biofilm formation, motility and the regulation of pathogenicity. This may be due to a bias in studying biofilm formation, which arguably plays an important role in pathogenicity (*86*). It is clear that more research will be needed to fully understand the role of light sensing in prokaryotes. The following chapters present biochemical and genetic studies on a number of light receptors in various bacterial species.

Table 1.1 Light receptors with confirmed functionalities. (NN indicates proteins for which no name was reported).

Protein	**Organism**	**Class**	**Function**	**Reference**
CarH	*Myxococcus xanthus*	B_{12}	Production carotenoids	(*50*)
BrBphP	*Bradhyrhizobium ORS278*	Bacteriophytochrome	Regulation expression photosynthesis genes	(*38*)
NN	*Rhodopseudomonas palustris*	Bacteriophytochrome	Regulation expression photosynthesis genes	(*38*)
BlsA	*Acinetobacter baumanni*	BLUF	Biofilms, motility, pathogenicity	(*87*)
NN	*Acinetobacter baylyi ADP1*	BLUF	Motility	(*88*)
PixD	*Synechocystis sp. PCC6803*	BLUF	Phototaxis	(*89*)
AppA	*Rhodobacter sphaeroides*	BLUF	Regulation expression photosynthesis genes	(*90*)

YcgF	*E. coli*	BLUF	Transcription regulation biofilm formation	(*83*)
RcaE	*Fremyella diplosiphon*	Cyanobacteriochrome	Chromatic adaptation	(*36*)
CcaS	*Synechocystis sp. PCC6803*	Cyanobacteriochrome	Chromatic adaptation	(*91*)
PixJ1	*Synechocystis sp. PCC6803*	Cyanobacteriochrome	Phototaxis	(*92, 93*)
LovR	*Caulobacter crescentus*	LOV	Cell attachment, regulation stressosome	(*94*)
NN	*Rhizobium leguminosum*	LOV	Exopolysaccharide, nodulation	(*95*)
BA-LOV-HK	*Brucella abortus*	LOV	Pathogenicity	(*96*)
NN	*Xanthomonas citri subsp. Citri*	LOV	Pathogenicity	(*97*)
YtvA	*Listeria monocytogenesis*	LOV	Pathogenicity, regulation stressosome	(*98*)
YtvA	*Bacillus subtilis*	LOV	Regulation stressosome	(*99*)
NN	*Pseudomonas syringiae*	LOV	Motility	(*100*)

BphB	*Pseudomonas aeruginosa*	Phytochrome		(*101*)
NN	*Pseudomonas syringiae*	Phytochrome	Motility	(*100*)
Cph2	*Synechocystis sp. PCC6803*	Phytochrome/ cyanobacteriochrome	Phototaxis, growth under blue light	(*102, 103*)
Il PYP	*Idiomarina loihiensis*	PYP	Biofilm formation	(*104*)
Ppr	*Rhodospirillum centenum*	PYP/Phytochrome	Aldolase activity, encystment	(*35*)
SRI, SRII	*Halobacterium salinarum*	Sensory rhodopsin	Phototaxis	(*105*)
ARS	*Anabaena PCC7120*	Sensory rhodopsin	Chromatic adaptation	(*5*)

References

1. G. T. Qualls, K. Stephens, D. White, Light-stimulated morphogenesis in the fruiting myxobacterium Stigmatella aurantiaca. *Science (New York, NY)* **201**, 444-445 (1978).
2. J. M. Christie *et al.*, Plant UVR8 Photoreceptor Senses UV-B by Tryptophan-Mediated Disruption of Cross-Dimer Salt Bridges. *Science (New York, NY)*, (2012).
3. R. A. Bogomolni, J. L. Spudich, Identification of a third rhodopsin-like pigment in phototactic Halobacterium halobium. *Proceedings of the National Academy of Sciences* **79**, 6250-6254 (1982).
4. J. L. Spudich, The multitalented microbial sensory rhodopsins. *Trends in Microbiology* **14**, 480-487 (2014).
5. K.-H. Jung, V. D. Trivedi, J. L. Spudich, Demonstration of a sensory rhodopsin in eubacteria. *Molecular Microbiology* **47**, 1513-1522 (2003).
6. O. A. Sineshchekov, V. D. Trivedi, J. Sasaki, J. L. Spudich, Photochromicity of Anabaena Sensory Rhodopsin, an Atypical Microbial Receptor with a cis-Retinal Light-adapted Form. *Journal Of Biological Chemistry* **280**, 14663-14668 (2005).
7. S. Y. Kim, S. R. Yoon, S. Han, Y. Yun, K.-H. Jung, A role of Anabaena sensory rhodopsin transducer (ASRT) in photosensory transduction. *Molecular Microbiology* **93**, 403-414 (2014).
8. R. Kort *et al.*, The xanthopsins: a new family of eubacterial blue-light photoreceptors. *The EMBO journal* **15**, 3209-3218 (1996).

9. J. Kyndt, T. Meyer, M. Cusanovich, Photoactive yellow protein, bacteriophytochrome, and sensory rhodopsin in purple phototrophic bacteria. *Photochemical & Photobiological Sciences* **3**, 519-530 (2004).

10. Y. Imamoto, M. Kataoka, Structure and Photoreaction of Photoactive Yellow Protein, a Structural Prototype of the PAS Domain Superfamily†. *Photochemistry and Photobiology* **83**, 40-49 (2007).

11. U. K. Genick *et al.*, Structure of a Protein Photocycle Intermediate by Millisecond Time-Resolved Crystallography. *Science (New York, NY)* **275**, 1471-1475 (1997).

12. T. E. Meyer *et al.*, The growing family of photoactive yellow proteins and their presumed functional roles. *Photochemical & Photobiological Sciences* **11**, 1495-1514 (2012).

13. J. A. Kyndt *et al.*, Rhodobacter capsulatus Photoactive Yellow Protein: Genetic Context, Spectral and Kinetics Characterization, and Mutagenesis. *Biochemistry* **43**, 1809-1820 (2004).

14. D. O. Jung, L. A. Achenbach, E. A. Karr, S. Takaichi, M. T. Madigan, A gas vesiculate planktonic strain of the purple non-sulfur bacterium Rhodoferax antarcticus isolated from Lake Fryxell, Dry Valleys, Antarctica. *Archives of Microbiology* **182**, 236-243-243 (2004).

15. E. Giraud, A. Vermeglio, Bacteriophytochromes in anoxygenic photosynthetic bacteria. *Photosynthesis Research* **97**, 141-153 (2008).

16. I. Chaves *et al.*, The Cryptochromes: Blue Light Photoreceptors in Plants and Animals. *Annu. Rev. Plant Biol.* **62**, 335-364 (2011).

17. C. Lin, T. Todo, The cryptochromes. *Genome Biology* **6**, 220 (2005).

18. A. Losi, W. Gärtner, The Evolution of Flavin-Binding Photoreceptors: An Ancient Chromophore Serving Trendy Blue-Light Sensors. *Annual Review of Plant Biology* **63**, 49-72 (2012).

19. J. Herrou, S. Crosson, Function, structure and mechanism of bacterial photosensory LOV proteins. *Nature Reviews Microbiology* **9**, 713-723 (2011).

20. J. P. Zayner, T. R. Sosnick, Factors that control the chemistry of the LOV domain photocycle. *PLoS ONE* **9**, e87074 (2014).

21. S. M. Harper, L. C. Neil, K. H. Gardner, Structural Basis of a Phototropin Light Switch. *Science (New York, NY)* **301**, 1541-1544 (2003).

22. A. Möglich, K. Moffat, Structural Basis for Light-dependent Signaling in the Dimeric LOV Domain of the Photosensor YtvA. *Journal of Molecular Biology* **373**, 112-126 (2007).

23. A. Möglich, R. A. Ayers, K. Moffat, Design and Signaling Mechanism of Light-Regulated Histidine Kinases. *Journal of Molecular Biology* **385**, 1433-1444 (2008).

24. R. P. Diensthuber, M. Bommer, T. Gleichmann, A. M glich, Full-Length Structure of a Sensor Histidine Kinase Pinpoints Coaxial Coiled Coils as Signal Transducers and Modulators. *Structure (London, England : 1993)* **21**, 1127-1136 (2013).

25. S. Masuda, Light Detection and Signal Transduction in the BLUF Photoreceptors. *Plant and Cell Physiology* **54**, 171-179 (2013).

26. V. Dragnea, A. I. Arunkumar, H. Yuan, D. P. Giedroc, C. E. Bauer, Spectroscopic Studies of the AppA BLUF Domain from Rhodobacter sphaeroides: Addressing

Movement of Tryptophan 104 in the Signaling State. *Biochemistry* **48**, 9969-9979 (2009).

27. Q. Wu, K. H. Gardner, Structure and Insight into Blue Light-Induced Changes in the BlrP1 BLUF Domain†,‡. *Biochemistry* **48**, 2620-2629 (2009).

28. Q. Wu, W.-H. Ko, K. H. Gardner, Structural Requirements for Key Residues and Auxiliary Portions of a BLUF Domain†. *Biochemistry* **47**, 10271-10280 (2008).

29. H. Yuan, V. Dragnea, Q. Wu, K. H. Gardner, C. E. Bauer, Mutational And Structural Studies Of The PixD BLUF Output Signal That Affects Light-Regulated Interactions With PixE. *Biochemistry*, 110620194047052 (2011).

30. T. R. M. Barends *et al.*, Structure and mechanism of a bacterial light-regulated cyclic nucleotide phosphodiesterase. *Nature* **459**, 1015-1018 (2009).

31. A. Winkler *et al.*, A ternary AppA–PpsR–DNA complex mediates light regulation of photosynthesis-related gene expression. *Nature Structural & Molecular Biology*, - (2013).

32. S. Ren, R. Sato, K. Hasegawa, H. Ohta, S. Masuda, A Predicted Structure for the PixD–PixE Complex Determined by Homology Modeling, Docking Simulations, and a Mutagenesis Study. *Biochemistry* **52**, 1272-1279 (2013).

33. W. L. Butler, K. H. Norris, H. W. Siegelman, S. B. Hendricks, Detection, assay, and preliminary purification of the prigment controlling photoresponsive development of plants. *Proceedings of the National Academy of Sciences of the United States of America* **45**, 1703-1708 (1959).

34. S. Davis, A. Vener, R. Vierstra, Bacteriophytochromes: Phytochrome-like photoreceptors from nonphotosynthetic eubacteria. *Science (New York, NY)* **286**, 2517-2520 (1999).

35. Z. Jiang *et al.*, Bacterial Photoreceptor with Similarity to Photoactive Yellow Protein and Plant Phytochromes. *Science (New York, NY)* **285**, 406-409 (1999).

36. D. Kehoe, A. Grossman, Similarity of a chromatic adaptation sensor to phytochrome and ethylene receptors. *Science (New York, NY)* **273**, 1409-1412 (1996).

37. H. Takala *et al.*, Signal amplification and transduction in phytochrome photosensors. *Nature* **509**, 245-248 (2014).

38. E. Giraud *et al.*, Bacteriophytochrome controls photosystem synthesis in anoxygenic bacteria. *Nature* **417**, 202-205 (2002).

39. B. Karniol, R. Vierstra, The pair of bacteriophytochromes from Agrobacterium tumefaciens are histidine kinases with opposing photobiological properties. *Proceedings of the National Academy of Sciences of the United States of America* **100**, 2807-2812 (2003).

40. G. Rottwinkel, I. Oberpichler, T. Lamparter, Bathy Phytochromes in Rhizobial Soil Bacteria. *Journal of Bacteriology* **192**, 5124-5133 (2010).

41. N. C. Rockwell *et al.*, Eukaryotic algal phytochromes span the visible spectrum. *Proceedings of the National Academy of Sciences* **111**, 3871-3876 (2014).

42. H. Li, J. Zhang, R. D. Vierstra, H. Li, Quaternary organization of a phytochrome dimer as revealed by cryoelectron microscopy. *Proceedings of the National Academy of Sciences* **107**, 10872-10877 (2010).

43. K. Evans, J. G. Grossmann, A. P. Fordham-Skelton, M. Z. Papiz, Small-Angle X-ray Scattering Reveals the Solution Structure of a Bacteriophytochrome in the Catalytically Active Pr State. *Journal of Molecular Biology* **364**, 655-666 (2006).

44. M. E. Auldridge, K. T. Forest, Bacterial phytochromes: More than meets the light. *Critical Reviews in Biochemistry and Molecular Biology* **46**, 67-88 (2011).

45. R. Banerjee, S. W. Ragsdale, The many faces of vitamin B12: catalysis by cobalamin-dependent enzymes. *Annual Review Of Biochemistry* **72**, 209-247 (2003).

46. M. T. Croft, A. D. Lawrence, E. Raux-Deery, M. J. Warren, A. G. Smith, Algae acquire vitamin B12 through a symbiotic relationship with bacteria. *Nature* **438**, 90-93 (2005).

47. M. J. Warren, E. Raux, H. L. Schubert, J. C. Escalante-Semerena, The biosynthesis of adenosylcobalamin (vitamin B12). *Natural Product Reports* **19**, 390-412 (2002).

48. Z. Cheng, K. Li, L. a. Hammad, J. a. Karty, C. E. Bauer, Vitamin B12 regulates photosystem gene expression via the CrtJ antirepressor AerR in Rhodobacter capsulatus. *Molecular Microbiology*, n/a-n/a (2014).

49. D. Ortiz de Orue Lucana, S. N. Fedosov, I. Wedderhoff, E. N. Che, A. E. Torda, The extracellular heme-binding protein HbpS from the soil bacterium Streptomyces reticuli is an aquo-cobalamin binder. *Journal Of Biological Chemistry*, (2014).

50. J. M. Ortiz-Guerrero, M. C. Polanco, F. J. Murillo, S. Padmanabhan, M. Elías-Arnanz, Light-dependent gene regulation by a coenzyme B12-based

photoreceptor. *Proceedings of the National Academy of Sciences* **108**, 7565-7570 (2011).

51. R. P. Burchard, M. Dworkin, Light-induced lysis and carotenogenesis in Myxococcus xanthus. *Journal of Bacteriology* **91**, 535-545 (1966).

52. M. Cervantes, F. J. Murillo, Role for vitamin B(12) in light induction of gene expression in the bacterium Myxococcus xanthus. *Journal of Bacteriology* **184**, 2215-2224 (2002).

53. J. J. López-Rubio *et al.*, Operator design and mechanism for CarA repressor-mediated down-regulation of the photoinducible carB operon in Myxococcus xanthus. *Journal Of Biological Chemistry* **279**, 28945-28953 (2004).

54. E. Leon *et al.*, A bacterial antirepressor with SH3 domain topology mimics operator DNA in sequestering the repressor DNA recognition helix. *Nucleic acids research* **38**, 5226-5241 (2010).

55. M. C. Perez-Marin, S. Padmanabhan, M. C. Polanco, F. J. Murillo, M. Elías-Arnanz, Vitamin B-12 partners the CarH repressor to downregulate a photoinducible promoter in Myxococcus xanthus. *Molecular Microbiology* **67**, 804-819 (2008).

56. C. Dong, S. Elsen, L. R. Swem, C. E. Bauer, AerR, a Second Aerobic Repressor of Photosynthesis Gene Expression in Rhodobacter capsulatus. *Journal of Bacteriology* **184**, 2805-2814 (2002).

57. O. V. Moskvin, S. Kaplan, M.-A. Gilles-Gonzalez, M. Gomelsky, Novel Heme-based Oxygen Sensor with a Revealing Evolutionary History. *Journal Of Biological Chemistry* **282**, 28740-28748 (2007).

58. R. V. Banerjee, S. R. Harder, S. W. Ragsdale, R. G. Matthews, Mechanism of reductive activation of cobalamin-dependent methionine synthase: an electron paramagnetic resonance spectroelectrochemical study. *Biochemistry* **29**, 1129-1135 (1990).

59. S. R. Harder, W. P. Lu, B. A. Feinberg, S. W. Ragsdale, Spectroelectrochemical studies of the corrinoid/iron-sulfur protein involved in acetyl coenzyme A synthesis by Clostridium thermoaceticum. *Biochemistry* **28**, 9080-9087 (1989).

60. W. P. Lu, B. Becher, G. Gottschalk, S. W. Ragsdale, Electron paramagnetic resonance spectroscopic and electrochemical characterization of the partially purified N5-methyltetrahydromethanopterin:coenzyme M methyltransferase from Methanosarcina mazei Gö1. *Journal of Bacteriology* **177**, 2245-2250 (1995).

61. S. Masuda *et al.*, Repression of Photosynthesis Gene Expression by Formation of a Disulfide Bond in CrtJ. *Proceedings of the National Academy of Sciences of the United States of America* **99**, 7078-7083 (2002).

62. W. Schumacher, C. Holliger, A. J. B. Zehnder, W. R. Hagen, Redox chemistry of cobalamin and iron-sulfur cofactors in the tetrachloroethene reductase of Dehalobacter restrictus. *Febs Letters* **409**, 421-425 (1997).

63. R. Narikawa, T. Kohchi, M. Ikeuchi, Characterization of the photoactive GAF domain of the CikA homolog (SyCikA, Slr1969) of the cyanobacterium Synechocystis sp PCC 6803. *Photochemical & Photobiological Sciences* **7**, 1253-1259 (2008).

64. J. E. Barrick, R. R. Breaker, The distributions, mechanisms, and structures of metabolite-binding riboswitches. *Genome Biology* **8**, R239 (2007).

65. D. A. Rodionov, A. G. Vitreschak, A. A. Mironov, M. S. Gelfand, Comparative genomics of the vitamin B12 metabolism and regulation in prokaryotes. *Journal Of Biological Chemistry* **278**, 41148-41159 (2003).

66. M. D. Lundrigan, W. Koster, R. J. Kadner, Transcribed sequences of the Escherichia coli btuB gene control its expression and regulation by vitamin B12. *Proceedings of the National Academy of Sciences of the United States of America* **88**, 1479-1483 (1991).

67. A. A. Richter-Dahlfors, D. I. Andersson, Cobalamin (vitamin B12) repression of the Cob operon in Salmonella typhimurium requires sequences within the leader and the first translated open reading frame. *Molecular Microbiology* **6**, 743-749 (1992).

68. S. Ravnum, D. I. Andersson, An adenosyl–cobalamin (coenzyme-B12)-repressed translational enhancer in the cob mRNA of Salmonella typhimurium. *Molecular Microbiology* **39**, 1585-1594 (2001).

69. X. Nou, R. J. Kadner, Adenosylcobalamin inhibits ribosome binding to btuB RNA. *Proceedings of the National Academy of Sciences of the United States of America* **97**, 7190-7195 (2000).

70. A. Nahvi *et al.*, Genetic control by a metabolite binding mRNA. *Chemistry & biology* **9**, 1043-1049 (2002).

71. K. A. Baker, M. Perego, Transcription antitermination by a phosphorylated response regulator and cobalamin-dependent termination at a B_{12} riboswitch contribute to ethanolamine utilization in Enterococcus faecalis. *Journal of Bacteriology* **193**, 2575-2586 (2011).

72. K. A. Fox *et al.*, Multiple posttranscriptional regulatory mechanisms partner to control ethanolamine utilization in Enterococcus faecalis. *Proceedings of the National Academy of Sciences of the United States of America* **106**, 4435-4440 (2009).

73. A. G. Vitreschak, D. A. Rodionov, A. A. Mironov, M. S. Gelfand, Regulation of the vitamin B12 metabolism and transport in bacteria by a conserved RNA structural element. *RNA* **9**, 1084-1097 (2003).

74. J. E. Johnson, F. E. Reyes, J. T. Polaski, R. T. Batey, B12 cofactors directly stabilize an mRNA regulatory switch. *Nature* **492**, 133-137 (2012).

75. Z. Weinberg *et al.*, Comparative genomics reveals 104 candidate structured RNAs from bacteria, archaea, and their metagenomes. *Genome Biology* **11**, (2010).

76. J. R. Lorsch, J. W. Szostak, In vitro selection of RNA aptamers specific for cyanocobalamin. *Biochemistry* **33**, 973-982 (1994).

77. D. Sussman, C. Wilson, J. C. Nix, The structural basis for molecular recognition by the vitamin B12 RNA aptamer. *Nature Structural Biology* **7**, 53-57 (2000).

78. A. Losi, W. Gaertner, Bacterial bilin- and flavin-binding photoreceptors. *Photochemical & photobiological sciences : Official journal of the European Photochemistry Association and the European Society for Photobiology* **7**, 1168-1178 (2008).

79. M. Kumauchi, M. Hara, P. Stalcup, A. Xie, W. Hoff, Identification of six new photoactive yellow proteins - Diversity and structure-function relationships in a bacterial blue light photoreceptor. *Photochemistry and Photobiology* **84**, 956-969 (2008).

80. C. Mandalari, A. Losi, W. Gärtner, Distance-tree analysis, distribution and co-presence of bilin- and flavin-binding prokaryotic photoreceptors for visible light. *Photochemical & photobiological sciences : Official journal of the European Photochemistry Association and the European Society for Photobiology* **12**, 1144-1157 (2013).

81. U. Römling, D. Amikam, Cyclic di-GMP as a second messenger. *Current Opinion in Microbiology* **9**, 218-228 (2006).

82. M. Gomelsky, W. D. Hoff, Light helps bacteria make important lifestyle decisions. *Trends in Microbiology* **19**, 441-448 (2011).

83. N. Tschowri, S. Busse, R. Hengge, The BLUF-EAL protein YcgF acts as a direct anti-repressor in a blue-light response of Escherichia coli. *Genes & Development* **23**, 522-534 (2009).

84. K. R. Fixen, A. W. Baker, E. A. Stojković, J. T. Beatty, C. S. Harwood, Apo-bacteriophytochromes modulate bacterial photosynthesis in response to low light. *Proceedings of the National Academy of Sciences* **111**, E237-E244 (2014).

85. N. Ivleva, T. Gao, A. LiWang, S. Golden, Quinone sensing by the circadian input kinase of the cyanobacterial circadian clock. *Proceedings of the National Academy of Sciences of the United States of America* **103**, 17468-17473 (2006).

86. L. Mulcahy, V. Isabella, K. Lewis, Pseudomonas aeruginosa Biofilms in Disease. *Microbial Ecology* **68**, 1-12-12 (2014).

87. M. A. Mussi *et al.*, The Opportunistic Human Pathogen Acinetobacter baumannii Senses and Responds to Light. *Journal of Bacteriology* **192**, 6336-6345 (2010).

88. M. Bitrian, R. H. Gonzalez, G. Paris, K. J. Hellingwerf, C. B. Nudel, Blue-light-dependent inhibition of twitching motility in Acinetobacter baylyi ADP1: additive involvement of three BLUF-domain-containing proteins. *Microbiology* **159**, 1828-1841 (2013).

89. K. Okajima *et al.*, Biochemical and functional characterization of BLUF-type flavin-binding proteins of two species of cyanobacteria. *Journal of Biochemistry* **137**, 741-750 (2005).

90. M. Gomelsky, S. Kaplan, appA, a novel gene encoding a trans-acting factor involved in the regulation of photosynthesis gene expression in Rhodobacter sphaeroides 2.4.1. *Journal of Bacteriology* **177**, 4609-4618 (1995).

91. Y. Hirose, T. Shimada, R. Narikawa, M. Katayama, M. Ikeuchi, Cyanobacteriochrome CcaS is the green light receptor that induces the expression of phycobilisome linker protein. *Proceedings of the National Academy of Sciences of the United States of America* **105**, 9528-9533 (2008).

92. D. Bhaya, A. Takahashi, A. Grossman, Light regulation of type IV pilus-dependent motility by chemosensor-like elements in Synechocystis PCC6803. *Proceedings of the National Academy of Sciences of the United States of America* **98**, 7540-7545 (2001).

93. S. Yoshihara, F. Suzuki, H. Fujita, X. X. Geng, M. Ikeuchi, Novel putative photoreceptor and regulatory genes required for the positive phototactic movement of the unicellular motile cyanobacterium Synechocystis sp PCC 6803. *Plant and Cell Physiology* **41**, 1299-1304 (2000).

94. E. Purcell, D. Siegal-Gaskins, D. Rawling, A. Fiebig, S. Crosson, A photosensory two-component system regulates bacterial cell attachment. *Proceedings of the National Academy of Sciences of the United States of America* **104**, 18241-18246 (2007).

95. H. R. Bonomi *et al.*, Light regulates attachment, exopolysaccharide production, and nodulation in Rhizobium leguminosarum through a LOV-histidine kinase photoreceptor. *Proceedings of the National Academy of Sciences* **109**, 12135-12140 (2012).

96. T. E. Swartz *et al.*, Blue-light-activated histidine kinases: two-component sensors in bacteria. *Science (New York, NY)* **317**, 1090-1093 (2007).

97. I. Kraiselburd *et al.*, The LOV Protein of Xanthomonas citri subsp. citri Plays a Significant Role in the Counteraction of Plant Immune Responses during Citrus Canker. *PLoS ONE* **8**, e80930 (2013).

98. N. Ondrusch, J. Kreft, Blue and Red Light Modulates SigB-Dependent Gene Transcription, Swimming Motility and Invasiveness in Listeria monocytogenes. *PLoS ONE* **6**, e16151 (2011).

99. M. Avila-Pérez, K. J. Hellingwerf, R. Kort, Blue light activates the sigmaB-dependent stress response of Bacillus subtilis via YtvA. *Journal of Bacteriology* **188**, 6411-6414 (2006).

100. L. Wu, R. S. McGrane, G. A. Beattie, Light Regulation of Swarming Motility in Pseudomonas syringae Integrates Signaling Pathways Mediated by a Bacteriophytochrome and a LOV Protein. *mBio* **4**, e00334-00313-e00334-00313 (2013).

101. K. Barkovits, B. Schubert, S. Heine, M. Scheer, N. Frankenberg-Dinkel, Function of the bacteriophytochrome BphP in the RpoS/Las quorum-sensing network of Pseudomonas aeruginosa. *Microbiology* **157**, 1651-1664 (2011).

102. P. Savakis *et al.*, Light-induced alteration of c-di-GMP level controls motility of Synechocystis sp. PCC 6803. *Molecular Microbiology* **85**, 239-251 (2012).

103. A. Wilde, B. Fiedler, T. Borner, The cyanobacterial phytochrome Cph2 inhibits phototaxis towards blue light. *Molecular Microbiology* **44**, 981-988 (2002).

104. M. A. van der Horst *et al.*, Locked chromophore analogs reveal that photoactive yellow protein regulates biofilm formation in the deep sea bacterium Idiomarina loihiensis. *Journal of the American Chemical Society* **131**, 17443-17451 (2009).

105. J. L. Spudich, R. A. Bogomolni, Mechanism of colour discrimination by a bacterial sensory rhodopsin. *Nature* **312**, 509-513 (1984).

Chapter 2 - Members of the PpaA family bind cobalamin

Summary

The PpaA family of proteins are proteins that contain a single SCHIC domain (sensor containing heme instead of cobalamin). In this study we show that PpaA from *Rhodobacter sphaeroides* is not a heme binding protein – as was previously thought – but a cobalamin binding protein instead. PpaA is able to interact with PpsR and activate expression of photosynthesis genes. Mutations in PpaA that cause a loss of cobalamin binding also disrupt PpaA antirepressor activity. We also tested a number of PpaA homologs from other species and found that cobalamin binding is indeed widespread among this family of proteins. This study thus shows that the SCHIC domain is in fact a cobalamin binding domain.

Introduction

The expression of photosynthesis genes is tightly regulated in anoxygenic photosynthetic prokaryotes. Early research has identified two key environmental factors that control photosystem synthesis: light and oxygen (*1*). Under high light intensity, pigment levels are reduced in order to appropriately balance the oxidation/reduction potential of the ubiquinone pool (*2, 3*). When grown under aerobic conditions, purple non-sulfur bacteria repress expression of the photosynthetic genes, and instead grow chemoheterotrophically. A number of regulatory elements involved in this process have been identified to date (reviewed in (*2, 4*)).

One of the main regulators controlling photosynthesis gene expression is PpsR

(also called CrtJ in some species). PpsR homologs can be found in almost all purple bacteria. Several species contain two functional copies of PpsR, each with its own functionality (*5*). For example, in *Bradyrhizobium* ORS278, PpsR1 acts as a redox-responsive activator while a second homolog PpsR2 acts as a light-regulated repressor in conjunction with a photoreceptor BphB2 (*6*).

Genes controlled by PpsR vary among different species, although most of the genes are indeed involved in photosynthesis, specifically enzymes involved in synthesis of the photopigments bacteriochlorophyll and carotenoids as well as the light harvesting and reaction center photosystem structural proteins (*5*). Other genes identified in the *R. capsulatus* and *R. sphaeroides* PpsR/CrtJ regulons include enzymes involved in heme biosynthesis and genes that code for cytochrome apoproteins (*7, 8*). Each of the known PpsR/CrtJ regulated promoters are known to contain a variant of the DNA recognition sequence TGT-N_{12}-ACA (*5*). This recognition sequence is present in tandem either 8 bp apart or at distant sites up to 240 bp apart (*9, 10*). Mutational studies indicate that PpsR/CrtJ bind cooperatively to these tandem sites (*6, 9, 11*).

The DNA-binding properties of PpsR is regulated, in part, by redox-dependent modifications of key cysteine residues present in the helix-turn-helix DNA binding region (*6, 11-13*). It has also been reported that a PAS domain of PpsR binds heme and that heme binding affects the DNA binding properties of PpsR (*14*). In addition to oxidation and heme, several proteins have been found to interact with and affect the DNA binding properties of PpsR. As mentioned above, the activity of PpsR2 from *Bradyrhizobium* ORS278 is inhibited by a light regulated interaction with a red-light absorbing phytochrome-like photoreceptor BphB2 (*6*). In *R. sphaeroides*, the activity of

PpsR is also known to be inhibited by interacting with the blue light absorbing-and redox responding antirepressor AppA (*11, 15*). AppA is known to convert PpsR from an active tetramer to an inactive dimer (*11*). The antirepressor activity of AppA is known to be regulated by both light absorption as well as by the presence of a AppA bound heme (*11, 16, 17*).

Recently, the DNA binding properties of CrtJ from *R. capsulatus* was shown to be inhibited by interaction with another antirepressor AerR (*18*). AerR (PpaA in some species) has homologs in almost all purple non-sulfur bacteria, and may therefore be the oldest regulator of PpsR activity. The PpaA/AerR homologs are characterized by a B_{12}-binding domain and an absence of enzymatic or other output domains. The B_{12}-binding domains of the PpaA/AerR homologs show some striking differences from those of B_{12}-dependent enzymes, leading to the hypothesis that this family no longer binds cobalamin but heme instead (*19*). Later studies with the truncated domains showed a preference for heme over cobalamin (*20*). However, recently work by Cheng and coworkers showed that AerR from *R. capsulatus* is in fact a bona fide cobalamin-binding protein (*18*). In this study AerR was readily purified with tightly bound cobalamin. Furthermore, mutation of the strongly conserved histidine in the B_{12} binding motif resulted in a loss of cobalamin binding (*18*). In vivo this mutation resulted in a loss of anti-repressor activity, further demonstrating the role of B_{12} binding in AerR.

While cobalamin has long been recognized as a cofactor in a number of enzymatic reactions, it has only recently become clear that cobalamin can also play a role as a sensor cofactor. In several bacteria the mRNA for the cobalamin transporter BtuB was shown to contain a B_{12}-binding riboswitch, which downregulates translation at

elevated cobalamin levels (*21, 22*). *Myxococcus xanthus* CarH regulates the light-dependent expression of carotenoid genes in a B_{12} dependent manner (*23*). In CarH the photolysis of adenosyl-cobalamin to hydroxyl cobalamin leads to a conformational change and the subsequent release of CarH from its target DNA (*23*). Likewise, hydroxyl cobalamin-bound AerR from *R. capsulatus* reduces the DNA-binding activity of CrtJ (*18*). What role this mechanism plays is not known, although it has been suggested that AerR, like CarH, acts as a light-receptor.

In the study below, I set out to test whether a close homolog of AerR, PpaA from *R. sphaeroides* is able to bind cobalamin. By overexpressing various mutants of PpaA in an AppA deletion strain, I was able to show that cobalamin binding is indeed the preferred mode of action of PpaA. I also tested a number of PpaA/AerR homologs from other purple non-sulfur bacteria for their ability to bind cobalamins.

Materials and Methods

Strains and plasmids

Rhodobacter sphaeroides strain HR was grown in Sistrom's minimal medium (*24*) with succinate and casamino acids as a carbon source or in LB at 30°C. *E. coli* was grown at 37°C in LB medium.

To make clean deletions, plasmid pAJV1 was used. Plasmid pAJV1 was constructed by fusing *sacB* from plasmid pZJD29a (*25*) to the *puc* promoter of *R. sphaeroides*. The resulting cassette was then inserted into BstB1 digested and blunted pJP5603 (*26*). The resulting plasmid confers both kanamycin resistance and sucrose sensitivity.

Flanking 500 bp regions of genes to be deleted were PCR amplified and than used as templates for a cross-over PCR reaction. The resulting product has the flanking regions linked by a 21 basepair nonsense reading frame. This construct was then inserted in SmaI digested pAJV1. The resulting plasmids were sequenced to ensure sequence fidelity of inserts.

Deletion plasmids were transferred into *R. sphaeroides* by conjugal mating with *E. coli* S17-1(λpir). *E. coli* S17-1(λpir) was transformed with the deletion plasmid and grown to exponential phase and washed twice to remove antibiotics. 750 μL washed cells were then mixed with 750 μL overnight culture of *R. sphaeroides*. Cells were pelleted and resuspended in 50 μL LB. The resuspended cells were then spotted on a LB plate in 50 μL aliquots and incubated for 24 – 48 hours at 30^{o}C. At that point the cells were restreaked onto LB agar with 25 μg/mL kanamycin. The selective plates also contained 5 μg/ml gentamycin to inhibit growth of *E. coli*. *R. sphaeroides* has some innate gentamycin resistance, and growth is not affected by gentamycin at low concentrations. The plates were incubated for 3 days at 30^{o}C after which several colonies were restreaked on LB agar with 50 μg/ml kanamycin. To select for double recombinants, mutants were streaked on LB without antibiotics supplemented with 10% (w/v) sucrose. Colonies were selected for complete segregation by testing for kanamycin sensitivity. Mutants were confirmed by colony PCR.

To overexpress PpaA in *R. sphaeroides,* plasmid pSRKKm (*27*) was used. pSRKkm is a broad-host-range plasmid with a multiple-cloning site with protein expression under control of a T7 promoter. This plasmid allows for induction of overexpression by the addition of IPTG. A PCR amplified *ppaA* gene was cloned into

NdeI,NotI digested pSRKkm. Several different mutations were subsequently introduced by using a quick change protocol (Agilent Technologies).

Bacterial two-hybrid screen

Interaction between PpaA and PpsR was tested by using the BacterioMatch II bacterial two-hybrid screen (Agilent Technologies). The genes encoding PpaA, PpsR and AppA were cloned in both pBT and pTRG plasmids. Interaction was tested by transforming Bacteriomatch II Validation cells with different combinations of bait and target plasmids. As positive control cells were transformed with pBT-LGF2 and pTRG-Gal11 plasmids that were supplied with the Bacteriomatch II kit. As negative control cell were transformed with a bait plasmid in combination with an empty target plasmid. The transformants were then plated on selective medium (M9, His drop out) and incubated for 48 hours at 30^{o}C in dark. Growth on selective medium indicates protein-protein interactions.

Protein purification

To overexpress various PpaA homologs, plasmid pET-MBP was used as a vector. pET-MBP was constructed by cloning the MBP domain and TEV site from plasmid pMHT-delta238 (*28*) into plasmid pET28a(+) (Novagen). The resulting plasmid encodes at His_6-tagged MBP domain that can be cleaved using TEV protease. Genes of interest were PCR amplified from genomic DNA (Rs-PpA, Rg-AerR, RPA1540 and Rc-AerR) or syntesized as codon-optimized genes (Eb-PpaA, Me-PpaA, Js-PpaA) (IDT, Coralville, IA). The program JCAT was used to optimize sequences for overexpression in *E. coli*

(*29*).

Proteins were overexpressed in *E. coli* BL21(DE3) in LB with 25 ug/mL kanamycin. Cultures were grown at 37^{o}C until OD_{600} ~ 0.3 and then incubated at 16^{o}C. After 1.5 hour overexpression was induced by adding IPTG to a final concentration of 0.4 mM. After 16-20 hours of growth at 16^{o}C cells were harvested and pellets stored at -80^{o}C.

Cell pellets were resuspended in lysis buffer (20 mM Tris-HCl, 150 mM NaCl, 10 mM imidazole) and lysed by three passages through a microfluidizer. Except when apo-protein was needed, hydroxy-cobalamin was added to a final concentration of 25 μM. Cell debris was removed by centrifuging for 30 minutes at 15,000 rpm (Sorvall SS-34 rotor) and filtered through a 0.45 um syringe filter. The clarified lysate was then applied a gravity nickel column. The column was washed with 30 mL wash buffer (as lysis buffer, with 30 mM imidazole). Bound protein was eluted with elution buffer (as lysis buffer, with 250 mM imidazole). The buffer was exchanged to 20 mM Tris (pH 8), 150 mM NaCl using a desalting column (Bio-Rad EconoPac 10DG).

When needed the His_6-MBP tag was cleaved by adding TEV protease in a 1:20 (TEV protease:MBP-tagged protein) molar ratio and incubating the reaction 2.5 hours at room temperature in buffer with 20 mM Tris (pH 8) and 150 mM NaCl. TEV protease, cleaved tags and uncleaved protein were then removed by first applying the protein to a column with amylose resin (NEB). The flowthrough was then applied to a nickel column and eluted with wash buffer. Finally the resulting protein was run over a Superose 12 column to remove aggregated protein. The final protein was concentrated using Amicon Ultra-4 centrifugal filter (Millipore, 10kDa MWCO).

Cofactor binding

To test for binding of different forms of cobalamin, protein was overexpressed in *E. coli* as described before. Cell lysate was then aliquoted in 6 equal amounts and different forms cobalamin was added to a final concentration of 25 μM. One aliquot was exposed to high intensity light for 5 minutes after addition of adenosylcobalamin. Other aliquots were kept in the dark. As control one aliquot was purified in absence of cobalamin. The lysates were incubated on ice for 1 hour. The lysate was clarified by centrifugation for 30 minutes at 15,000 rpm (Sorvall SS-34). Proteins were then purified using amylose resin. All procedures were performed in dark under dim red safety light. A pink color and the presence of absorbance peaks in the 500 -550 nm region were used as indicators of cobalamin binding.

Photosynthetic growth

To test for *in vivo* functionality, a *ΔappA* mutant was transformed with plasmid pSRK-*ppaA* and the various mutants. As a control, *ΔappA* was transformed with pSRKkm. Aerobic cultures were grown until log phase and inoculated in fresh Sistrom's medium with 4%(w/v) succinate and 0.2%(w/v) casamino acids at an OD_{660}~0.3. The cultures were transferred to screw cap tubes filled to the top. When needed, expression was induced with IPTG at a final concentration of 1 mM. The cultures were incubated in incandescent light for 48 hours at 30^{o}C. 10 ml of the cultures was harvested and resuspended in 20 mM Tris (pH 8), 150 mM NaCl and lysed by sonication. The lysates were centrifuged at maximum speed for 10 minutes. The UV/vis absorbance spectrum

was measured from 300 to 900 nm and normalized to protein content.

Results

Cofactor binding of R. sphaeroides *PpaA*

First we tested whether full length PpaA from *R. sphaeroides* is able to bind cobalamin. When hydroxy-cobalamin (OH-Cbl) is added to the cell lysate the protein elutes in a pink-colored fraction. Addition of adenosyl-cobalamin (ado-Cbl), followed by exposure to high-intensity light also led to protein-bound cobalamin, while addition of ado-Cbl without light excitation did not. The UV-vis spectrum resembles hydroxy-cobalamin, albeit that the α- and β-peaks are more separated. The cobalamin remained associated with the protein in subsequent buffer exchange and gel filtration steps, showing that PpaA binds hydroxy-cobalamin tightly.

We also tested specificity of cobalamin binding by full length PpaA. The PpaA homolog from *R. capsulatus*, AerR, has a high degree of binding specificity for hydroxy-cobalamin (OH-Cbl) over that of adenyl-, cyano- and methyl-cobalamin (ado-Cbl, CN-Cbl and Met-Cbl, respectively). These latter cobalamin derivatives have bulkier and tighter upper axial ligands to the centrally coordinated cobalt. As is the case with AerR, none of the other cobalamin derivatives containing tighter upper ligands were able to significantly bind apo-PpaA, indicating that, like AerR, full length PpaA is also selective for hydroxy-cobalamin (Table 2.1). Finally, light excitation of ado-Cbl results in well-characterized photohydrolysis of the upper axial ligand to generate OH-Cbl as a product. Thus, addition of adenosyl-cobalamin (ado-Cbl) to apo-PpaA in the presence of high intensity light, led to PpaA with bound OH-Cbl, while addition of ado-Cbl without light -

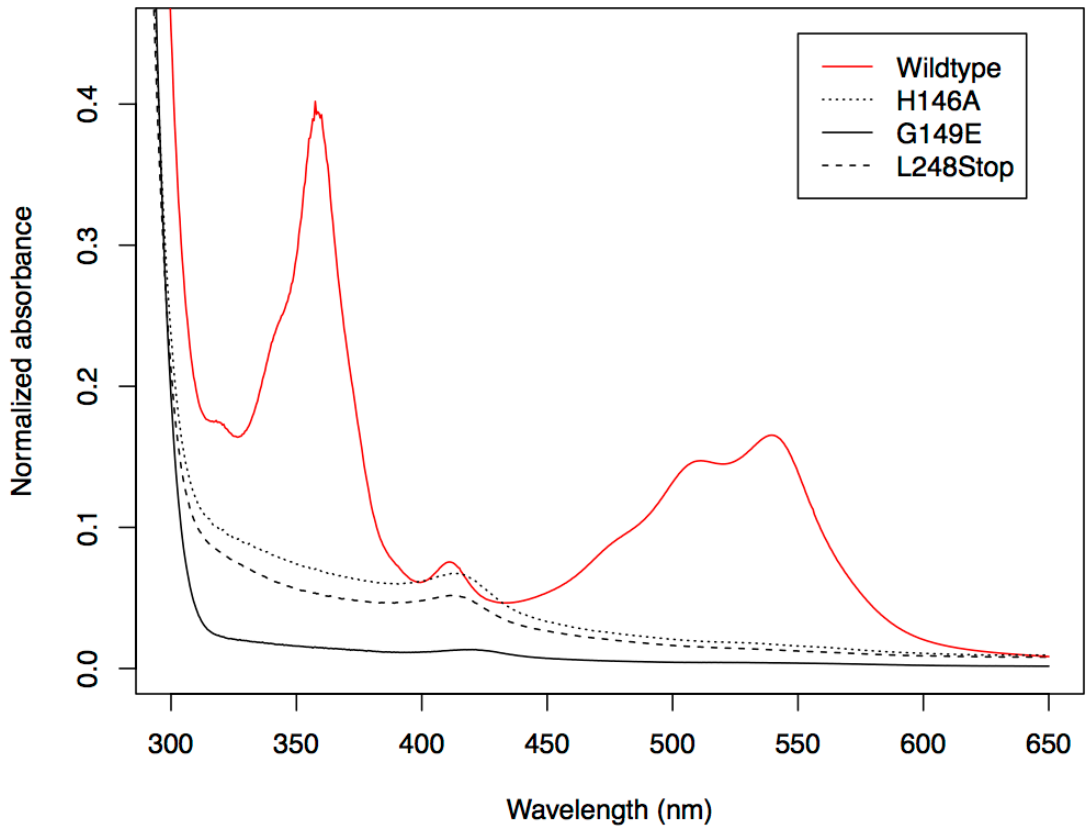

Figure 2.1 Absorption spectra of Rs-PpaA purified in the presence of hydroxycobalamin. Wildtype PpaA copurifies with cobalamin, while truncated (L248Stop) or single residue mutants all lost their ability to bind hydroxycobalamin. Interestingly, a small peak around 412 nm is still visible in these mutants, indicating sub-stoichiometric heme-binding. All proteins were His_6-MBP-tagged.

excitation did not. Similar photohydrolysis-mediated cobalamin binding was also observed to occur with AerR (*18*).

A previous study by Moskvin et al. (*20*) suggested that PpaA from *R. sphaeroides* is a heme binding protein that is unable to bind cobalamin. However, in their experiments they used a truncated variant of PpaA that contained just the SCHIC domain fused to an MBP domain. To test whether this truncation influences cofactor binding we introduced a stop codon at Leu248 mimicking the C-terminal truncation that was used in their study. Interestingly, the L248Stop mutant was no longer able to bind cobalamin, which indicates that the carboxyl domain of PpaA (beyond codon 248) is important for OH-Cbl binding (Figure 2.1). This result shows that the heme-binding reporter before is mostly likely an artifact of the introduced truncations.

To test the importance of the strongly conserved DxHxxG motif, which is a signitature motif for B_{12}-binding domains we introduced mutation in this motif and assayed for cobalamin binding. His145 in AerR (His146 in PpaA) has been shown to form the lower axial ligand to OH-Cbl (*18*). When we mutated this histidine to alanine PpaA was no longer able to bind OH-Cbl (Figure 2.1). Similar results have been reported for AerR (*18*). A glycine to glutamate mutation three residues downstream of the histidine also abrogated cobalamin binding (Figure 2.1). A similar glycine to glutamate mutation is found in the heme-binding SCHIC domain of AppA (Figure 2.2). This mutation was hypothesized to be one of the reasons why AppA is not able to bind cobalamin, despite the sequence similarities to B12 binding domains (*30*).

Table 2.1 The ability of a number of PpaA homologs to bind cobalamin. (OH-Cbl: hydroxycobalamin, CN-Cbl: cyanocobalamin, Met-Cbl: methylcobalamin, Ado-Cbl: adenosylcobalamin).

Species	**Protein**	**OH-Cbl**	**CN-Cbl**	**Met-Cbl**	**Ado-Cbl**
Rhodobacter sphaeroides HR	Rs-PpaA	+	-	-	-
Rubrivivax gelatinosus IL-144	Rg-AerR	+	-	-	-
Methylobacterium extorquens PA1	Me-PpaA	+	-	-	-
Rhodopseudomonas palustris	RPA1540	-	-	-	-
Jannaschia sp. CCS1	Js-PpaA	+	-	+	+
Rhodospirillum centenum	Rc-AerR	+	+	+	+
Erythrobacter sp. NAP1	Eb-PpaA	+	+	+	+

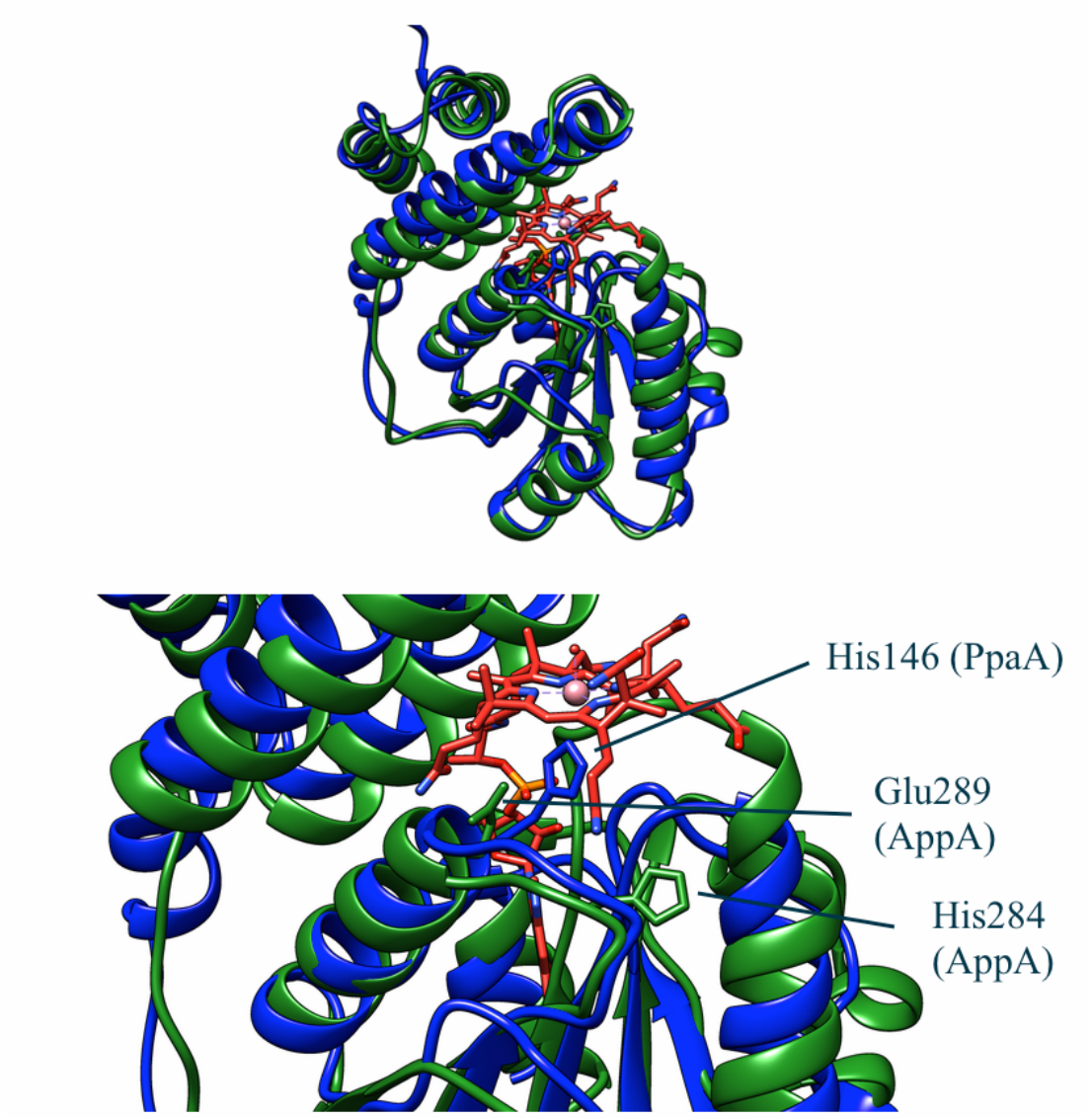

Figure 2.2 Comparison of PpaA with the structure of the AppA SCHIC domain (PDB: 4HEH). PpaA is depicted in blue, AppA in green and cobalamin in red. The structure of PpaA was predicted using the Phyre homology modeler. The strongly conserved histidine is shown in stick representation in both structures. The glutamate that replaces a strongly conserved glycine in AppA is also shown in stick representation. This glutamate is in close proximity to the phosphate group of the DMBI tail of cobalamin and may explain why AppA does not bind cobalamin but heme instead.

We also introduced mutations in the strongly conserved glycine three residues downstream of the conserved histidine that is also part of the strongly conserved DxHxxG B_{12}-binding motif. We mutated this glycin to a glutamate, thus mimicking the AppA SCHIC domain, which is a related structure that is known to bind heme but not cobalamin (*17, 30*). In AppA the presence of a glutamate at this position presumably introduces a negative charge repelling the phosphate group of the tail of cobalamin, and also provides a steric hindrance which prevents the 5,6-dimethylbenzimidazole (DMBI) tail form inserting into the Rossman fold of the protein thereby allowing AppA to bind heme over that of cobalamin (Figure 2.2).

PpaA purified in absence of added cobalamin shows a small UV/vis absorption peak around 412 nm suggesting substoichiometric heme-binding (data not shown). The same peak shows in the spectra of mutant forms of PpaA. We tried to increase the amount of bound heme by incubating purified wildtype or mutant apo-PpaA with free hemin. All forms of PpaA showed some heme-binding as indicated by a red-shift of the Soret peak from 385 nm for free hemin to 412 nm for bound hemin (Figure 2.3). This red-shift was less obvious in the H146A mutant (Figure 2.3) indicating that a fraction of heme is coordinating with His146. This histidine however is not essential for heme-binding as was hypothesized by Moskvin *et al*. (*20*). The G149E mutant showed a more pronounced red-shift and binds heme better than the wildtype protein does.

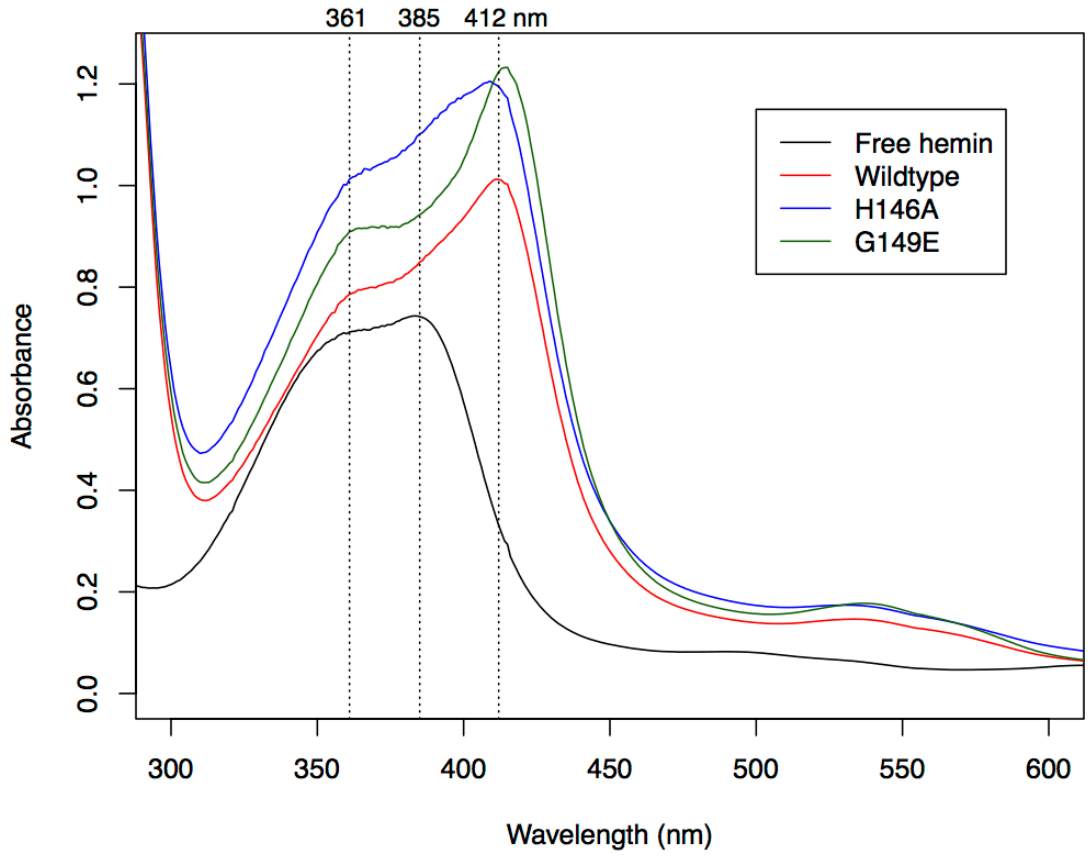

Figure 2.3 Reconstitution of nickel purified His_6-MBP-PpaA with hemin (vertical dotted lines at 361, 412 nm). Purified protein was mixed with hemin in a 1:1 molar ratio and incubated overnight at 4°C. The spectrum of heme is red-shifted, suggesting that PpaA does have some heme binding capacity. Heme-binding by the H146A mutant is less apparent, while the G149E mutant shows a more pronounced spectral change.

In vivo analysis of PpaA

In most purple bacterial species the *ppaA* gene is located just upstream of the *ppsR* gene that codes for a well-characterized repressor of photosystem gene expression. In *R. capsulatus* the isolated PpaA homolog AerR was shown to physically interact with the PpsR homolog CrtJ *in vitro* by co-elution during gel filtration (*18*). In this study we extended this interaction by addressing whether PpaA can interacts with PpsR *in vivo* using a bacterial-two-hybrid screen. The results of this analysis indicate that PpaA can indeed interact with PpsR (Figure 2.4). Thus, PpsR in *R. sphaeroides* appears to have two structurally related regulators: PpaA and AppA, one of which binds cobalamin (PpaA) and the other of which binds heme (AppA) (Figure 2.2).

Previous studies suggested that PpaA only plays a minor role in regulating the expression of photosynthetic genes in *R. sphaeroides* (*31*). At the same time AppA plays a major role in regulating DNA-binding activity of PpsR so much so that a deletion of *appA* leads to a complete loss of pigmentation and photosynthetic growth (*32*). To further assess the biological ability of PpaA, we overexpressed PpaA in an *appA* deletion mutant using a broad host range overexpression construct (pSRK-*ppaA*). Interestingly overexpression of PpaA by the addition of IPTG does indeed restore pigmentation (Figure 2.5) and photosynthetic growth (Table 2.2). This indicates that overexpression of PpaA relieves PpsR repression of bacteriochloryphyll gene expression even in the absence of AppA.

Using this overexpression system we also tested the ability of several PpaA mutants to function as an antirepressor of PpsR. The PpaA H146A mutant that did not show cobalamin-binding *in vitro* was also not able of restore growth under

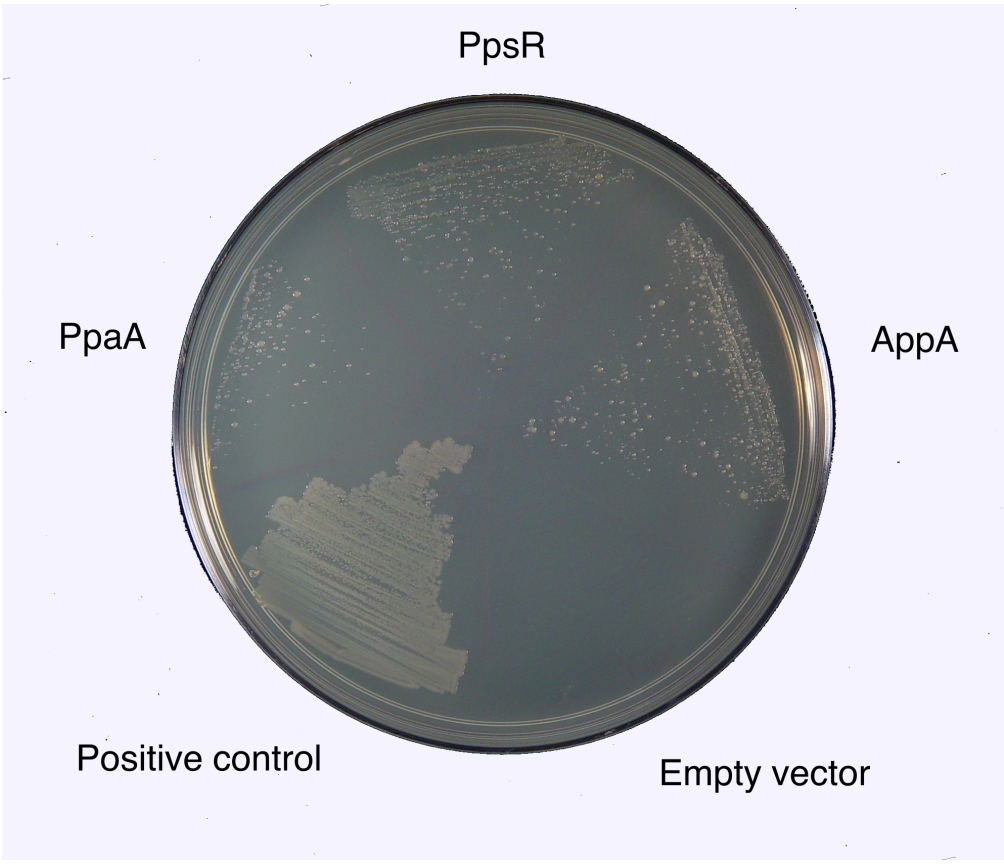

Figure 2.4 Bacterial two hybrid screen with PpsR as bait. The different targets are indicated. The screen shows interaction between PpsR and PpaA. This interaction may be weaker than the interaction between PpsR and AppA and the interaction of PpsR with itself as this strain shows less vigourous growth. The positive control is a strain transformed with pBT-LGF2 and pTRG-Gal11 as supplied as part of the Bacteriomatch II kit.

photosynthetic conditions when overexpressed (Table 2.2, Figure 2.5). This shows that coordination of cobalamin by the conserved histidine is essential for the function of PpaA. Similarly, the G149E mutant which also is defective in cobalamin binding also did not restore photosynthetic growth. The fact that this heme-preferring mutant is inactive shows that the functionality of PpaA is indeed dependent on cobalamin and not binding of heme.

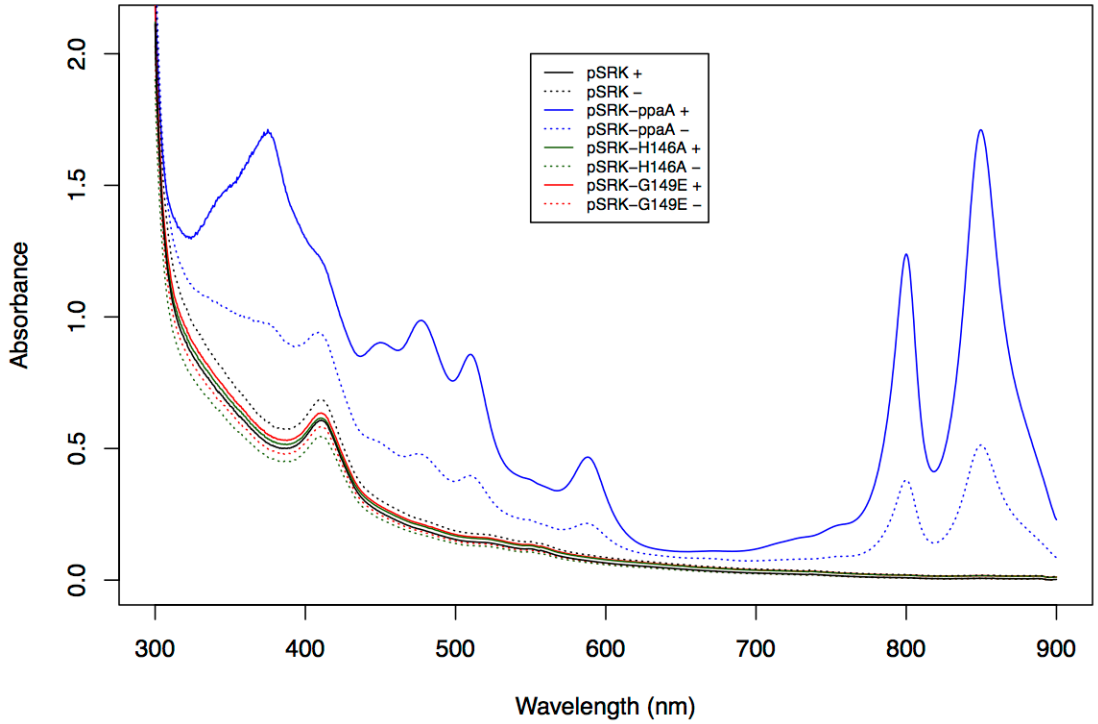

Figure 2.5 Extracted pigments of ΔappA::pSRK-ppaA grown photosynthetically in the presence (solid line) or absence (dotted line) IPTG. Overexpression of ppaA leads to restoration of pigment production and allows for photosynthetic growth.

Table 2.2 Growth of *appA* knockout strains complemented with various *ppaA* mutants under photosynthetic conditions. (-: no growth, +: growth).

	- IPTG	**+ IPTG (1 mM)**
ΔappA::pSRK	-	-
ΔappA::pSRK-ppaA	-	+
ΔappA::pSRK-ppaA H146A	-	-
ΔappA::pSRK-ppaA G149E	-	-

Homologs

Next we asked whether B_{12}-binding was wide-spread among PpaA/AerR homologs from various species. We expressed a number of homologs (Table 2.1) as MBP-fusion proteins and purified them in the presence of various cobalamins. All of the tested homologs were able to bind cobalamin, with the exception of RPA1540 from *Rhodopseudomonas palustris*. The *R. palustris* PpaA homolog is an outlier as it is not upstream of a PprR gene and is instead upstream of a heme-oxygenase. Given that we did not observe binding of cobalamin by this protein, we also tested for binding of biliverdin, the end product of the reaction catalyzed by heme oxygenase. No binding of biliverdin could be detected (data not shown).

We observed that PpaA homologs from *Methylobacterium extorquens* PA1 (Me-PpaA) and *Rubrivivax gelatinosus* IL-144 (Rg-AerR) showed only interaction with hydroxy-cobalamin and not with other forms of cobalamin (Table 2.1). This is similar to AerR from *R. capsulatus* and PpaA from *R. sphaeroides.* The PpaA homologs of *Jannaschia* sp. CCS1 (Js-PpaA), *Rhodospirillum centenum* (Rc-AerR) and *Erythrobacter* sp. NAP1 (Eb-PpaA) showed binding to all forms of cobalamin, with the exception of Js-PpaA which did not show binding to cyano-cobalamin. Interestingly, *Jannaschia* and *Erythrobacter* are both aerobic anoxygenic phototrophs. Whether the ability of binding multiple forms of cobalamin is more widespread in this group of bacteria compared to the anaerobic anoxygenic phototrophs is not known.

Another interesting observation is that the α- and β-peaks of the absorption spectra of Me-PpaA and Rc-AerR are red-shifted by about 25 nm compared to the spectra of other PpaA homologs (Figure 2.6). The spectra of the other homologs are very similar

to the spectrum of free OH-Cbl, with some red-shifting of the γ- and β-peaks, but not of the α-peak (Figure 2.6). The absorption spectra of Me-PpaA and Rc-AerR show some resemblance to the absorption spectrum of free ado-Cbl, albeit more red-shifted. It could be that the bound cobalamins are in fact a mixed population with predominantly ado-Cbl. Interestingly Me-PpaA did not show ado-Cbl binding in previous experiments. All spectra strongly resemble the spectra reported for CarH from *Myxococcus xanthus* in dark (Rc-AerR, Me-PpaA) or light form (the other homologs).

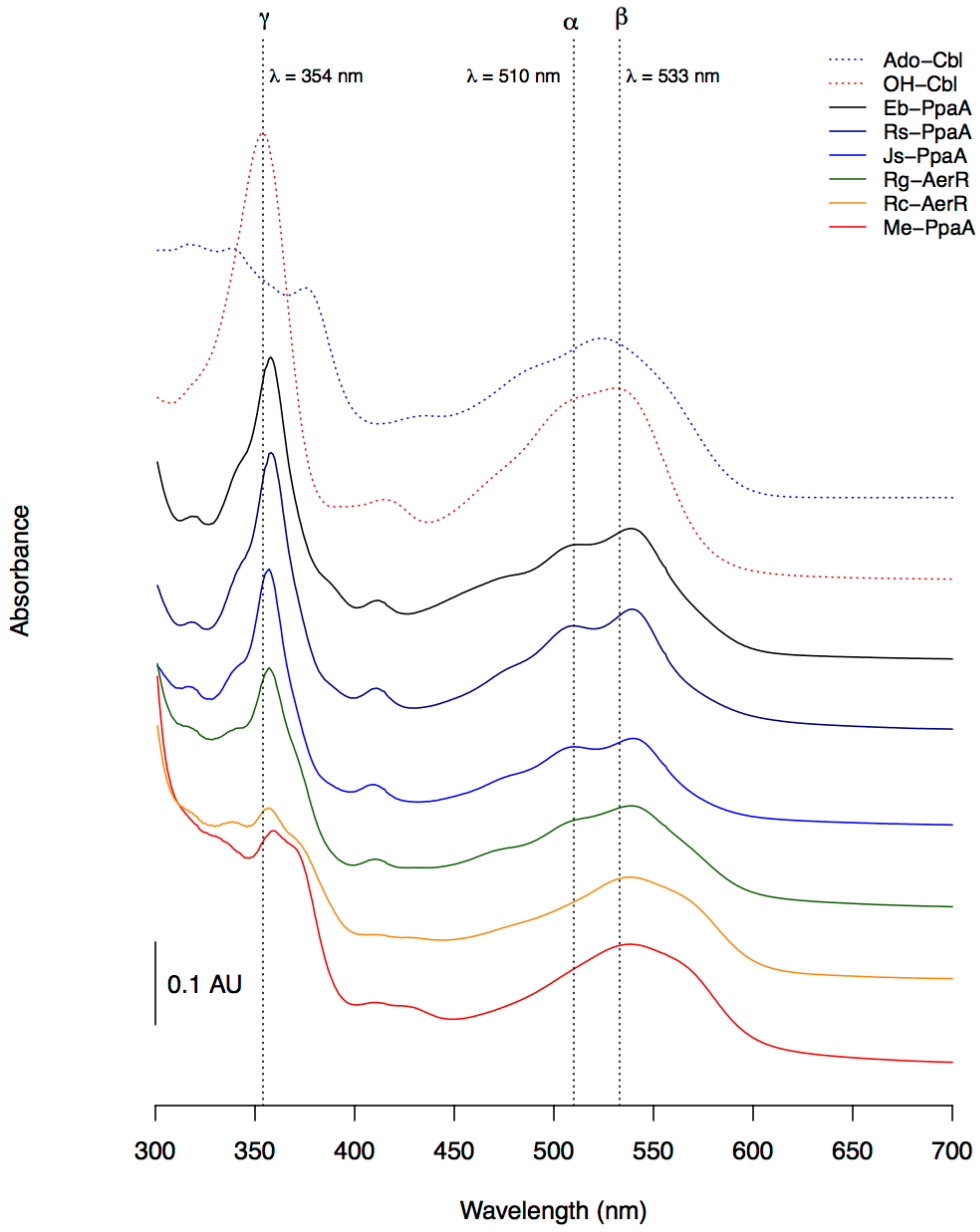

Figure 2.6 Absorption spectra of purified PpaA homologs. All spectra were recorded after removal of the His6-MBP tag. Eb-PpaA, Rs-PpaA and Js-PpaA all show spectra similar to free hydroxycobalamin. The spectrum of Rg-AerR appears to be more red-shifted. The α- and β-peaks (around 500 – 550 nm) of Rc-AerR and Me-PpaA are more strongly red-shifted, while the γ-peak (~350 nm) is strongly reduced. (For abbreviations see Table 2.1).

Discussion

PpaA from *R. sphaeroides* was previously reported to be a heme-binding protein (*20*). However, our analysis shows that Rs-PpaA selectively and effectively binds hydroxycobalamin over both heme and other forms of cobalamin that contain a more tightly bound upper ligand. Full length PpaA does have some heme-binding capacity, but it cannot be readily reconstituted to stoichiometric amounts by the addition of exogenous heme thereby indicating PpaA has a lower affinity for heme than for cobalamin. Several differences between our study and the Moskvin *et al*. study (*20*) is that we added excess hydroxyl-cobalamin to the PpaA overexpressing *E. coli* cell lysate while Moskvin et al. used cyano-cobalamin added to the growth medium (*20*). Another explanation for the observed differences is that the Moskvin study used a PpaA truncation that contained just the SCHIC domain. Our results show that an arginine-rich C-terminus that was deleted in the Moskvin study is necessary for incorporation of hydroxycobalamin.

The additional PpsR antirepressor AppA is known to bind heme at its SCHIC domain (*17, 30*). This domain contains sequence resemblance to the B_{12}-binding domain of PpaA and of other well-characterized B_{12} binding proteins. One notable difference is the presence of a bulky charged glutamate instead of the canonical glycine in the DxHxxG signature motif for B_{12}-binding domains. Recent crystal structures of the AppA SCHIC domain show that the presence of this glutamate could provide electrostatic repulsion to the phosphate group in cobalamin thereby affecting its binding to this tetrapyrrole (*15, 30*). When we introduced a Gly to Glu mutation in PpaA it indeed resulted in loss of cobalamin-binding in favor of heme-binding. Interestingly, in

Methylobacterium extorquens the PpaA homolog has a cysteine instead of glycine in the B_{12} binding motif without disrupting cobalamin-binding. This indicates that Gly at this location is not absolutely necessary for cobalamin binding.

A chromosomal deletion of PpaA does not lead to an appreciable difference in pigmentation under photosynthetic conditions indicating that the role of PpaA in controlling photopigment synthesis is minimal (*31*). This is contrasted by a much stronger reduction in photopigment synthesis observed by a deletion of the PpaA homolog AerR in *R. capsulatus* (*18*). Indeed the phenotype of the *aerR* deletion in *R. capsulatus* is more like that of an AppA deletion in *R. sphaeroides,* which also exhibits a significant reduction in pigment synthesis. AppA and AerR are both known to function as antirepressors of PpsR/CrtJ (*18, 33*). It therefore seems likely that PpaA also may have a similar antirepressor role on PpsR in *R. sphaeroides*. In support of this conclusion is our observation that overexpression of PpaA in a *ΔappA* mutant background does indeed lead to a restoration of photopigment synthesis and subsequent photosynthetic growth. This latter result indicates either that AppA has taken over the antirepressor role of PpaA and that PpaA is a cryptic antirepressor or that under some growth conditions AppA is the main PpsR antirepressor, while under other conditions PpaA controls PpsR activity. In support of this latter possibility, PpaA was identified as an activator of bacteriochlorophyll genes under (micro)aerobic conditions (*31*).

One possibility is that PpaA is functioning as both as a light and as a redox sensor. In regards to light sensing, PpaA selectively binds hydroxyl-cobalamin, which is known to be generated as a photohydrolysis product of light excitation of adenosyl-cobalamin. Thus the selectivity hydroxyl-cobalamin may be a means to allow PpaA to

indirectly sense the presence of light by interacting with the product of adeno-cobalamin photolysis. In regards to redox sensing, cobalt is redox active with able to easily transition from Co(III) in the oxidized state to Co(II) and then to Co(I) in a series of one electron transfers. The stability of the axial ligands to Co is weakened as the Co is reduced from Co(III) to Co(II). Specifically, Co(III) has both upper and lower axial ligands as well as the four ligands from the pyrrole ring (termed 6 coordinate) while Co(II) is 5 coordinate as it has a loss of either the upper or lower axial ligand. Further reduction of Co(I) produces 4 coordinate cobalamin that has lost both upper and lower axial ligands and just retains the four pyrrole ligands. These Co redox events are known to occur under physiologically relevant potentials (-350 mV to >150 mV) (*34*), and in the case of methionine synthase, involves both molecular oxygen and flavodoxin as oxidants and reductants respectively (*35*). One could therefore envision that PpaA may function as a redox sensor as changes in the oxidation state of cobalamin could affect the structure of PpaA via alterations in the binding of relevant axial amino acid ligands to Co.

Finally, all of the tested homologs for other species bound cobalamin with half specific for hydroxy-cobalamin. The set of homologs tested here is very limited, but it is curious to see that two of the three more promiscuous homologs are from aerobic anoxygenic phototrophs (AAnP), a group of purple non-sulfur bacteria that are obligatly aerobic and use photosynthesis under aerobic conditions (*36*). The third promiscuous species is AerR from *R. centenum*. *R. centenum* shows much less reduction of pigmentation under aerobic conditions than typical purple non-sulfur bacteria (*37*). Collectively these results suggest that the clade of proteins previously designated as SCHIC proteins actually preferentially bind cobalamin over that of heme. The one outlier

appears to be AppA which has undergone a distinct mutational changes in the cobalamin binding domain that allow AppA to uniquely bind heme over that of cobalamin. The challenge going forward wil be to obtain better understanding of the completing roles of PpaA and AppA in controlling the DNA binding activity of PpsR.

References

1. G. Cohen-Bazire, W. R. Sistrom, R. Y. Stanier, Kinetic studies of pigment synthesis by non-sulfur purple bacteria. *Journal of Cellular and Comparative Physiology* **49**, 25-68 (1957).
2. C. Bauer, S. Elsen, L. Swem, D. Swem, S. Masuda, Redox and Light Regulation of Gene Expression in Photosynthetic Prokaryotes. *Philosophical Transactions: Biological Sciences* **358**, 147-154 (2003).
3. J. Wu, C. E. Bauer, RegB Kinase Activity Is Controlled in Part by Monitoring the Ratio of Oxidized to Reduced Ubiquinones in the Ubiquinone Pool. *mBio* **1**, e00272-00210-e00272-00218 (2010).
4. J. Gregor, G. Klug, Regulation of bacterial photosynthesis genes by oxygen and light. *Fems Microbiology Letters* **179**, 1-9 (1999).
5. S. Elsen, M. Jaubert, D. Pignol, E. Giraud, PpsR: a multifaceted regulator of photosynthesis gene expression in purple bacteria. *Molecular Microbiology* **57**, 17-26 (2005).
6. M. Jaubert *et al.*, Light and redox control of photosynthesis gene expression in Bradyrhizobium: dual roles of two PpsR. *The Journal of biological chemistry* **279**, 44407-44416 (2004).
7. O. V. Moskvin, L. Gomelsky, M. Gomelsky, Transcriptome Analysis of the Rhodobacter sphaeroides PpsR Regulon: PpsR as a Master Regulator of Photosystem Development. *Journal of Bacteriology* **187**, 2148-2156 (2005).

8. J. L. Smart, J. W. Willett, C. E. Bauer, Regulation of hem gene expression in Rhodobacter capsulatus by redox and photosystem regulators RegA, CrtJ, FnrL, and AerR. *Journal of Molecular Biology* **342**, 1171-1186 (2004).

9. S. Elsen, S. N. Ponnampalam, C. E. Bauer, CrtJ Bound to Distant Binding Sites Interacts Cooperatively to Aerobically Repress Photopigment Biosynthesis and Light Harvesting II Gene Expression in Rhodobacter capsulatus. *The Journal of biological chemistry* **273**, 30762-30769 (1998).

10. S. N. Ponnampalam, C. E. Bauer, DNA Binding Characteristics of CrtJ. *Journal Of Biological Chemistry* **272**, 18391-18396 (1997).

11. S. Masuda, C. E. Bauer, AppA is a blue light photoreceptor that antirepresses photosynthesis gene expression in Rhodobacter sphaeroides. *Cell* **110**, 613-623 (2002).

12. Z. Cheng *et al.*, Activity of the tetrapyrrole regulator CrtJ is controlled by oxidation of a redox active cysteine located in the DNA binding domain. *Molecular Microbiology* **85**, 734-746 (2012).

13. S.-H. Cho, S.-H. Youn, S.-R. Lee, H.-S. Yim, S.-O. Kang, Redox property and regulation of PpsR, a transcriptional repressor of photosystem gene expression in Rhodobacter sphaeroides. *Microbiology (Reading, England)* **150**, 697-706 (2004).

14. L. Yin, V. Dragnea, C. E. Bauer, PpsR, a regulator of heme and bacteriochlorophyll biosynthesis, is a heme-sensing protein. *The Journal of biological chemistry* **287**, 13850-13858 (2012).

15. A. Winkler *et al.*, A ternary AppA–PpsR–DNA complex mediates light regulation of photosynthesis-related gene expression. *Nature Structural & Molecular Biology*, - (2013).

16. Y. Han, S. Braatsch, L. Osterloh, G. Klug, A eukaryotic BLUF domain mediates light-dependent gene expression in the purple bacterium Rhodobacter sphaeroides 2.4.1. *Proceedings of the National Academy of Sciences of the United States of America* **101**, 12306-12311 (2004).

17. Y. Han, M. H. F. Meyer, M. Keusgen, G. Klug, A haem cofactor is required for redox and light signalling by the AppA protein of Rhodobacter sphaeroides. *Molecular Microbiology* **64**, 1090-1104 (2007).

18. Z. Cheng, K. Li, L. a. Hammad, J. a. Karty, C. E. Bauer, Vitamin B12 regulates photosystem gene expression via the CrtJ antirepressor AerR in Rhodobacter capsulatus. *Molecular Microbiology*, n/a-n/a (2014).

19. O. V. Moskvin, S. Kaplan, M.-A. Gilles-Gonzalez, M. Gomelsky, Novel Heme-based Oxygen Sensor with a Revealing Evolutionary History. *Journal Of Biological Chemistry* **282**, 28740-28748 (2007).

20. O. V. Moskvin, M.-A. Gilles-Gonzalez, M. Gomelsky, The PpaA/AerR regulators of photosynthesis gene expression from anoxygenic phototrophic proteobacteria contain heme-binding SCHIC domains. *Journal of Bacteriology* **192**, 5253-5256 (2010).

21. A. Nahvi, J. E. Barrick, R. R. Breaker, Coenzyme B12 riboswitches are widespread genetic control elements in prokaryotes. *Nucleic acids research* **32**, 143-150 (2004).

22. A. Nahvi *et al.*, Genetic control by a metabolite binding mRNA. *Chemistry & biology* **9**, 1043-1049 (2002).

23. J. M. Ortiz-Guerrero, M. C. Polanco, F. J. Murillo, S. Padmanabhan, M. Elías-Arnanz, Light-dependent gene regulation by a coenzyme B12-based photoreceptor. *Proceedings of the National Academy of Sciences* **108**, 7565-7570 (2011).

24. W. R. Sistrom, A Requirement for Sodium in the Growth of Rhodopseudomonas spheroides. *Journal of General Microbiology* **22**, 778-785 (1960).

25. S. Masuda, C. E. Bauer, Null Mutation of HvrA Compensates for Loss of an Essential relA/spoT-Like Gene in Rhodobacter capsulatus. *Journal of Bacteriology* **186**, 235-239 (2004).

26. R. J. Penfold, J. M. Pemberton, An improved suicide vector for construction of chromosomal insertion mutations in bacteria. *Gene* **118**, 145-146 (1992).

27. S. R. Khan, J. Gaines, R. M. Roop, S. K. Farrand, Broad-Host-Range Expression Vectors with Tightly Regulated Promoters and Their Use To Examine the Influence of TraR and TraM Expression on Ti Plasmid Quorum Sensing. *Applied and Environmental Microbiology* **74**, 5053-5062 (2008).

28. P. G. Blommel, B. G. Fox, A combined approach to improving large-scale production of tobacco etch virus protease. *Protein Expression and Purification* **55**, 53-68 (2007).

29. A. Grote *et al.*, JCat: a novel tool to adapt codon usage of a target gene to its potential expression host. *Nucleic acids research* **33**, W526-W531 (2005).

30. L. Yin *et al.*, Redox and Light Control the Heme-Sensing Activity of AppA. *mBio* **4**, e00563-00513-e00563-00513 (2013).

31. L. Gomelsky *et al.*, Identification and in vivo characterization of PpaA, a regulator of photosystem formation in Rhodobacter sphaeroides. *Microbiology (Reading, England)* **149**, 377-388 (2003).

32. M. Gomelsky, S. Kaplan, appA, a novel gene encoding a trans-acting factor involved in the regulation of photosynthesis gene expression in Rhodobacter sphaeroides 2.4.1. *Journal of Bacteriology* **177**, 4609-4618 (1995).

33. M. Gomelsky, S. Kaplan, Molecular genetic analysis suggesting interactions between AppA and PpsR in regulation of photosynthesis gene expression in Rhodobacter sphaeroides 2.4.1. *Journal of Bacteriology* **179**, 128-134 (1997).

34. W. Schumacher, C. Holliger, A. J. B. Zehnder, W. R. Hagen, Redox chemistry of cobalamin and iron-sulfur cofactors in the tetrachloroethene reductase of Dehalobacter restrictus. *Febs Letters* **409**, 421-425 (1997).

35. M. Koutmos, S. Datta, K. A. Pattridge, J. L. Smith, R. G. Matthews, Insights into the reactivation of cobalamin-dependent methionine synthase. *Proceedings of the National Academy of Sciences* **106**, 18527-18532 (2009).

36. V. V. Yurkov, J. T. Beatty, Aerobic anoxygenic phototrophic bacteria. *Microbiology and molecular biology reviews : MMBR* **62**, 695-724 (1998).

37. S. Masuda, J. Berleman, B. M. Hasselbring, C. E. Bauer, Regulation of aerobic photosystem synthesis in the purple bacterium Rhodospirillum centenum by CrtJ and AerR. *Photochemical & photobiological sciences : Official journal of the*

European Photochemistry Association and the European Society for Photobiology **7**, 1267-1272 (2008).

Chapter 3 - Exploring The Role Of BLUF, LOV, Bacteriophytochrome, and PYP-Bacteriophytochrome Photoreceptors In *Rhodospirillum centenum* Using Transcriptomics

Summary

Genome sequencing of *Rhodospirillum centenum* has revealed the presence of four reading frames that encode for light sensing photoreceptors, specifically a PYP-bacteriophytochrome hybrid histidine kinase (Ppr), a bacteriophytochrome histidine kinase, a stand alone blue light using flavin (BLUF) domain, and a flavin binding light oxygen voltage (LOV)-histidine kinase protein. To identify the roles of these photoreceptors, we constructed in-frame gene deletions and then assayed these deletion strains for genome wide changes in RNA transcript abundance using next generation deep sequencing RNAseq technology. Our results indicate that Ppr functions as a global regulator controlling the expression of numerous metabolic genes as well as many genes that code for methyl accepting chemoreceptors (MCP's). On the other hand, deletion of the BLUF and bacteriophytochrome genes only led to expression changes in genes encoding the flagellar machinery. This indicates that the BLUF and bacteriophytochrome photoreceptors are dedicated to the control motility in response to light. Interestingly, deletion of the LOV-histidine kinase photoreceptor did not result in any significant changes in gene expression levels. This suggests that the LOV protein phosphorylates a target protein(s) that does not regulate gene expression and instead controls a downstream response. To our knowledge, this is the first reported genetic and genomic study of all

identified light photoreceptors in a purple anoxygenic photosynthetic bacterium. This study also illustrates how transcriptomics can be used as a facile tool for identifying functions of photoreceptors to guide further research.

Introduction

Over the last decade, it has become increasingly clear that light reception plays an important role in the regulation of many biological cellular processes. Indeed, sequences encoding light responsive proteins can be found in the Bacteria, Archaea and Eukarya domains where they control a wide variety of responses. For example, blue light-sensing BLUF proteins can control gene expression, phototaxis and cyclic nucleotide synthesis (c-di-GMP and cAMP) and are frequently found in bacteria with a few examples in algal cells (*1, 2*). Blue light absorbing LOV domains are present in a wide range of bacteria, archea, fungi, alga and plants and appear to control a variety of functions ranging from biofilm formation in bacteria to phototropism in plants (*3*). Cryptochromes are present in bacteria, archaea, plants and animals where they are involved in light driven DNA repair, the control of plant growth and development and the control of circadian rhythms (*4*). Phytochromes that contain a light absorbing GAF domain are present in many bacteria as well as in nearly all plants and algae where they typically function in light regulated signal transduction that controls gene expression in response to a wide range of wavelengths from blue to red light (*5-7*). Rhodopsins are present in bacteria, archaea and eukaryotes where they are involved in such diverse processes as phototaxis, photosynthesis, ion transport and vision (*8*).

Recent analyses of bacterial genome sequences show that the majority of available genomes code for at least one photoreceptor. In fact, one study found 22% of analyzed bacterial genomes contain both a phytochrome and a flavin-based (BLUF or LOV) photoreceptor sequence (*9*). The high frequency of these occurrences underscore that light sensing is a widespread feature of members of the bacterial domain. Despite the prominence of light absorbing photoreceptors, relatively little is known about the role individual photoreceptors play in regulating bacterial physiology, and importantly, why bacteria contain multiple photoreceptors many of which exhibit overlapping wavelength absorbance characteristics. Furthermore, light sensing GAF, BLUF, PYP and LOV domains appear to be rather "plastic" in that they can be present as stand alone domains or attached to a diverse array of effector output domains such as histidine kinase domains, di-cGMP synthases, nucleotidyl cyclases etc. (*9, 10*). As is the case of Ppr, there are also several examples of proteins that contain more than one type of photoreceptor domain allowing a protein to respond to multiple wavelengths of light.

Even though the presence of photoreceptors is nearly ubiquitous among bacterial species, there are only a few photoreceptors that are well characterized. For example, the BLUF domain containing protein AppA from *Rhodobacter sphaeroides* is known to function as blue light regulated antirepressor that controls the synthesis of the photosystem in response to light intensity (*11*). Additional bacterial BLUF photoreceptors have been shown to control di-cGMP levels and phototaxis (*12-14*). Only a few blue light-sensing LOV proteins have been characterized, the most notable being the LOV-histidine kinase LovK that regulates surface attachment of *Caulobacter crescentus* in response to light (*15*). In *Bacillus subtilis* the blue light-sensing LOV

protein YcfA regulates a light-dependent stress response although deletion of *ycfA* does not completely eliminate this pathway, suggesting a complex network involved in the process (*16*). Furthermore, integration of multiple light inputs has been found in the regulation of phototaxis in *Synechocystis*, where multiple light receptors including a cyanobacteriochrome (PixJ1) and a BLUF protein (PixD) have been found to play a role (*14, 17*).

The genome of the cyst-forming purple non-sulfur bacterium *Rhodospirillum centenum* is typical of many purple bacterial species as it encodes four different light absorbing photoreceptors (*18*). These photoreceptors are a blue light absorbing BLUF receptor, a LOV domain containing histidine kinase, a bacteriophytochrome comprised of PAS- GAF-PHY domains and a histidine kinase domain and the hybrid blue and red light absorbing bacteriophytochrome Ppr comprised of a PYP domain, a PAS-GAF-PHY domain and a histidine kinase domain (Figure 3.1). Of these proteins, only Ppr has been biochemically and genetically studied, although those studies have mostly focused on spectroscopic and structural properties of the PYP domain (*19*). As a result, little is known about the biological role of these photoreceptors in *R. centenum*.

To probe the roles of the multitude of photoreceptors in *R. centenum* we have utilized RNA-Seq technique that allows high-throughput genome wide sequencing of mRNA levels to obtain an overview of light regulated cellular responses at a transcriptional level (*20*). By comparing transcription levels of wild type and photoreceptor deletion strains under both light and dark conditions we were able to obtain roles for each of these photoreceptors *in vivo*.

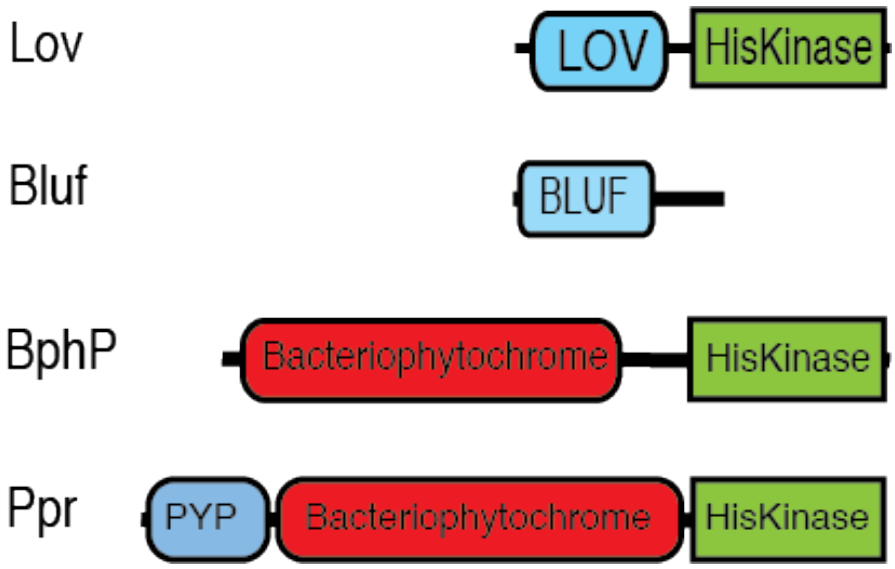

Figure 3.1 Domain architecture of the different light receptors in this study. HisKinase refers to a histidine kinase domain, Bacteriophytochrome indicates a PAS-GAF-PHY chromophore-binding domain).

Materials and Methods

Strains and culture conditions

E. coli strains were grown on LB medium. When appropriate, chloramphenicol was added to a final concentration of 30 μg/ml. *Rhodospirillum centenum* strains were cultured in CENS medium at 42^{o}C or 37^{o}C unless specified otherwise. Growth of *R. centenum* under controlled dark or illuminated conditions involved duplicate wild type and mutant cultures grown in 60 mL Pyrex test tubes containing 35 mL of CENS medium. To ensure sufficient aeration, the cultures were vigorously bubbled with air. The tubes were wrapped in aluminum foil and incubated in a water bath that was kept at 39^{o}C. When the cultures reached OD_{660} ~ 0.15 the aluminum foil was removed from one set of tubes and the cultures were exposed to incandescent light. After 1.5 hours (OD_{660} ~ 0.3) the cultures were quickly cooled in an ice water bath and cells were then harvested in 5 mL aliquots with cell pellets stored at -80^{o}C.

Deletion construction

The construction of the ppr deletion strain C145 has been previously described (*21*). Clean deletions for the remaining photoreceptor genes made using a previously reported double recombination technique (*22, 23*). In short, gene fragments of approximately 1 kb long containing 500 bp DNA flanking the targeted gene were amplified by crossover PCR with primers listed in Table 3.1. The PCR products were sequenced, subcloned into the gentamicin (Gm)-resistant pZJD29a suicide vector (*21*). The resulting constructs have the flanking regions and a short reading frame that replaces the original gene of interest. All constructed plasmids were confirmed by sequencing.

Suicide plasmids with correct sequences transformed into E. coli S-17(λpir). The *E. coli* strain was grown in LB medium with 10 μg/mL gentamycin) exponential phase, at which point 750 μL was harvested and washed 2 times with fresh CENS medium. The resulting pellet was resuspended in 750 μL overnight *R. centenum* culture (CENS) and pelleted again. The supernatant was removed and cells were then resuspended in 50 μL CENS and spotted onto CENS plates without antibiotics. The plates were incubated for 6 hours at 37^{o}C, after which the cells were streaked onto selective medium (CENS with 25 μg/mL kanamycin and 10 μg/mL gentamycin). Colonies were visible on the selective plates after incubation for 2 days at 42^{o}C. Several colonies were then restreaked onto selective medium, and subsequently on CENS with 5% sucrose. Mutants were screened for double crossover recombination events by patching colonies on both CENS and CENS with 10 μg/mL gentamycin. The genotypes of the mutants were confirmed by colony PCR.

Table 3.1 Primers used to construct suicide plasmids.

Target Gene	**Primer Name**	**Primer Sequence (5'-3')**
lov	1lov_sacIf	GGCGCTGAGCTCCGACGACATCGATGTCGAGGG
lov	2lov_crossr	TCAACGACGAGAATCGTGGCCCAGCATCTCCCGCTCCCGCAT
lov	3lov_crossf	ATGCGGGAGCGGGAGATGCTGGGCCACGATTCTCGTCGTTGA
lov	4lov_xbaIr	AATTCCCGCAGCAGGCGCGCCTCTAGACCGTGT
bluf	1bluf_sacIf	CTGGGCGAGCTCGACGCCCAACCCTGGAGGA
bluf	2bluf_crossr	CTACACCTCCACGAGGTTGTCGAGCAGCGCGTCGTCGGTCAT
bluf	3bluf_crossf	ATGACCGACGACGCGCTGCTCGACAACCTCGTGGAGGTGTAG
bluf	4bluf_xbaIr	GGGCGGTCTAGAGCTCGACCTGTCCGCGATC
bphP	1bphp_sacIf	CTATGTGAGCTCTCTCGTCCGCGGGATGGTC
bphP	2bphp_crossr	TCAGCCGTGCCATTGTAGCCGGACCTGGTCAATCACGTCCAC
bphP	3bphp_crossf	GTGGACGTGATTGACCAGGTCCGGCTACAATGGCACGGCTGA
bphP	4bphp_xbaIr	GCGGCCTCTAGAAAGGCGCGGCGGCATCTCT

RNAseq

Frozen cell pellets were resuspended in 350 μL TRI-Reagent (MRC, Inc.) and heated for 5 minutes at 95^{o}C. RNA was then extracted using the Direct-zol kit (Zymo Research) following the manufacturer's instructions. DNA contaminants were removed by digestion with DNaseI (NEB). To remove DNaseI the preps were cleaned up once more with the Direct-zol kit. Concentration of the RNA samples was determined using a NanoDrop spectrophotometer. The quality of the RNA preps was determined using the Bioanalyzer 2100 with RNA 6000 Nano chips (Agilent). High quality RNA was submitted to the University of Wisconsin Gene Expression Center for all library preparation and deep sequencing. Ribosomal RNA was removed using the RiboZero kit and libraries were constructed per standard protocols established at the UW Gene Expression Center. Sequencing was done using an Illumina HiSeq in 100 bp reads on single ends.

The sequencing reads were trimmed to a PHRED quality score of 30 using FASTQ Quality Trimmer on Galaxy (*24*). The resulting files were then aligned using BWA (version 0.7.5a-r405) and the number of reads per feature was calculated using HTSeq-count (version 0.5.4p5) (*25, 26*). The data was then further processed using DESeq (version 1.16.0) (*27*). For all steps default settings were used. For all comparisons mutants were compared to wild type cells grown under equal conditions (absence or presence of light).

For further analysis only genes that were expressed differentially with a p_{adj} value of 0.05 were considered. The results were not filtered for fold change in expression

levels. Selected genes were then assigned to COG categories (*28*) using the COG automatic classification tool on the MicroScope website (https://www.genoscope.cns.fr/agc/microscope/genomic/classifCOG.php?). The COG categories used are listed in Table 3.2. Unassigned genes were manually classified by similarity to homologous known proteins, or by identifying protein domains using Pfam. Assigning genes to multiple COG categories was avoided, as was assignment to categories indicating unknown functionality (COG classes R and S).

Table 3.2 COG assignments used in this study. Most genes were annotated using the automated annotation tool on the MicroScope website (see Methods). Where possible assignment to the R and S classes was avoided.

Process	**COG**	**Description**
Cellular processes and signaling	D	Cell cycle control, cell division, chromosome partitioning
	M	Cell wall/membrane/envelope biogenesis
	N	Cell motility
	O	Posttranslational modification, protein turnover, chaperones
	T	Signal transduction mechanisms
	U	Intracellular trafficking, secretion, and vesicular transport
	V	Defense mechanisms
	W	Extracellular structures
Information storage and processing	B	Chromatin structure and dynamics
	J	Translation, ribosomal structure and biogenesis
	K	Transcription
	L	Replication, recombination and repair
Metabolism	C	Energy production and conversion
	E	Amino acid transport and metabolism
	F	Nucleotide transport and metabolism

	G	Carbohydrate transport and metabolism
	H	Coenzyme transport and metabolism
	I	Lipid transport and metabolism
	P	Inorganic ion transport and metabolism
	Q	Secondary metabolites biosynthesis, transport and catabolism
Poorly characterized	R	General function prediction only
	S	Function unknown

Motility assays

To test for swimming motility cultures were grown overnight to log phase. Cells were concentrated 20 fold by pelleting and resuspending in fresh medium. 5 Microliter aliquots were spotted onto CENMED minimal medium (*29*), solidified with 0.25%(w/v) agar (Bacto-Agar). The plates were incubated at 42^{o}C for 48 hours. After incubation motility rates were determined by measuring the diameters of the colonies. Significance of different observations was determined using Welch's two-sample t-test in R.

Results

The Use Of RNA-Seq To Define Photoreceptor Function.

As is the case of many species, the role of individual photoreceptors is poorly defined in *R. centenum*. To characterize a role of individual photoreceptors, we constructed in-frame deletions of each of the photoreceptor genes *ppr*, *bluf*, *lov*, and *bphP*. Strains that contained individual photoreceptor deletions were initially grown aerobically in the dark and then split into duplicate cultures one that remained in the dark and the other was illuminated with approximately 80 μE/m^2/s of white light. After a 90-minute incubation period triplicate biological replicates of these cultures were chilled in an ice water bath, harvested by centrifugation and then extracted for RNA that was analyzed for expression levels using RNA-Seq technology. Briefly, (details are provided in Methods) the RNA was first depleted of rRNA, converted to cDNA and then used for

library construction and analyzed for copy number using a Hiseq2000 deep sequencing platform. An average of 13.5 million RNA-Seq reads were obtained per sample with 97.2% mapped to the genome of *R. centenum*. This data set resulted in an average of 300-fold coverage per nucleotide. Genes were considered differentially expressed with a false-discovery-rate (p_{adj}) less than 0.05. The sections below discuss the identification and analysis of genes that were differentially expressed as a consequence of deletion of individual photoreceptors. To facilitate analysis and discussion individual genes were categorized into one of 20 unique "clusters of orthologous groups" (COG) (Table 3.2).

The Δlov strain shows no changes in expression levels

Expression profiles in the Δ*lov* strain showed no difference from the wildtype strain. The LOV protein encoded by *lov* has to our knowledge not been studied *in vitro* and is therefore not confirmed to be a true light receptor. This protein does however contain the signature motif with the conserved cystein that forms a covalent bond with the flavin group upon light excitation (*30*). It is possible that this Lov protein does not play a role under the conditions tested here. A similar pattern was reported for YtvA in *Bacillus subtilis* where an effect of deleting *ytvA* was only observable when a light impulse was combined with salt stress (*16*). It is well possible that Lov plays a role in a similar multidimensional regulation mechanism.

Directly upstream of *lov* is a partially overlapping reading frame encoding a single domain response regulator. While most response regulators contain output domains, a substantial group of response regulators lack these output domains. These response regulators are thought to act on other proteins or to play a phosphorelay role

(*31*). This fits the hypothesis that Lov is part of a signaling cascade with multiple sensory inputs. Alternatively Lov may be part of a phototaxis signaling pathway: *R. centenum* shows negative phototaxis in blue-green light (λ<600 nm). Typical LOV photoreceptors however sense blue light (λ=450 nm) while the strongest negative phototaxis response was observed between 550 and 660 nm (*32*).

Bluf And BphP Share Many Differentially Expressed Genes

Analysis of differentially expressed genes in the Δ*bluf* data set and in the Δ*bphB* data set showed a remarkable overlap in the number and type of differentially expressed genes (DEGs) are caused by deletion of these different photoreceptors (Figure 3.2). Collectively there are a total of 17 DEGs present in the Δ*bluf* light and dark data sets. Interestingly, all of the BLUF DEGs are also present in the Δ*bphB* dark and light data sets indicating that there is a complete overlap in the genes that are affected by these very different photoreceptors. As shown in the Venn diagram in Figure 3.2, there are an additional 16 genes present in the Δ*bphB* data set that are not present in the Δ*bluf* data set so the number of genes regulated by the BphP photoreceptor is nearly double that of the BLUF photoreceptor.

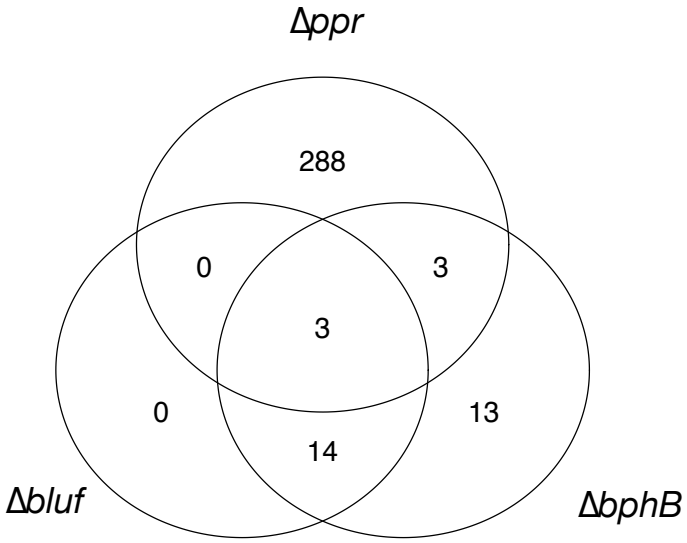

Figure 3.2 Overlap of differentially expressed genes in the data sets (not to scale). The diagram shows how the Δbluf dataset completely overlaps with the ΔbphB dataset, whereas in the Δppr data set only six genes were also identified in the other datasets.

Table 3.3 Overlapping differentially expressed genes in the bluf and bphB deletion strains. All numbers represent log2 fold change expression. (ns; not significant; FGC4: flagellar gene cluster 4; cgrE: gene cluster upstream of the CRP homolog cgrE)

		Δ*bluf*		Δ*bphB*	
Role	**Gene**	**Dark**	**Light**	**Dark**	**Light**
FGC4	*flgF*	2.44	2.15	3.18	2.5
	flgG	ns	2.41	3.28	3.02
	flgA	3.3	3.07	3.21	2.95
	flgH	ns	ns	2.87	2.23
	flgI	ns	ns	2.74	2.99
	cheL	ns	ns	3.13	3.3
	RC1_1395	ns	2.21	ns	3.82
	fliK	ns	2.38	2.93	4.04
	flgD	2.54	2.21	3.53	2.48
	RC1_1399	2.05	1.62	2.9	ns
FGC5	*flgE*	2.74	2.25	3.33	2.11
	flgK	2.98	2.58	3.48	2.45
	flgL	2.57	2.21	3.2	2.34
C-di-GMP	RC1_1539	ns	2.25	2.2	3.62
SLT	RC1_1631	1.89	2.21	2.72	3.5
cGMP	RC1_3784	ns	-1.99	ns	-2.33
	RC1_3785	-3.07	ns	-3.48	ns
	RC1_3786	-2.48	ns	-2.6	-2.51

	RC1_3787	-2.45	ns	-2.67	ns

Analysis of the 17 DEG that are present in both the BLUF and BphP data sets indicate that half comprise flagellar structural genes (Table 3.3). *R. centenum* exhibits two forms of motility; swimming motility in liquid and swarming on a solid surface (*33*). Swimming motility depends on a single polar flagellum, while swarming motility is powered by multiple lateral flagella (*34*). Previous studies have shown that polar and lateral flagella are coded by separate sets of structural genes (*18, 35*). The genome of *R. centenum* contains 5 flagellar gene clusters (FGC) with the largest FGC1 containing all genes needed to encode a complete lateral flagellum (*18*). The remaining four smaller FGC's contain structural genes for the polar flagellum (*18, 32, 35*). The flagellar DEGs affected by both the BLUF and BphP photoreceptors (*flgF*, *flgG*, *flgA*, *fliK*, *flgD*, *flgE*, *flgK* and *flgL*) are all structural components of the basal body and hook indicating that these photoreceptors affect synthesis of early components of the flagella. These DEGs are all present in the smaller polar FGC4 (*flgF*, *flgG*, *flgA*, *fliK*, *flgD*, RC1_1399) and polar FGC5 (*flgE*, *fliK* and *flgL*) indicating that they affect synthesis of the polar flagellum used for swimming motility. Furthermore, the flagellar expression levels are ~4-6 fold higher in the wild type cells relative to the Δ*bluf* and Δ*bphB* data sets indicating that these photoreceptors are involved in enhancing polar flagellum expression. While light effects on expression are modest, in 7 of 8 cases the polar flagellum gene expression levels are higher in the dark than in the light indicating that light excitation may impede polar flagellum synthesis.

Bluf and BphB both also appear to play a role in regulating intracellular c-di-GMP levels as a GGDEF protein coded by RC1_1539 was found to be upregulated under both dark and light conditions (Table 3.3). GGDEF proteins catalyze the formation of c-

di-GMP from GTP. Cyclic-di-GMP levels are known to regulate a number of processes including motility, cell differentiation and biofilm formation. The majority of BLUF proteins are single domain proteins, similar to the BLUF protein studied here however, the single BLUF domain protein PapB from *Rhodopseudomonas palustris* was found to regulate c-di-GMP levels through an interaction with the phosphodiesterase PapA (*13*). Exposure of the PapBA complex to blue light leads to an increase of c-di-GMP hydrolysis activity. A similar activity is found in BlrP1 from *Klebsiella pneumonia* where there is a fusion of a BLUF domain with an EAL domain (*12*). In fact a recent study showed that 40% of multi-domain proteins that contain at least one BLUF domain also contain a GGDEF or EAL domain (*9*). This suggests that many BLUF domains are involved in light regulation of c-di-GMP levels. BphB on the other hand sports a histidine kinase domain and therefore it likely utilizes a different mechanism promote the same outcome.

Several genes thought to be involved in cGMP production (*gcyB* encoded by RC1_3786 and *gcyC* encoded by RC1_3787) are expressed ~4 to 5-fold lower in the Δ*bluf* and Δ*bphP* mutants under both light and dark conditions. Cyclic-GMP plays a key regulatory role in initiating cyst cell encystment, which is a developmental process that occurs when cells are faced with nutrient starvation or desiccation (*36-38*). Deletion of *gcyB* or *gcyC* (resp. RC1_3786 and RC1_3787) result in loss of cGMP production and are thought to code for subunits of a guanylyl cyclase enzyme complex (*38*). The expression of short reading frames RC1_3784 and RC1_3785 which are located just upstream of *gcyB* and *gcyC* were found to be expressed ~5 to 6.5-fold lower in the BLUF and BphP mutants. RC1_3784 features a ribbon-helix-helix (RHH4) domain, which may

act as a DNA-binding motif. Expression of RC1_3784 is downregulated under both light and dark conditions in the *bluf* or *bphB* knockout, but only under light conditions is this effect significant. Finally, expression of the CgrA transcription factor coded by RC1_3788 that binds cGMP to regulate cyst development gene expression, is also 2 to 3-fold lower in the BphP strain under light conditions (Table 3.4).

There are several hypothetical genes that are co-regulated by Bluf and BphB with the most notable being RC1_1631 that is upregulated in both mutant strains. RC1_1631 encodes a hypothetical protein with some similarity to a transglycosylase domain. These lysozyme-like domains are thought to play a role in remodeling of the peptidoglycan layer and may be important for transport processes (*39, 40*). Whether or not RC1_1631 actually has transglycosylase activity remains to be studied

Differentially Expressed Genes Unique To The BphP Knockout

In the Δ*bphB* mutant six ORFs encoding transposases were upregulated in both dark and light conditions (RC1_0483, RC1_1690, RC1_1730, RC1_1731, RC1_2731 and RC1_3675). RC1_1690 and RC1_1731 share strong sequence similarity with each other. The other four share strong sequence similarity among themselves, where RC1_1730 seems to be N-terminally truncated. In total 6 transposases were upregulated under both light and dark conditions (Table 3.4). Of these transposases 4 are almost identical to each other, while the other two are similar to one another (Figure 3.3). While transposases are abundant in bacterial genomes their regulation is thought to be tightly controlled in order to prevent genome damage (*41*). Transpose genes were also found to be upregulated in bacteria colonizing the rhizosphere (*42, 43*). Genetic reorganizations during root

colonization have been found in several *Azospirillum* species, and possibly constitute a regulation mechanism (*44*).

Table 3.4 Differentially expressed genes unique to the ΔbphB mutant.

Gene	**Dark (LFC)**	**Light (LFC)**	**Description**
RC1_1630	ns	2.48	FAD linked oxidase, putative
RC1_1731	1.64	1.44	transposase
RC1_1690	3.04	2.05	transposase
RC1_3675	2.65	2.29	transposase
RC1_0483	3.25	2.7	transposase
RC1_2731	3.82	3.64	transposase
RC1_1730	3.94	3.79	transposase
RC1_0033	ns	-1.22	hypothetical protein
RC1_3219	ns	-1.17	hypothetical protein
RC1_2141	ns	-1.09	hypothetical protein
RC1_3444	ns	1.1	hypothetical protein
RC1_0671	ns	1.48	hypothetical protein

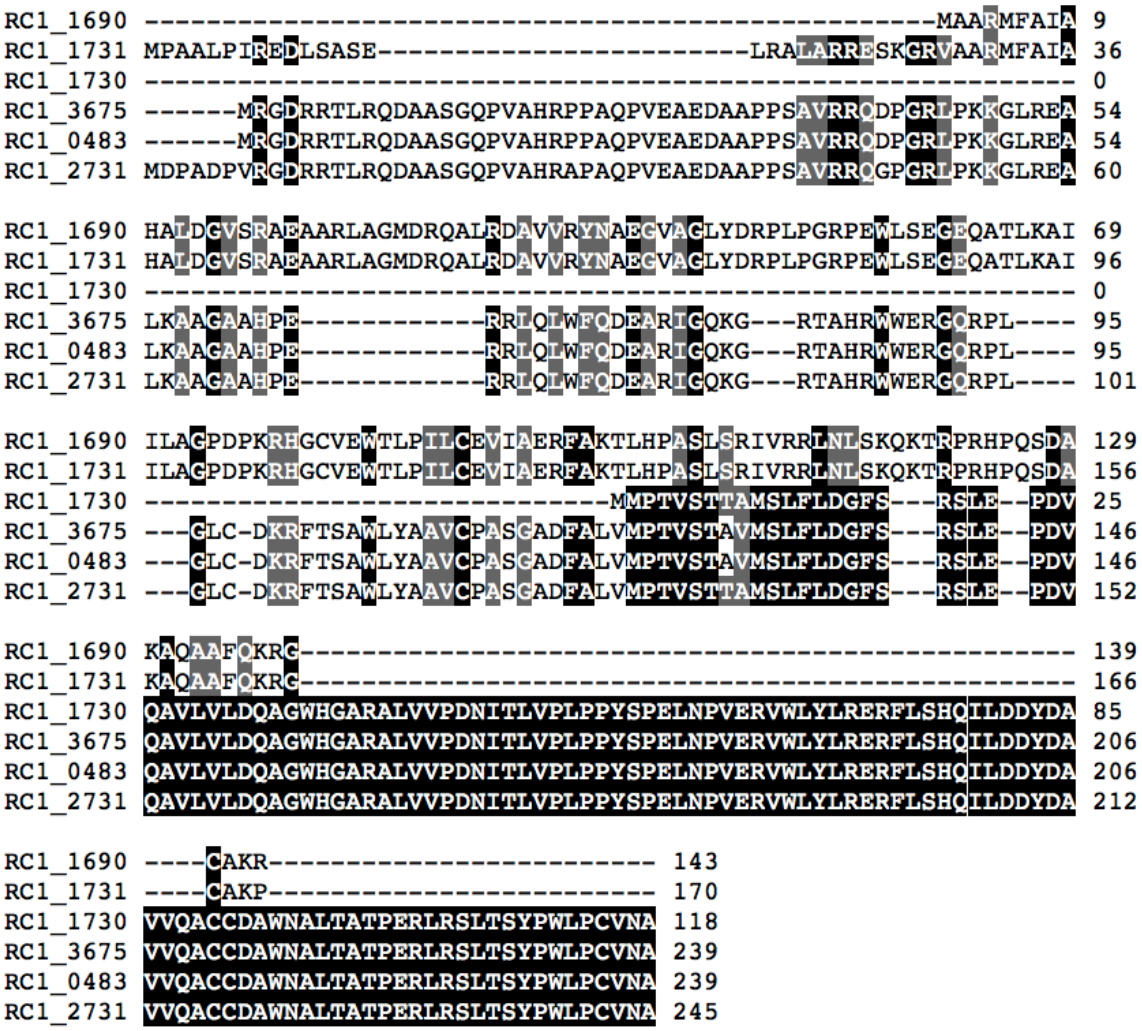

Figure 3.3 Alignment of transposases that were found to be upregulated in the ΔbphB mutant. The transposases are nearly identical to one another.

ppr knockout

The *ppr* knockout shows large changes in expression compared to the wildtype under both dark and light conditions. In total 294 genes were found to be expressed differentially under light and dark conditions combined. Under dark conditions 28 genes were differentially expressed and 286 under light conditions (Figure 3.4). Under light conditions a large number of genes showed moderate changes in expression (less than 2-fold change), while under dark conditions all changes are larger than 2-fold (Figure 3.5). Under dark conditions the deletion of *ppr* mostly affected motility and signal transductions genes, while under light conditons transcriptional responses across a wide range of functionalities were found (Figure 3.6). The differentially expressed genes show little overlap with genes expressed differentially in either Δ*bluf* of Δ*bphB* mutant (Figure 3.2).

Of the light receptors studied here only the function of Ppr has been established. Previously it had been shown that light exposure causes a Ppr-dependent increase in expression of the chalcone synthase ChsA (*21*). ChsA is strongly upregulated during the encystment process and may play a key role in this process (*45*). Expression levels are elevated in the presence of infrared light, while addition of blue or white light repressed expression. In our results the expression of *chsA* is not significantly affected in the Δ*ppr* strain regardless of illumination conditions. It is possible that the light source used in our study provides insufficient infrared light for activation of Ppr.

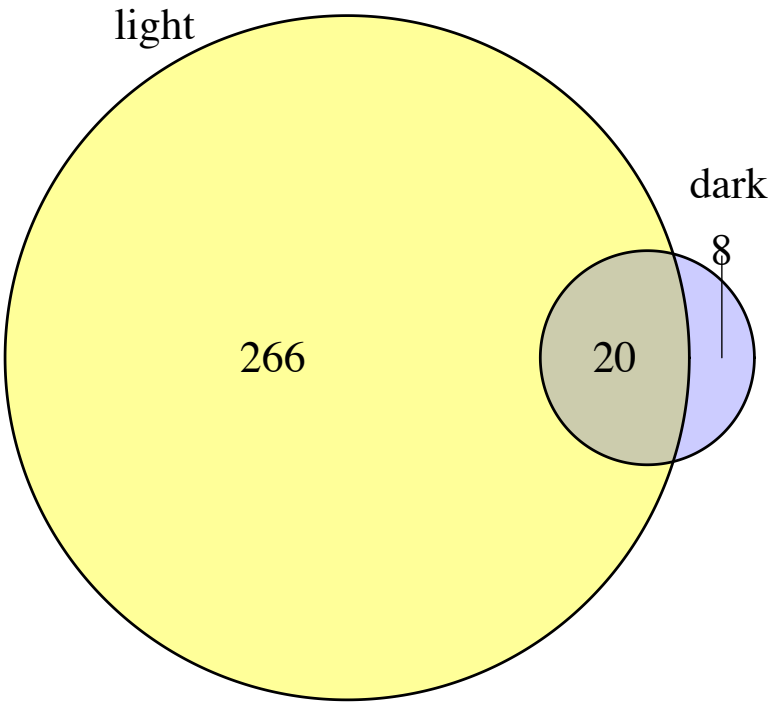

Figure 3.4 Overlap of Δppr light and dark datasets. A total of 294 genes was found to be differentially expressed in the Δppr mutant. Exposure to light increased the difference between the wildtype and mutant strain.

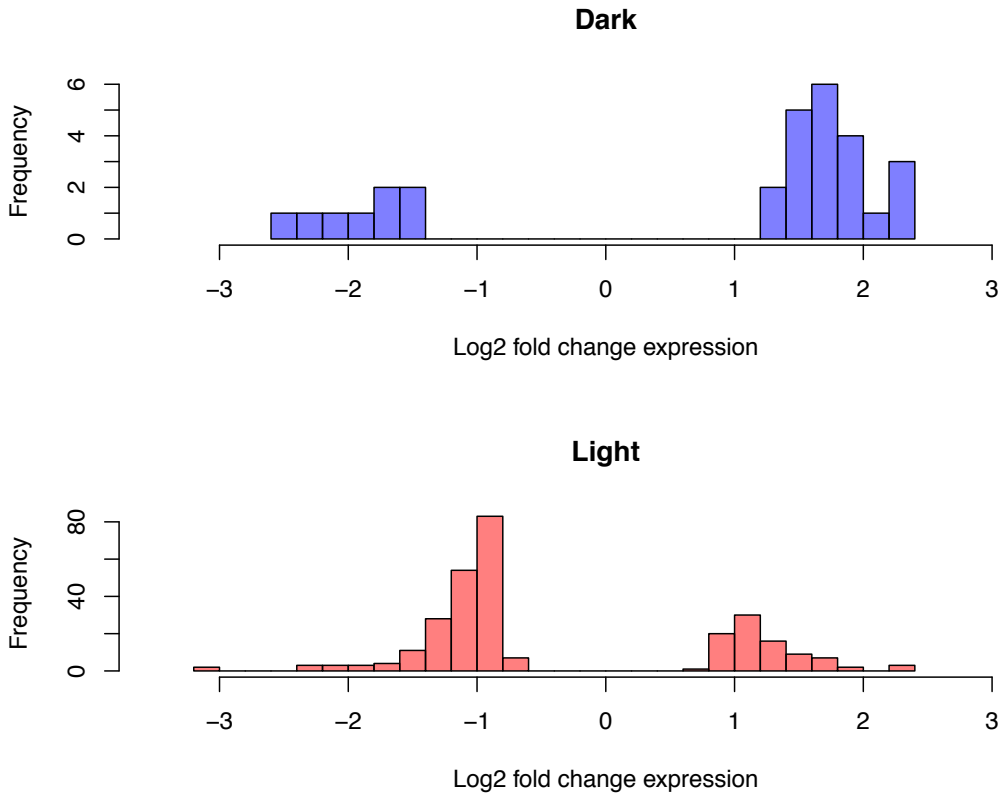

Figure 3.5 Histograms showing the distribution of log2 fold changes in expression under dark and light conditions. Under light conditions expression more repressed. Interestingly a large portion appears to be moderately affected (less or equal to a 2-fold change in expression).

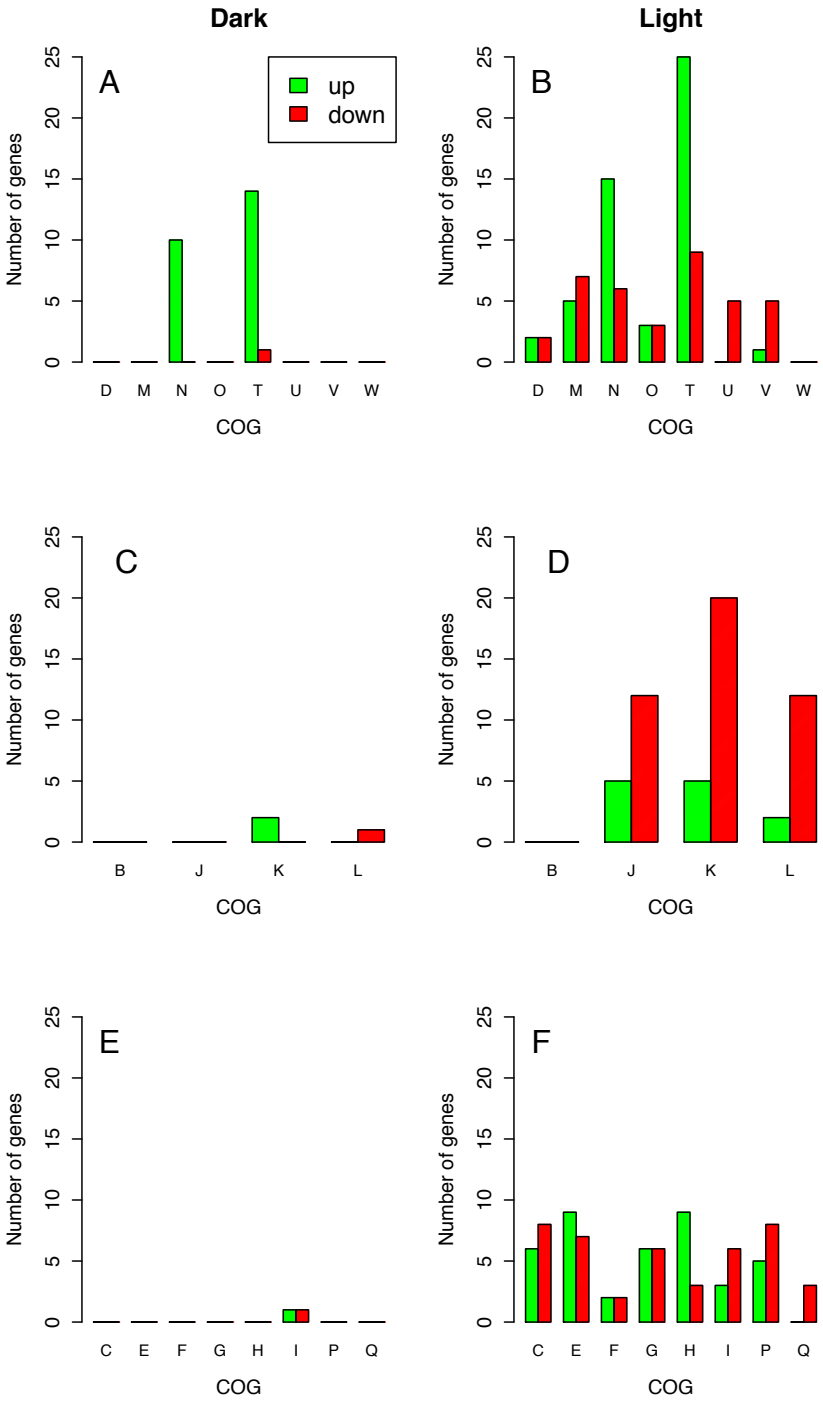

Figure 3.6 Functional categories and the direction of the changes in expression levels under dark (A,C,E) or light conditions (B,D,F). (A,B) Cellular processes, (C,D) information storage and processing, (E,F) metabolism. The letters indicate the different COG categories.

Large portions of the differentially expressed genes play a role in signal transduction (37 out of 294 genes). Under dark conditions 15 genes were upregulated and none were down regulated, while under light conditions 25 genes were upregulated and expression of 9 genes was repressed. Fifteen out of 32 MCP homologs encoded in the genome were upregulated under dark or light conditions (Table 3.5). With the exception of RC1_0327 all were upregulated under both light and dark conditions. The group of MCPs include five small single MCP domain proteins, two aerotaxis MCPs and several MCPs predicted to sense extracellular ligands (CACHE, 4HB_MCP1 and CHASE2 domains). A histidine kinase annotated as *divJ* was also upregulated, closer inspection revealed that this histidine kinase does contain an extracellular CHASE4 domain, indicating a role in sensing extracellular ligands.

Not surprisingly, the regulation of transcription is greatly affect by the deletion of ppr. Under dark conditions two transcriptional regulators were significantly upregulated, RC1_1405 and RC1_0848. These two transcription regulators were also upregulated under light conditions. No transcriptional regulators were found to be downregulated under dark conditions. A number of transcription regulators and DNA binding proteins is expressed differentially in the Δ*ppr* mutant under light conditions (Table 3.6). With a few exceptions all were downregulated. Unfortunately none of these transcription regulators have been studied before, and nothing is known about their target sequences.

Deletion of *ppr* has a pronounced effect on the expression of a substantial set of genes involved in various aspects of metabolism. Genes found are predicted to play a role in a wide range of processes. Typically the differential expression show smaller fold changes in expression and higher false discovery rates (p_{adj}). This suggests more noise

and it is likely that these observations are due to indirect effects. One interesting aspect about this category is the presence of a number of transporters (Table 3.7). Most notable is the strong downregulation of *atoE*, a gene encoding a short fatty acid transporter. Presence of the four-carbon fatty acid butyrate promotes encystment (*46*). Since deletion of *ppr* seems to inhibit cyst formation (*22*) it is tempting to speculate that AtoE plays a key role in this process. While the genes found here are only a fraction of the transporters encoded in the genome it does show a shift in how *R. centenum* interacts with its surroundings. What the meaning of this shift is remains a question and requires further study.

Deletion of *ppr* caused changes in the expression levels of a large number of genes. The broad range of gene functionalities represented in this gene set suggests that *ppr* acts as a master life style regulator. Most of the DEGs found play a role in signal transduction or motility. Thus it is likely that these changes in turn could result in a multiplication of the effects, thus increasing the impact of *ppr* deletion. At this point no cognate response regulator is known for Ppr, and more work will be needed to reveal the initial events leading to the large changes found.

Table 3.5 Differentially expressed MCP homologues in the ppr mutant. (Abbreviations: LFC: log2 fold change expression; ns: not significant). CACHE, CHASE3 and 4HB_MCP1 domains mostly likely sense environmental signals. Aer2 and Aer3 are homologs of the E. coli aerotaxis MCP Aer.

Gene	**Dark (LFC)**	**Light (LFC)**	**Domain architecture**
RC1_0295	2.21	1.59	CACHE-HAMP-MCP
RC1_0297	1.63	1.17	MCP
RC1_0327	1.33	ns	PAS-PAS-MCP
RC1_0354	ns	1.10	MCP
RC1_0477	1.79	0.87	4HB_MCP1-HAMP-MCP
RC1_0540	1.41	0.89	4HB_MCP1-HAMP-MCP
RC1_0872	1.68	0.79	MCP
RC1_1179	1.47	1.12	HAMP-MCP
RC1_2174	ns	1.19	MCP
RC1_2261	NS	1.31	MCP
RC1_2697	1.68	1.43	HAMP-MCP
RC1_3024	1.73	1.09	CACHE-HAMP-MCP
aer2	ns	0.93	MCP-PAS
aer3	ns	0.97	MCP-PAS
RC1_4093	1.92	1.35	CHASE3-HAMP-MCP

Table 3.6 Transcription/two-component related genes that are expressed differentially in the Δppr mutant.

Gene	**Dark (LFC)**	**Light (LFC)**	**Domain architecture**
RC1_0848	ns	1.86	RR-HTH
RC1_0849	2.22	2.23	RR-HTH
RC1_1405	1.86	1.57	RR-HTH
agmR1	ns	-0.88	RR-HTH
narL	ns	-0.92	HTH-RR
RC1_1368	ns	-1.34	RR
RC1_2399	ns	1.11	RR
RC1_1779	ns	1.14	RR-HPt
RC1_1473	ns	-0.88	HK
barA	ns	1.70	GAF-2PAS-HK
pleC2	ns	1.15	PAS-HK
divJ3	ns	-0.89	HK
divJ4	ns	1.29	CHASE4-PAS4_HK
dksA	ns	-0.94	dksA/traR C4-type zinc finger

Table 3.7 Genes encoding transport proteins. With the exception of atoE, RC1_3440 and RC1_3441 expression of these genes was only moderately affected.

Gene	**Dark (LFC)**	**Light (LFC)**	**Description**
atoE	-2.17	-3.17	short chain fatty acid transporter, putative
RC1_2482	ns	1.01	long chain fatty acid transporter, putative
RC1_0027	ns	-1.09	TonB-dependent receptor, putative
RC1_1174	ns	0.83	TonB-dependent copper receptor, putative
RC1_3738	ns	-1.04	TonB-dependent receptor, putative
RC1_1200	ns	-0.75	outer membrane protein, putative
eamA	ns	-1.03	amino acid metabolite efflux pump, probable
RC1_1511	ns	-0.97	amino acid metabolite efflux pump, probable
RC1_1513	ns	1.5	amino acid permease, putative
RC1_3440	ns	2.24	outer membrane autotransporter barrel domain protein
RC1_3441	ns	2.27	efflux transporter component, putative

Swim assays

To test whether increase in expression of motility genes does indeed lead to an increase in motility I performed swim assays. Cells were grown for 48 hours on semi-solid agar plates. The resulting colonies all showed a dark red core of high cell density with an fainter aura emanating from the core. The cells showed little difference in motility when incubated under dark or light conditions (data not shown). This compares to the findings of the RNA-seq data that showed similar differential expression levels under both dark and light conditions. Both Δ*bluf* and Δ*ppr* strains showed a significant increase in swimming motility ($p<<0.05$, Welch two-sample t-test) while the Δ*lov* an Δ*bphB* strains showed no significant changes ($p=0.3687$ and $p=0.2525$ resp.) (Figure 3.7). Despite the similarities in expression levels the phenotypes of Δ*bluf* and Δ*bphB* are strikingly different. This shows that motility cannot be explained by expression levels of motility genes alone. The Δ*ppr* mutant showed a downregulation of a different set of motility genes.

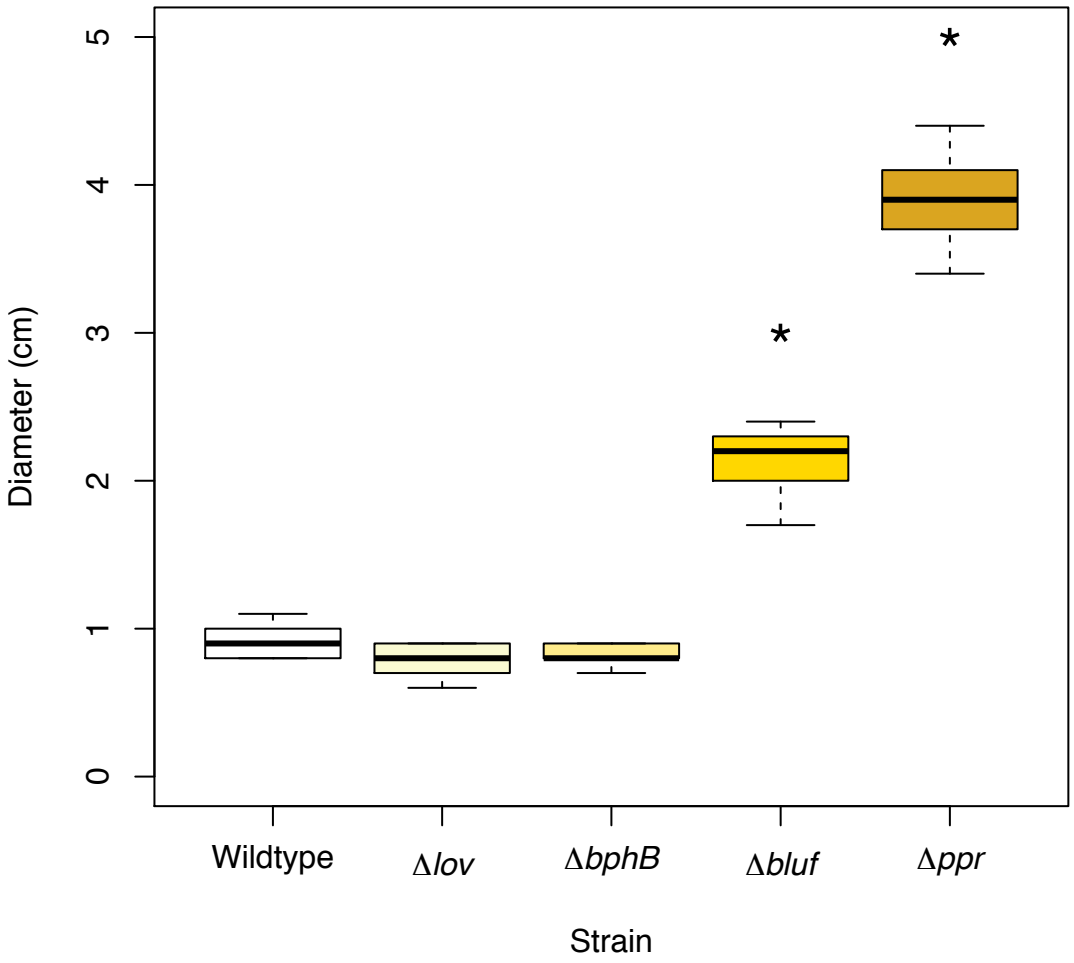

Figure 3.7 Swimming activity of the different strains. All swimming assays were done in triplicate, with a total of 21 observations per strain. Both bluf and ppr knockouts show a significant increase in swimming motility (* Student's t-test $p << 0.05$). The lov and bphB mutants show a decrease in motility compared to the wildtype (Student's t-test $p < 0.01$), although also in the wildtype very little spreading beyond the growth zone was observed.

Discussion

Here I described the use of transcriptomics to identify the role of different light receptors in *R. centenum*. One of the most surprising findings is that Bluf and BphB appear to regulate the same processes, despite the differences in the wavelength of light they sense and their output domains. Both Bluf and BphB appear to play a role in the regulation of flagellum biosynthesis, although in motility assays these mutants showed quite different phenotypes. The regulons of Lov and Ppr were less clear: either no differences in transcription levels were found (in the case of Lov), or wide-ranging changes were found (Ppr). The large changes in the Δ*ppr* mutant indicate that Ppr acts as a master regulator for several processes.

This study is to my knowledge also the first time all light receptors of an organism were deleted and tested for their function. Light receptors have been proposed as key regulators for life style adaptations (*47*). Light has been shown to impact the formation of biofilms in several species. In *Acinetobacter baumanni* for example blue light represses the formation of biofilms (*48*). A similar response was seen in *Idiomarina loihiensis*, even though this bacterium is mainly found in deep-sea enviroments (*49*). In contrast *Caulobacter crescentus* increases the formation of cell aggregates upon exposure to blue light (*15*). Light exposure also increased the shift from free living to pathogenicity in both *A. baumanni* and *Brucella abortis* (*48, 50*). Recently Ppr was shown to be implicated in the encystment process, perhaps an even more dramatic life style change than biofilm formation (*22*). Although more studies are needed, the data presented here supports the hypothesis that Ppr controls life style changes in *R. centenum*. Similarly,

Bluf appears to promote motility. Whether biofilm formation is regulated by these light receptors remains a question.

The life style changes mentioned above are gross phenotypes and provide little insight in the molecular mechanism behind these adaptations. Application of transcriptomics may provide insights in these processes. Recent application of RNA-seq to studies of the process of rice root colonization by *Azospirillum lipoforum* 4B or infection of the chicken cecum with *Campylobacter jejuni* showcase the potential of RNA-seq to reveal cellular responses to new conditions (*42, 51*). Like the study presented here these studies don't provide insight in the details of the regulation processes involved, but they do provide valuable insights that will benefit hypothesis generation.

References

1. M. Gomelsky, G. Klug, BLUF: a novel FAD-binding domain involved in sensory transduction in microorganisms. *Trends in Biochemical Sciences* **27**, 497-500 (2002).
2. S. Masuda, Light Detection and Signal Transduction in the BLUF Photoreceptors. *Plant and Cell Physiology* **54**, 171-179 (2013).
3. U. Krauss *et al.*, Distribution and Phylogeny of Light-Oxygen-Voltage-Blue-Light-Signaling Proteins in the Three Kingdoms of Life. *Journal of Bacteriology* **191**, 7234-7242 (2009).
4. I. Chaves *et al.*, The Cryptochromes: Blue Light Photoreceptors in Plants and Animals. *Annu. Rev. Plant Biol.* **62**, 335-364 (2011).
5. M. E. Auldridge, K. T. Forest, Bacterial phytochromes: More than meets the light. *Critical Reviews in Biochemistry and Molecular Biology* **46**, 67-88 (2011).
6. B. Karniol, J. Wagner, J. Walker, R. Vierstra, Phylogenetic analysis of the phytochrome superfamily reveals distinct microbial subfamilies of photoreceptors. *Biochemical Journal* **392**, 103-116 (2005).
7. N. C. Rockwell, J. C. Lagarias, A brief history of phytochromes. *Chemphyschem : a European journal of chemical physics and physical chemistry* **11**, 1172-1180 (2010).
8. J. L. Spudich, The multitalented microbial sensory rhodopsins. *Trends in Microbiology* **14**, 480-487 (2014).

9. C. Mandalari, A. Losi, W. Gärtner, Distance-tree analysis, distribution and co-presence of bilin- and flavin-binding prokaryotic photoreceptors for visible light. *Photochemical & photobiological sciences : Official journal of the European Photochemistry Association and the European Society for Photobiology* **12**, 1144-1157 (2013).

10. T. E. Meyer *et al.*, The growing family of photoactive yellow proteins and their presumed functional roles. *Photochemical & Photobiological Sciences* **11**, 1495-1514 (2012).

11. M. Gomelsky, S. Kaplan, Molecular genetic analysis suggesting interactions between AppA and PpsR in regulation of photosynthesis gene expression in Rhodobacter sphaeroides 2.4.1. *Journal of Bacteriology* **179**, 128-134 (1997).

12. T. R. M. Barends *et al.*, Structure and mechanism of a bacterial light-regulated cyclic nucleotide phosphodiesterase. *Nature* **459**, 1015-1018 (2009).

13. T. Kanazawa *et al.*, Biochemical and Physiological Characterization of a BLUF Protein−EAL Protein Complex Involved in Blue Light-Dependent Degradation of Cyclic Diguanylate in the Purple Bacterium Rhodopseudomonas palustris. *Biochemistry* **49**, 10647-10655 (2010).

14. K. Okajima *et al.*, Biochemical and functional characterization of BLUF-type flavin-binding proteins of two species of cyanobacteria. *Journal of Biochemistry* **137**, 741-750 (2005).

15. E. Purcell, D. Siegal-Gaskins, D. Rawling, A. Fiebig, S. Crosson, A photosensory two-component system regulates bacterial cell attachment. *Proceedings of the*

National Academy of Sciences of the United States of America **104**, 18241-18246 (2007).

16. M. Avila-Pérez, K. J. Hellingwerf, R. Kort, Blue light activates the sigmaB-dependent stress response of Bacillus subtilis via YtvA. *Journal of Bacteriology* **188**, 6411-6414 (2006).
17. S. Yoshihara, F. Suzuki, H. Fujita, X. X. Geng, M. Ikeuchi, Novel putative photoreceptor and regulatory genes required for the positive phototactic movement of the unicellular motile cyanobacterium Synechocystis sp PCC 6803. *Plant and Cell Physiology* **41**, 1299-1304 (2000).
18. Y.-K. Lu *et al.*, Metabolic flexibility revealed in the genome of the cyst-forming alpha-1 proteobacterium Rhodospirillum centenum. *BMC Genomics* **11**, 325 (2010).
19. J. Kyndt, T. Meyer, M. Cusanovich, Photoactive yellow protein, bacteriophytochrome, and sensory rhodopsin in purple phototrophic bacteria. *Photochemical & Photobiological Sciences* **3**, 519-530 (2004).
20. N. J. Croucher, N. R. Thomson, Studying bacterial transcriptomes using RNA-seq. *Current Opinion in Microbiology* **13**, 619-624 (2010).
21. Z. Jiang *et al.*, Bacterial Photoreceptor with Similarity to Photoactive Yellow Protein and Plant Phytochromes. *Science (New York, NY)* **285**, 406-409 (1999).
22. K. He, Indiana University, (2013).
23. S. Masuda, J. Berleman, B. M. Hasselbring, C. E. Bauer, Regulation of aerobic photosystem synthesis in the purple bacterium Rhodospirillum centenum by CrtJ and AerR. *Photochemical & photobiological sciences : Official journal of the*

European Photochemistry Association and the European Society for Photobiology **7**, 1267-1272 (2008).

24. D. Blankenberg *et al.*, Manipulation of FASTQ data with Galaxy. *Bioinformatics (Oxford, England)* **26**, 1783-1785 (2010).

25. H. Li, R. Durbin, Fast and accurate long-read alignment with Burrows-Wheeler transform. *Bioinformatics (Oxford, England)* **26**, 589-595 (2010).

26. S. Anders, P. T. Pyl, W. Huber, HTSeq–A Python framework to work with high-throughput sequencing data. *Bioinformatics (Oxford, England)* **31**, 166-169 (2015).

27. S. Anders, W. Huber, Differential expression analysis for sequence count data. *Genome Biology* **11**, R106 (2010).

28. R. L. Tatusov *et al.*, The COG database: an updated version includes eukaryotes. *BMC Bioinformatics* **4**, 41 (2003).

29. J. Favinger, R. Stadtwald, H. Gest, *Rhodospirillum centenum, sp. nov.*, a thermotolerant cyst-forming anoxygenic photosynthetic bacterium. *Antonie Van Leeuwenhoek Journal of Microbiology* **55**, 291-296 (1989).

30. J. Herrou, S. Crosson, Function, structure and mechanism of bacterial photosensory LOV proteins. *Nature Reviews Microbiology* **9**, 713-723 (2011).

31. M. Y. Galperin, Diversity of structure and function of response regulator output domains. *Current Opinion in Microbiology*, (2010).

32. L. Ragatz, Z. Y. Jiang, C. E. Bauer, H. Gest, Macroscopic phototactic behavior of the purple photosynthetic bacterium Rhodospirillum centenum. *Archives of Microbiology* **163**, 1-6 (1995).

33. D. Nickens, C. J. Fry, L. Ragatz, C. E. Bauer, H. Gest, Biotype of the purple nonsulfur photosynthetic bacterium, Rhodospirillum centenum. *Archives of Microbiology* **165**, 91-96 (1996).

34. L. L. McCarter, Dual Flagellar Systems Enable Motility under Different Circumstances. *Journal of Molecular Microbiology and Biotechnology* **7**, 18-29 (2004).

35. J. McClain, D. R. Rollo, B. G. Rushing, C. E. Bauer, Rhodospirillum centenum Utilizes Separate Motor and Switch Components To Control Lateral and Polar Flagellum Rotation. *Journal of Bacteriology* **184**, 2429-2438 (2002).

36. S. R. Chowdury, Indiana University, (2013).

37. J. N. Marden, (2010).

38. J. N. Marden, Q. Dong, S. Roychowdhury, J. E. Berleman, C. E. Bauer, Cyclic GMP controls Rhodospirillum centenum cyst development. *Molecular Microbiology* **79**, 600-615 (2011).

39. G. Koraimann, Lytic transglycosylases in macromolecular transport systems of Gram-negative bacteria. *Cellular and Molecular Life Sciences* **60**, 2371-2388-2388 (2003).

40. A. R. Mushegian, K. J. Fullner, E. V. Koonin, E. W. Nester, A family of lysozyme-like virulence factors in bacterial pathogens of plants and animals. *Proceedings of the National Academy of Sciences* **93**, 7321-7326 (1996).

41. J. Mahillon, M. Chandler, Insertion Sequences. *Microbiology And Molecular Biology Reviews* **62**, 725-774 (1998).

42. B. Drogue, H. Sanguin, S. Borland, C. Prigent-Combaret, F. Wisniewski-Dyé, Genome wide profiling of Azospirillum lipoferum 4B gene expression during interaction with rice roots. *FEMS Microbiology Ecology* **87**, 543-555 (2014).

43. M. A. Matilla, M. Espinosa-Urgel, J. J. Rodríguez-Herva, J. L. Ramos, M. I. Ramos-González, Genomic analysis reveals the major driving forces of bacterial life in the rhizosphere. *Genome Biology* **8**, R179 (2007).

44. L. Vial *et al.*, Phase variation and genomic architecture changes in Azospirillum. *Journal of Bacteriology* **188**, 5364-5373 (2006).

45. J. E. Berleman, B. M. Hasselbring, C. E. Bauer, Hypercyst Mutants in Rhodospirillum centenum Identify Regulatory Loci Involved in Cyst Cell Differentiation. *Journal of Bacteriology* **186**, 5834-5841 (2004).

46. J. Berleman, C. Bauer, Characterization of cyst cell formation in the purple photosynthetic bacterium Rhodospirillum centenum. *Microbiology* **150**, 383-390 (2004).

47. M. Gomelsky, W. D. Hoff, Light helps bacteria make important lifestyle decisions. *Trends in Microbiology* **19**, 441-448 (2011).

48. M. A. Mussi *et al.*, The Opportunistic Human Pathogen Acinetobacter baumannii Senses and Responds to Light. *Journal of Bacteriology* **192**, 6336-6345 (2010).

49. M. A. van der Horst *et al.*, Locked chromophore analogs reveal that photoactive yellow protein regulates biofilm formation in the deep sea bacterium Idiomarina loihiensis. *Journal of the American Chemical Society* **131**, 17443-17451 (2009).

50. T. E. Swartz *et al.*, Blue-light-activated histidine kinases: two-component sensors in bacteria. *Science (New York, NY)* **317**, 1090-1093 (2007).

51. M. E. Taveirne, C. M. Theriot, J. Livny, V. J. DiRita, The Complete Campylobacter jejuni Transcriptome during Colonization of a Natural Host Determined by RNAseq. *PLoS ONE* **8**, 1-1 (2013).

Chapter 4 - The Role Of The PixD-PixE Complex In Regulating Phototaxis in *Synechocystis* sp. PCC6803

Summary

Synechocystis sp. PCC6803 shows phototactic responses to a range of different wavelengths. One of the light receptors involved, PixD, interacts with the PatA homolog PixE forming a light-responsive complex (*1*). The function of the PixD-PixE complex, or of PixE itself is not known. While a deletion of *pixD* caused cells to move away from light, a deletion of *pixE* did not significantly change phototaxis. PixE contains a response regulator domain, indicating a role in two-component signaling. Truncation of this response regulator domain did not abrogate binding with PixD *in vitro*. Besides the interaction between PixD and PixE, a bacterial-two-hybrid screen showed interaction between PixD, PixE and an EAL protein (Slr1692) encoded by an ORF upstream of *pixD-pixE*. Deletion of *slr1692* lead to loss of motility and poor growth under white light conditions. These results suggest a complicated network of interactions and a combination of two-component and c-di-GMP signaling controlled by PixD.

Introduction

The cyanobacterium *Synechocystis* sp. PCC6803 (*Synechocystis* hereafter) shows complicated motility, with many factors playing a role in its regulation: for example, calcium (*2*), cAMP (*3, 4*), c-di-GMP (*5*), the RNA chaperone Hfq (*6*), and light (*7, 8*) have all been shown to play a role. A recent paper describing the molecular evolution of

several laboratory strains identified a number of additional, to date unstudied mutations causing changes in motility (*9*). *Synechocystis* also shows phototactic responses to a wide range of wavelengths, suggesting the involvement of multiple light receptors (*7, 10*). To date four light receptors have been identified: PixJ1 (or TaxD1) (*11, 12*), Cph2 (*13*), UirS (or PixA) (*14, 15*), and PixD (*16*).

Exposure of wild type cells to red or white light leads to positive phototaxis towards the light source whereas a strain deleted for *pixD* exhibites negative phototaxis away from the light source (*16*). PixD contains a BLUF domain, but no output domain. It is therefore expected that PixD functions through interaction with a second protein. Upstream of *pixD* is a reading frame encoding a PatA homolog called PixE. PixE was shown to interact with PixD in a yeast-two-hybrid screen (*16, 17*). The light-dependent interaction between PixD and PixE was later confirmed in vitro (*1, 18*). Work by Masuda *et al.* showed that mutations in PixD that abrogated interaction with PixE *in vitro* also led to negative phototaxis *in vivo* (*18*). These results strongly suggest the involvement of PixE in the regulation of phototaxis.

The function of PixE is not yet known. It is interesting though, that three of the six PatA homologs encoded in the *Synechocystis* genome have been shown to be involved in regulating phototaxis or motility in general (*12, 14, 15, 19*). Indeed in all three chemotaxis operons in this species the first ORF encodes a PatA homolog (*10, 20*). Like other PatA homologs, PixE features a so-called PATAN domain and a C-terminal response regulator domain (Figure 4.1) (*21*). The response regulator of PixE has a glutamate instead of the conserved aspartate group that would receive a phosphate group from its partnering histidine kinase (*22*).

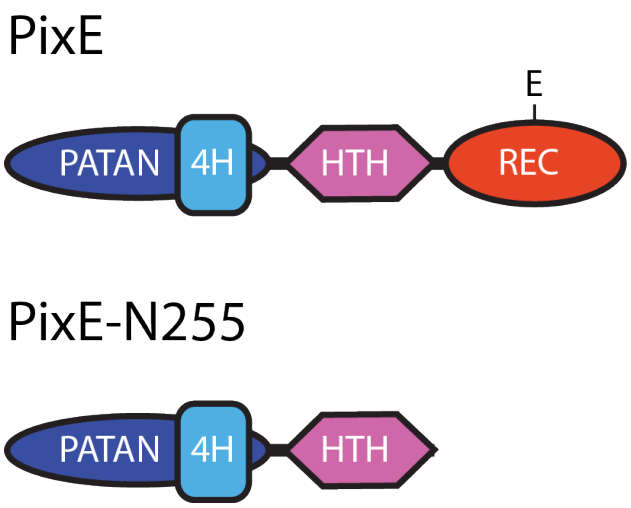

Figure 4.1 Domain organization of PixE. The HTH domain indicated here can not be detected by Pfam or SMART algorithms. PixE features a receiver domain with the conserved aspartic acid mutated to a glutamic acid residue. (Figure adapted from (21)).

Several BLUF proteins contain or interact with EAL domains that are involved in the degradation of the ubiquitous second messenger c-di-GMP (e.g. BlrP1, PapA-PapB, BluF) (*23-25*). In that sense, it is interesting that upstream of *pixE* and *pixD* is an ORF (*slr1692*) that encoding an EAL protein. C-di-GMP signaling plays an important role in lifestyle changes, for example in the switch from a motile, planktonic lifestyle to biofilm formation (*26, 27*). Like many other bacteria, *Synechocystis* contains a number of c-di-GMP synthesizing and degrading proteins. One of which is Cph2: a phytochrome-like light receptor with both GGDEF and EAL domains. Cph2 was shown to be involved in the regulation of phototaxis, presumably through its ability to alter c-di-GMP concentrations (*5*).

Here we describe our research on the structure of the PixD-PixE protein complex, the *in vivo* role of PixE, transcription of *slr1692, pixE and pixD*, and interaction between Slr1692, PixD and PixE.

Materials and Methods

Strains and plasmids

Wildtype and *pixD*$^{-}$ strains of *Synechocystis* sp. PCC6803 were kindly donated by Dr. Shinji Masuda. Deletion plasmid pDEL was made by cloning the PCR amplified *aphX-sacB* cassette from pPSBA2KS (*28*) into pGEM-7Zf. On both sides of the *aphX-sacB* cassette NotI, PmeI and PacI, AscI restriction sites were added to allow insertion of the flanking regions of genes to be deleted. To delete genes 1 kb flanking regions of genes of interest were PCR amplified and cloned into plasmid pDEL. The resulting

plasmid was transformed into *Synechocystis* using a method described by Lagarde *et al.* (*28*). In short, cells were grown to OD_{750}~0.8. Aliquots of the cells (10 mL) were pelleted and resuspended in 1 mL fresh BG-11 medium without antibiotics. 3 μg of deletion plasmid was added to 150 μL resuspended cells. The cells were then incubated at 30°C for 5 hours under fluorescent light after which 1 mL of fresh BG-11 was added and the cells were incubated overnight at 30°C on a shaker under light. After incubations the cells were plated on BG-11 agar plates containing 10 μg/mL kanamycin. Mutants were selected for several rounds at increasing concentration of kanamycin (10 – 150 μg/mL). For stronger selection in later rounds neomycin (30 μg/mL) was used. To make clean deletions, mutants were transformed with pGEM-7Zf plasmids containing 7 codon nonsense reading frames with 1kb flanking regions of the genes of interest. After transformation cells were plated on BG-11 agar containing 0.5 to 2% (w/v) sucrose.

To overexpress the PixD-PixE complex, *pixE* with an N-terminal TEV site was cloned into MCS1 of the pCDFDuet-1 plasmid (Novagen). Followed by subsequenct cloning of *pixD* into MCS2 yielded plasmid pCDF-PixDE-TEV. Plasmid pCDF-PixDE-N255 was made by introducing a PixE(Pro256Stop) mutation using a quick change protocol (Agilent QuickChange). The PixD-PixE complex was overexpressed by growing E. coli BL21(DE3) transformed with plasmid pCDF-PixDE-TEV or pCDF-PixDE-N255 in autoinducing medium (LBE5052) with 50 mg/L spectinomycin. Cultures were grown for several hours at 37°C and then incubated on a shaker at 16°C for at least 18 hours.

Several constructs were made to overexpress Slr1692 fused to a variety of solubility-enhancing domains (MBP, CBP-intein, SUMO or Trx). Various

overexpression conditions were tested, including induction time, incubation temperature and media.

Motility assays

To test the role of Slr1692, PixE and PixD mutants for the respective genes were tested using an agar plate or glass slide assay. For the agar plate assay BG-11 agar plates were prepared with 0.4%(w/v) agar. Strains were spotted onto the agar plate in 1μL spots and allowed to dry until excess medium had disappeared. The plates were then incubated in an aquarium with a layer of water to prevent further drying out. Lateral light was provided by a fluorescent light bulb.

To test individual phototactic responses cells were diluted to $OD_{750} \sim 0.25$. Five microliters of this culture was placed on microscope slides (Fisher Superfrost) and covered with 22 mm cover slides. The edges were sealed with nail polish or black electrical tape to prevent liquid flow as a result of evaporation. The prepared slides were incubated in dark for at least 30 minutes. Time-lapse movies were recorded on a Nikon Eclipse Ni with a Hamatsu camera at 20x magnification. Pictures were taken at 10-second intervals for a duration of 5 minutes. To minimize the influence of the condenser light an 850 nm long-pass filter was placed between the condenser and the slide. The intensity of the condenser light was kept as low as possible (light levels were to low to be measured reliably). Individual cells were tracked using the ImageJ plug-in Manual Tracker.

A Nikon light source was used to provide lateral illumination of the slide. Light intensities were kept at 10 $\mu E.m^{-2}.s^{-1}$. The cells were allowed to acclimatize for 10 minutes before movies were recorded.

Purification of the PixD-PixE and PixD-PixE-N255 complex

Cells co-expressing PixD and PixE or PixE-N255 were lysed in lysis buffer (20 mM Tris (pH 7.5), 300 mM NaCl, 20 mM imidazole, 0.05%(v/v) Tween-20, 10%(v/v) glycerol) by three passages through a microfluidizer. Cell lysates were cleared by centrifuging for 30 minutes at 15,000 rpm (Sorvall SS-34 rotor). The supernatant was then applied to a gravity column with 1 mL Ni-NTA resin (GE Healthcare). The column was washed with 75 column volumes of wash buffer (as lysis buffer, minus Tween-20 and 60 mM instead of 20 mM imidazole). The protein complex was then eluted with elution buffer (as wash buffer, with 250 mM imidazole). The eluted protein was then further purified using a Superose 6 gel filtration column with 20 mM Tris (pH 7.5), 100 mM sodium chloride as running buffer. The peak corresponding to complexed protein was collected and the protein concentrated using Ultracel centrifugal filters with a cut off value of 10 kDa (Millipore).

If removal of the histidine tags was desired, protein eluted from the Ni-NTA resin was first ran over a desalting column (Bio-Rad) to change the buffer to 20 mM Tris (pH7.5), 100 mM NaCl. TEV protease was then added in 1:3 molar ratio (TEV protease:PixDE complex). The reaction mixture was incubated at room temperature for 3 hours. Incompletely cleaved protein complex and TEV protease were then removed by adding imidazole to a final concentration of 40 mM and running the mixture over a Ni-

NTA column. The protein complex was then further purified by gel filtration as described above.

Purification of Slr1692

To purify Slr1692 from inclusion bodies cells from 100 mL LB culture were lysed by sonication in 20 mM Tris (pH 7.5), 10 mM EDTA, and 1%(v/v) Triton X-100. Inclusion bodies were collected by centrifugation for 10 minutes at 10,000 x g. The pellet was washed once in lysis buffer and then resuspended in lysis buffer with 10%(w/v) urea, incubated at room temperature for 30 minutes and centrifuged for 10 minutes at 10,000 x g. The resulting pellet was weighed and resuspended to 1 mg/mL in 50 mM CAPS (pH 11), 0.3%(w/v) N-lauroyl sarcosyl. Solubilized protein was centrifuged 10 minutes at 10,000 x g at 21^{o}C. The resulting supernatant was then added in 1 mL bursts to 750 mL refolding buffer (50 mM Tris (pH 8.5), 240 mM NaCl, 10 mM KCl, 0.01% Tween-20). The refolded protein was then loaded onto a Ni column overnight at 4^{o}C. The next day the column was washed with refolding buffer without Tween-20 and 75 mM imidazole. Refolded Slr1692 was eluted with a 0 - 0.5 M linear gradient of imidazole. The eluted protein was then diluted 15-fold with 25 mM Tris (pH 8). The protein was then filtered (0.22 μm) and applied to a DEAE column and eluted using a sodium chloride gradient (50 mM – 1 M). To test the oligomerization state eluted protein was applied to a calibrated Superose 12 column (column volume 28 mL).

Cryo-electron microscopy and single particle reconstruction

Purified full length PixD-PixE complex was diluted to a final concentration of 0.1 mg/mL. The final buffer was diluted to 10 mM Tris (pH7.5), 50 mM NaCl to reduce background signal. Five microliter of protein was applied to Quantifoil R1.2/1.3 grids that had been cleaned with acetone and glow discharging. Grids were blotted for 0.5 seconds and then quickly dropped in hexane just above freezing temperature. Frozen grids were stored in liquid nitrogen. Imaging was done using a JEOL 3200 electron microscope at 300 kV. Images were recorded using a Gatan camera. All procedures were performed under red and green safety light.

Single particle reconstruction was attempted using a very limited data set using the Eman2 software package (*29*).

Crystallography

To crystallize the truncated PixD-PixE complex, purified protein was concentrated to a final concentration of 5 mg/mL. Hanging drops were created on siliconized cover slips by adding 1 uL protein to 1 uL buffer. The slides were then used to cover wells filled with 150 uL buffer. All steps, including visual inspection of the drops, were done under red or green safety light.

Crystals were screened for diffraction using an in house X-ray facility.

Bacterial two-hybrid screening

To test for interaction between Slr1692 and PixE or PixD a bacterial-two-hybrid screen was used (Agilent, BacterioMatchII). Full length ORFs were cloned into the

supplied pBT and pTRG plasmids using the NotI and XhoI restriction sites. Interactions were tested following the manufacturer's instructions. Plates were incubated for 1 or 2 days at 37^{o}C in darkness.

Transcriptional organization

To test whether *slr1692, pixE* and *pixE* are organized in a single operon RT-PCR was used. RNA was extracted from wildtype *Synechocystis* that had been grown under continuous light until an OD_{750} of approximately 0.3. Fifty milliliter cultures were rapidly cooled in a dry ice/ethanol bath. Cells were harvested by centrifugation at 4^{o}C. The pellets were resuspended in 1 mL PGTX. Suspensions were then stored at -80^{o}C until further processing. RNA was extracted using the protocol described in (*30*). The extracted RNA was treated with DNase and further purified using the Qiagen RNEasy kit following the manufacturer's instruction.

Primers for the reverse transcription were designed for the 3' end of each of the three ORFs. Reverse transcription was performed using SuperScript III (Invitrogen), followed by PCR reactions using primers specific for the approximately 200 bp at the 5' end of each ORF.

To identify the exact transcription start site for the three genes 5'-RACE was used. For each reaction 12 ng total RNA was split in two fractions: one of each was treated with RppH. The reactions were cleaned up and RNA adapter sequences were ligated to the 5' end. Again reactions were cleaned up and the resulting RNA was used in a reverse transcription reaction. Reverse transcription was followed by using a forward primer specific for the adapter sequence and gene-specific reverse primers. Bands of

interest were excised from the agarose gel and ligated in pGEM-T Easy. The resulting plasmids were then sequenced.

Results

Purification and crystallization of the PixD-PixE complex

The PixD-PixE complex can readily be purified from an *E. coli* strain overexpressing both proteins, one of which (PixE) containing an affinity tag. Truncation of the receiver domain of PixE (PixE-N255, Figure 4.1) yielded a protein that still forms a complex with PixD. Like the full-length PixE- PixD complex, this complex readily dissociates when exposed to light (Figure 4.2). Further truncations of either the amino- or carboxy-terminus of PixE led to loss of interaction (data not shown). These results show that the N-terminus of PixE interacts with PixD. Further truncations presumably either cause misfolding of PixE, or disrupt essential PixD-PixE binding interfaces.

Purified PixD-PixE-N255 complex appears to contain less contamination, but it should be noted that the major contaminant of the PixD-PixE complex is about 28 kD which is comparable to the predicted molecular weight of PixE-N255 (29.6 kDa). This contaminant may still be present, while being undetected using SDS-PAGE.

Purified PixD-PixE complex showed some tendency to crystallize in several conditions. Unfortunately these results were not reproducible. Crystallization of the PixD-PixE-N255 complex on the other hand was more reproducible. Optimization of the crystallization conditions eventually yielded crystals that diffracted to approximately 9.1 A (data not shown). We then decided to further truncate the complex by cleaving off the

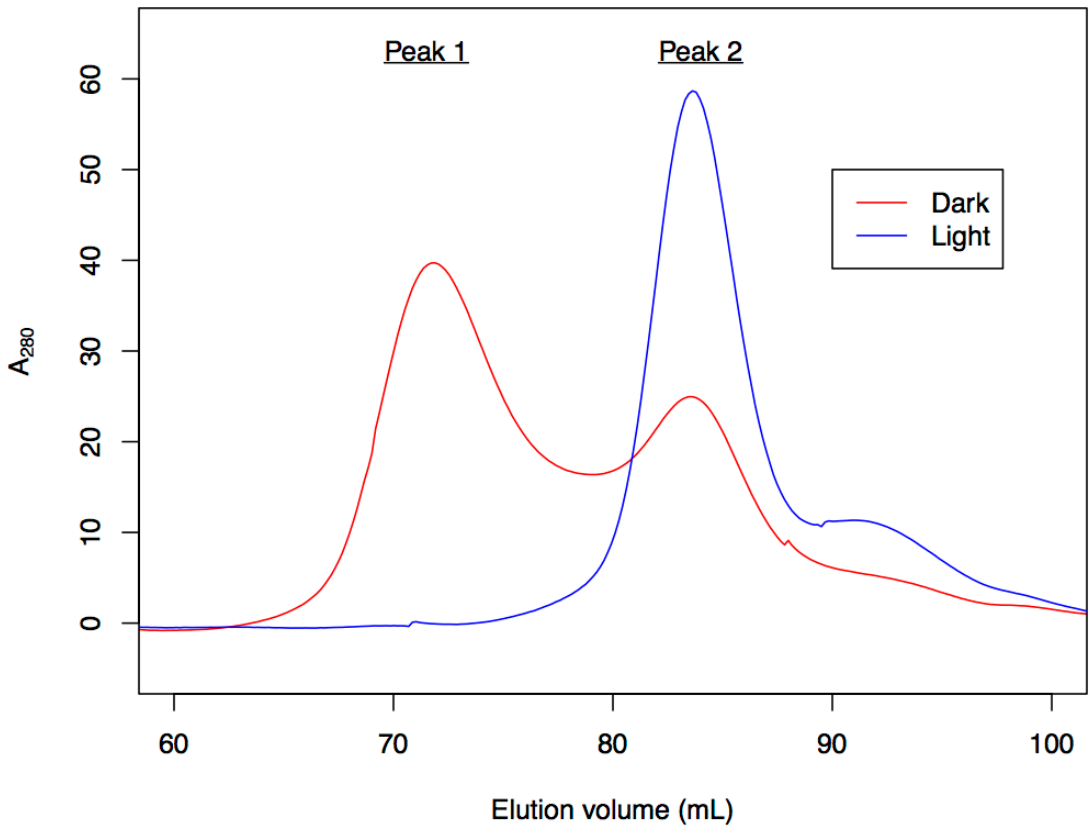

Figure 4.2 Truncation of PixE and interaction with PixD. Superose 6 elution profile of the PixD-PixE_N255 complex. Peak 1 contains complex, while peak 2 contains dissociated proteins. Like a complex with full-length PixE, the truncated complex is light-sensitive.

N-terminal histidine tag. This gave conditions that overnucleated and yielded a multitude of crystalline plates.

Full-length PixE cannot be readily purified by itself. Truncated PixE however, could be purified albeit at low concentrations. The protein is not very stable and tends to precipitate when stored overnight at 4^{o}C. A small amount of protein remains in solution (~ 0.5 mg/mL).

Cryo-electron microscopy

Using cryo-electron microscopy we were able to visualize the PixD-PixE complexes. At a concentration of 0.1 mg/mL the particles are well separated. Most particles are pentagonal with an apparent central cavity (Figure 4.3). This shape resembles the topview of the PixD crystal structure (*31*). A possible explanation could be that one face of the complex is hydrophobic, causing the complex to accumulate at the air-liquid interface. Imaging the samples under various angles confirmed that most particles are indeed in one orientation (data not shown).

Bacterial-two-hybrid screening

A bacterial-two-hybrid screen showed interaction between Slr1692, PixD and PixE (Figure 4.4). No self-activation was detected, further indicating that interactions between the three proteins occure. Since the bacterial-two-hybrid screen did not allow for incubation in light, we employed a mutant of PixD that is locked in its lit state (Q50A) (*32*). This mutant PixD still showed interaction with Slr1692, although this interaction

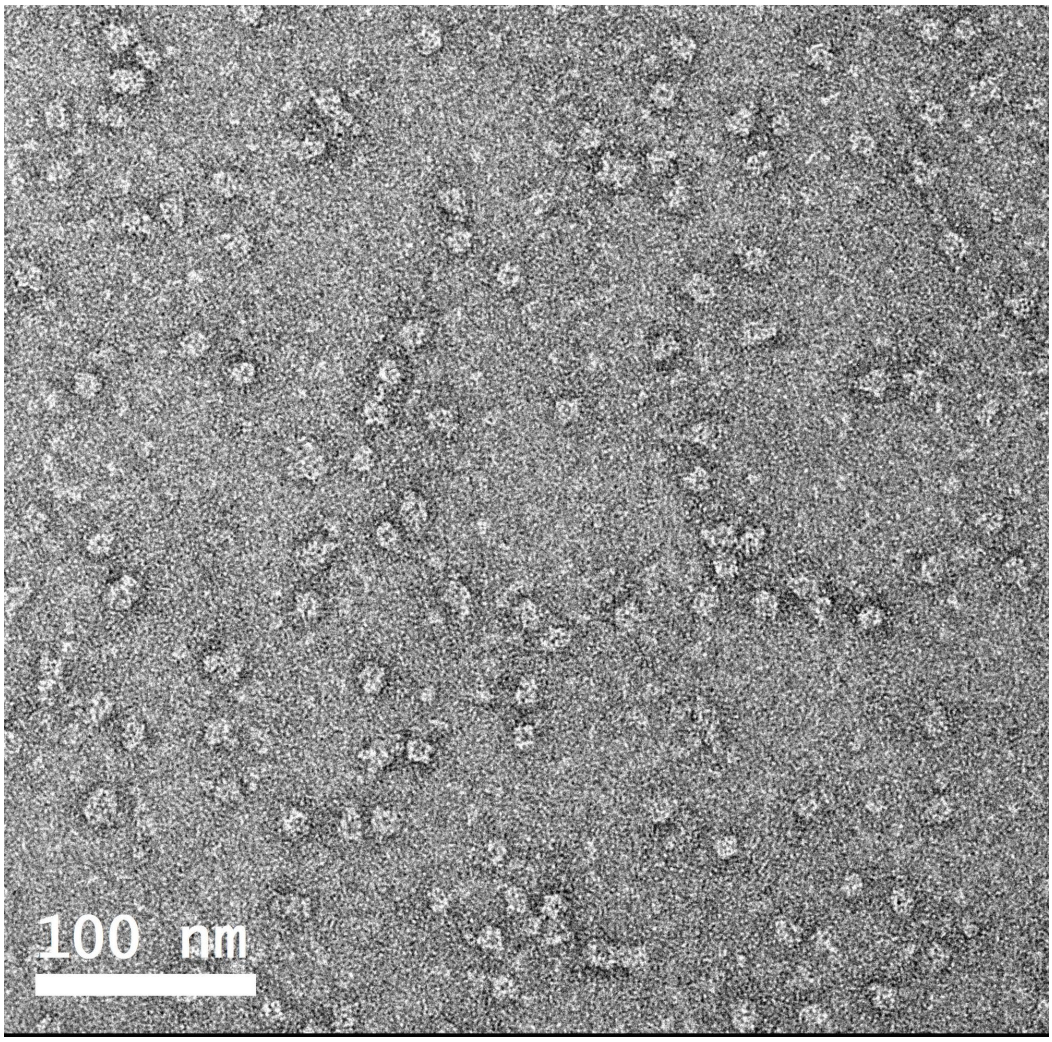

Figure 4.3 Cryoelectronmicrograph of the PixD-PixE complex. Most particles show a pentagonal shape with a central cavity.

appears to be weaker as shown by diminished growth on selective plates. One should be careful with this observation as PixD_Q50A and PixE showed some interaction in this screen, while this interaction was not shown *in vitro* (*32*).

An interaction between Slr1692 and PixD or PixE was not shown in a large scale yeast-two-hybrid screen (*17*). We tested interactions in a yeast-two-hybrid screen and only found light-independent interaction between PixD and PixE, and self-interaction of PixD (data not shown). Whether the interaction with Slr1692 as seen in the bacterial-two-hybrid screen is an artifact, or whether the lack of interaction in the yeast-two-hybrid screen is due to a lack of a cofactor remains a question.

Purification of Slr1692

Overexpressed Slr1692 showed very poor solubility. In order to solve this problem several solubility enhancing domains (e.g. maltose-binding protein, chitin-binding/intein, SUMO) were tested. None of these seemed to alleviate this poor solubility. Expression of *slr1692* in *E. coli* strains that overexpressed various combinations of chaperones appeared to result in some solubility, but separating Slr1692 from the chaperones by addition of 10 mM ATP and casein (5 mg/mL) did alleviate this problem somewhat, but never completely solved contamination problems.

Treating overexpressed insoluble Slr1692 as inclusion bodies was more successful. We eventually established a solubilization and refolding protocol that yielded soluble Slr1692. However, in size exclusion chromatography all protein eluted in the void volume, indicating the formation of high molecular weight aggregates.

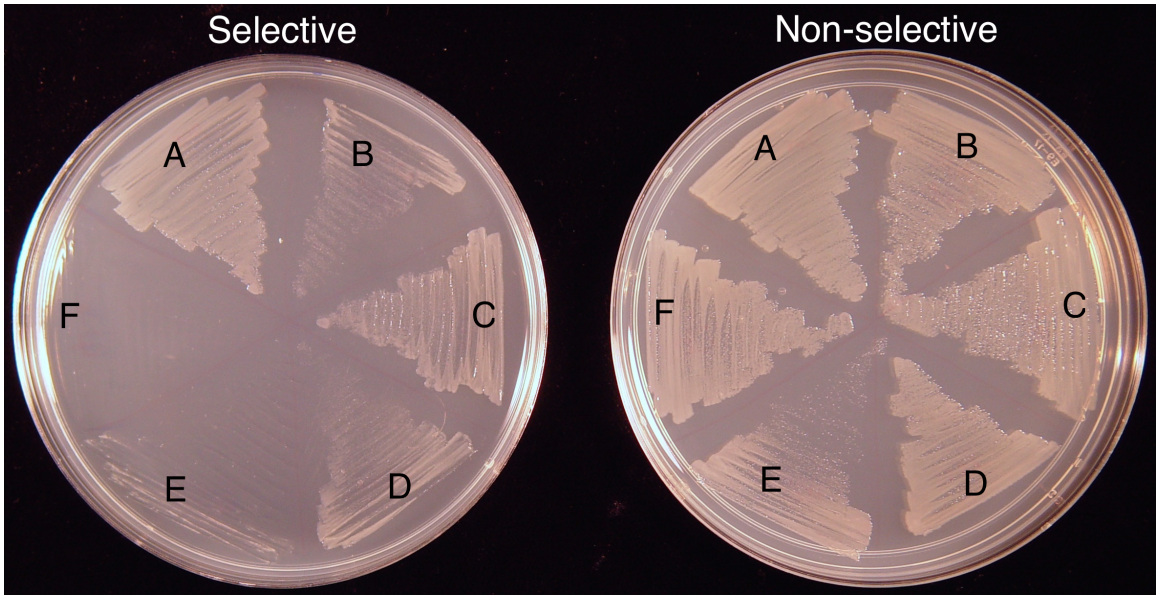

Figure 4.4 Bacterial two hybrid screen using Slr1692 as bait. The screens shows interaction between Slr1692 and PixD or PixE. Since the use of tetracyclin prohibited exposure to light, a PixD_Q50A mutant was used instead. Previous studies showed this mutant to be locked in the lit state (32). Interaction between Slr1692 and PixD_Q50A seems to be slightly weaker than the interaction between Slr1692 and wildtype PixD. (A: positive control (strain transformed with pBT-LGF2 and pTRG-GalII); B: PixD_Q50A; C: PixD; D: PixE; E: Slr1692; F: empty target vector).

Deletion of slr1692, pixE and pixD

Both *pixE* and *pixD* could be deleted from the chromosome using the method described by Lagarde *et al.* (*28*). Initial attempts to delete pixD were unsuccessful due to an unintended mutation of the stop codon of *pheT* on the opposite strand. Consequently most of the work described below was done using a $pixD^-$ strain constructed by Masuda *et al.* (*33*). This strain has a spectinomycin cassette inserted in the pixD ORF. To avoid polarity effects, the *pixE* reading frame was replaced by a 7 codon nonsense reading frame.

To achieve a complete deletion of *slr1692* the selective agar plate cultures had to be incubated under red LED light. While these cultures did grow under fluorescent light, they did maintain at least one copy of wild type *slr1692*. The *slr1692* mutants grew slower than the wild type cells and also appeared to be non-motile on agar plates and on glass slides. Attempts to transform the resulting strain with a clean deletion plasmid were unsuccessful. This could be due to a lack of pili formation (*12*). Taken together these observations do suggest a light dependent role of *slr1692* in the regulation of motility.

Transcriptional organization

The structure of the *slr1692-pixE-pixD* operon was tested by reverse transcription using primers for *pixE* or *pixD* followed by PCR using gene-specific primers (Figure 4.5). The results suggested that indeed the three reading frames are cotranscribed (Figure 4.6).

To confirm this, I performed 5'-RACE to identify the transcription start sites (TSS) for each of the reading frames. For *slr1692* the TSS was found to be 130 bp upstream of the start codon. This is consistent with the results reported by Mitschke *et al.* (*34*). The TSSs for *pixE* and *pixD* proved to be more difficult to identify, which could be due to lower transcription levels, or less efficient reverse transcription or PCR amplification. We did find a TSS between the *slr1692* and the *pixE* reading frames. The TSS found here was 5 bp upstream of the TSS reported by Mitschke *et al*. (*34*). It should be noted that the 5'-RACE PCR product contained another 19 bp that could not be aligned to the genome. It is well possible that this 25 bp difference is an artifact introduced by the 5'-RACE procedure.

Despite this artifact, it does seem that *pixE* has its own TSS. The presence of a second TSS does not exclude cotranscription. However, Mitschke *et al.* reported lower transcription levels of *pixE* and *pixD* as compared to *slr1692*. It is therefore most likely that our initial results are due to read-through.

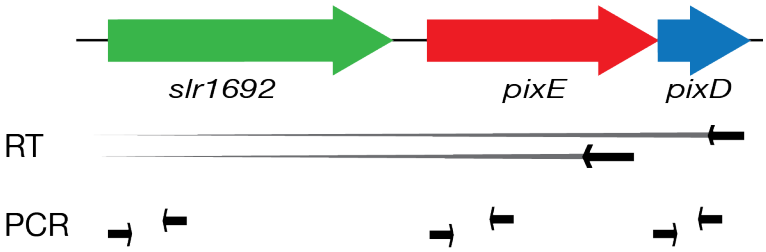

Figure 4.5 Probing transcriptional organization. Primers specific for pixE and pixD were used to produce cDNA, followed by PCR using gene-specific primers for each of the the three genes. As a control RTase reactions without RTase were included.

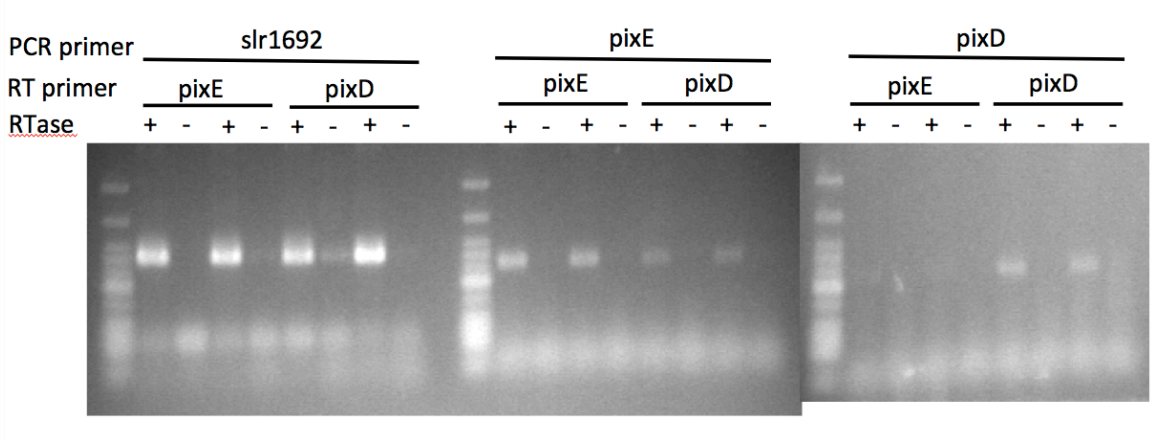

Figure 4.6 slr1692 is cotranscribed with pixE and pixD. An slr1692 or pixE fragment can readily be amplified from cDNA generated with pixE or pixD specific primers, showing that these genes are indeed co-transcribed. As a control pixD can only be amplified from cDNA generated with a pixD specific primer.

Motility assays

The *pixE* deletion mutants show positive phototaxis under white light (Figure 4.7, Figure 4.8, Figure 4.9). The mutant seemed to move more vigorously on agar plates, with fewer cells remaining at the inoculation spot as compared to wild type cells. The *pixD*$^{-}$ mutant showed negative phototaxis, as has been reported before (*33*).

When tested for phototaxis using the glass slide based assay, the *pixD*$^{-}$ mutant cells did appear to move less vigorously than the wild type cells (Figure 4.7, Figure 4.8). This however is based on very limited data (17 to 22 individual cells, no biological replicate). The *pixD*$^{-}$ strain showed mostly negative phototaxis in this assay. The wild type cells migrate over a longer distance, and in general show positive phototaxis. Both *pixD* and *pixE* mutants appear to move less and also show less orientation along the light axis (Δx). Interestingly, the phototaxis efficiencies of these different strains seem to be comparable (Figure 4.9) indicating that for all strains the light sensing component is equally sensitive. This could mean that PixD and PixE work in a system separate from the phototaxis system.

The two main differences between the methods used here are the time scales (minutes versus days), and individual versus group behavior. In general the behaviors observed in both assays are comparable, but the difference in activity of the *ΔpixE* mutants is interesting. Obviously the results presented here are based on an insufficient data set, but it does illustrate the benefit of studying phototaxis using both assays.

Figure 4.7 Phototaxis on 0.4% BG-11 agar. The agar plates were incubated at 30^{o}C in an aquarium under lateral white light for 7 days. (WT: wildtype strain; Δslr1692: mutant strain, slr1692 replaced by kanR sacB cassette; ΔpixE: clean deletion strain of pixE; ΔpixE kanR: pixE replaced by kanR-sacB cassette; ΔpixD: pixD replaced by kanR-sacB cassette, at least one copy of wildtype pixD present; pixD^{-}: pixD mutant strain, with spectinomycin resistance cassette inserted in the pixD ORF (18).

The pixE clean deletion strain shows positive phototaxis and possibly more vigorous motility compared to wildtype. The pixD^{-} strain shows negative phototaxis, while the incompletely segregated ΔpixD strain shows positive phototaxis.

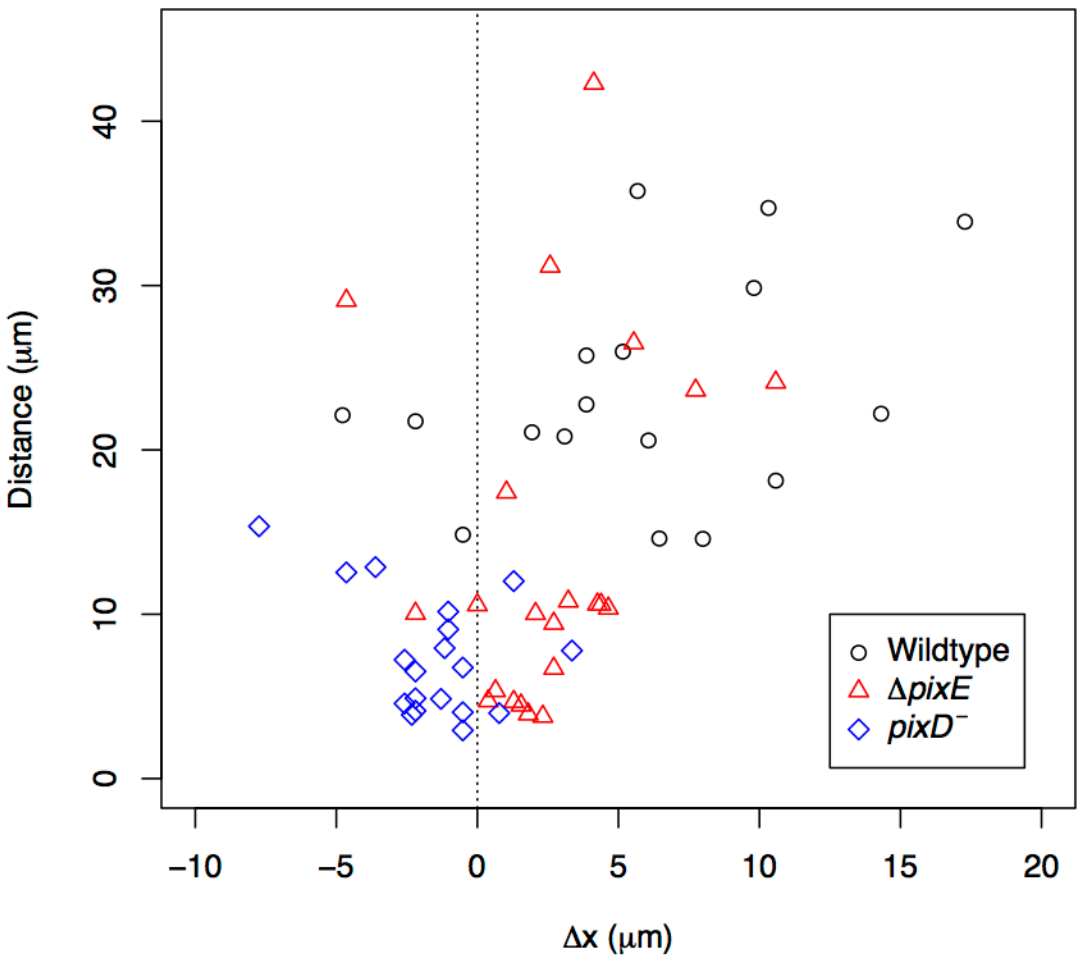

Figure 4.8 Motility in a glass slide based assay. Cells were observed as they moved glass microscope slides exposed to lateral light. Individual cells were tracked over a period of 5 minutes and the total distance traveled and the total displacement along the light axis (**Δ**x) were measured.

(A)

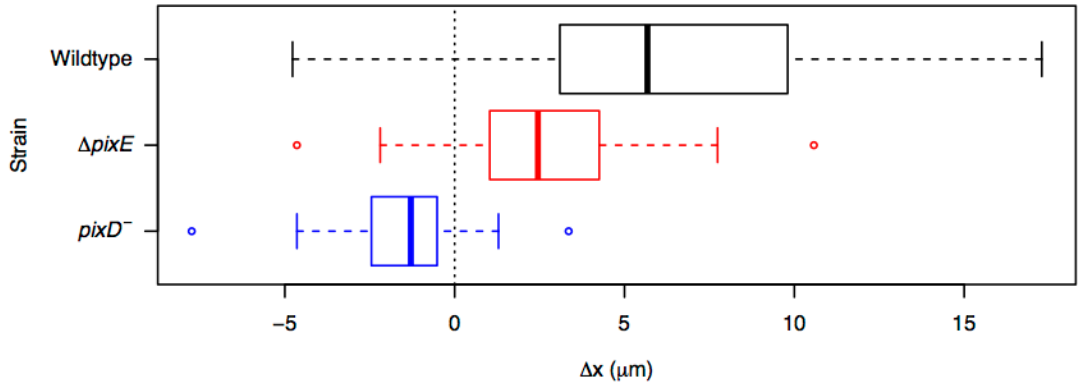
Wildtype
ΔpixE
pixD⁻
Strain
−5
0
5
10
15
Δx (μm)

(B)

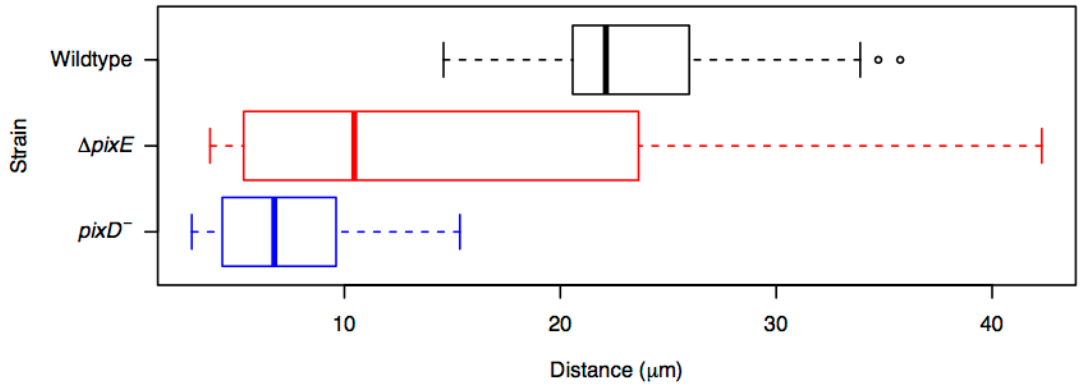
Wildtype
ΔpixE
pixD⁻
Strain
10
20
30
40
Distance (μm)

(C)

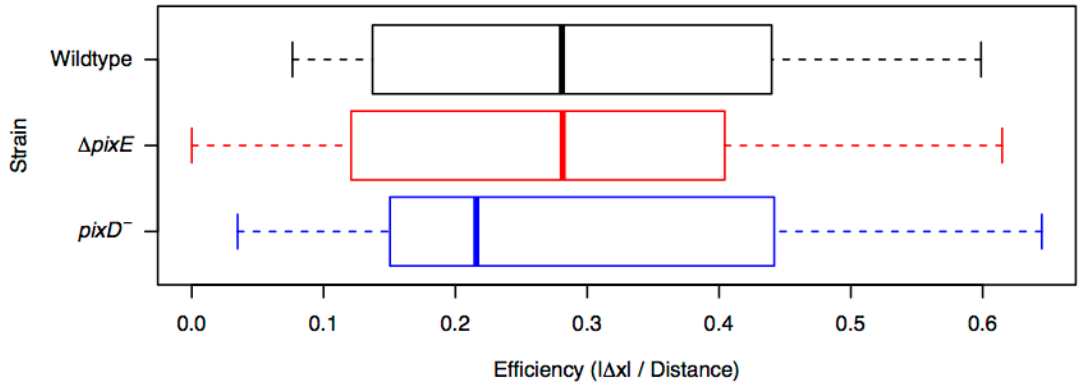
Wildtype
ΔpixE
pixD⁻
Strain
0.0
0.1
0.2
0.3
0.4
0.5
0.6
Efficiency (|Δx| / Distance)

Figure 4.9 Phototaxis during short time scales. Individual cells were tracked over a 5 minute period with 10 second intervals. (A) The displacement along the light axis shows that both wildtype and pixE deletion mutants generally positive phototaxis, while pixD- shows negative phototaxis. (B) The total distance each of the cells traveled shows that pixD- cells are in general less motile than wildtype cells. pixE mutants show great variance in their motility. (C) The efficiency was calculated by dividing the absolute displacement along the light axis by the total distance traveled. All strains seem to have a similar efficiency, indicating that none is better at finding the light source.

Discussion

The majority of proteins containing BLUF domains are short single domain proteins. Currently 465 sequences of single domain BLUF proteins are known (Pfam, accessed June 2014). Despite their presence in many genomes, only two interaction pairs have yet been identified: PixD-PixE and PapB-PapA from *Rhodopseudomonas palustris* (*24*). PapA (RPA0521) contains both a GGDEF and an EAL domain, the former, however, does not contain the conserved GGDEF motif and is thought to be inactive (*24*). Light appears not to affect the interaction between PapB (RPA0522) and PapA, although the phosphodiesterase activity of PapA does increase when PapB is light excited (*24*). Unlike the PapB-PapA complex, the PixD-PixE complex dissociates upon light-excitation (*1*). What role dissociation plays in the function of PixD is not clear. A *pixD* deletion strain showed a phototaxis motility phenotype in white and red light, but not in blue light (*16, 18*). In white light the PixD-PixE complex dissociated *in vitro*, while red light does not affect this complex (*1*). This indicates that whether or not PixE is complexed with PixD, PixE does not have an effect on its own, but rather must work in conjunction with some other signal. Could it be that free PixE inverts whatever signal is present?

Synechocystis moves by twitching motility, a form of surface motility that depends on extension and retraction of type IV pili. Work on *Pseudomonas aeruginosa* showed that extension of pili is dependent on PilB, while PilT retracts the pilus (*35*). Both PilB and PilT are ATPases that respectively catalyze the assembly or disassembly of pili (*36*). The action of PilB and PilT is regulated by PilG and PilH, respectively (*37*).

PilG and PilH are both CheY homologs encoded by two reading frames at the start of the *pil-chp* chemotaxis gene cluster that also contains two CheY homologs (*38, 39*). Likewise, the chemotaxis gene clusters found in *Synechocystis* all contain two CheY homologs (*10*) suggesting that the regulation of motility in *Synechocystis* may work in a similar fashion as in *P. aeruginosa*. Indeed, deletion of a *pilH* homolog in *Synechocystis,* the second CheY homolog in the *pil* gene cluster, led to longer and more thicker pili and a complete loss of motility, suggesting a reduced retraction of pili (*19*). However, deletion of *pilG*, the first CheY homolog, showed no changes in motility or piliation (*19*). PilG is one of six PatA homologs encoded in the genome of *Synechocystis* so there may be redundancy in the function of these PatA homologs. To date five light receptors have been found to influence phototaxis, three of these are associated directly or indirectly with PatA homologs (*1, 11-16, 40*). It is therefore tempting to speculate that these PatA homologs act on the same pilus motor and thus allow convergence of different light sensing signaling pathways. However, to date little is known about what other proteins these PatA homologs interact with.

Our bacterial-two-hybrid results suggest that PixD is able to form a complex with Slr1692, an EAL protein. About 36% of known BLUF proteins are BLUF-EAL hybrid proteins (Pfam, accessed June 2014). EAL domains have phosphodiesterase activity and are involved in reducing the c-di-GMP levels in cells through its conversion to GMP (*26*). Several instances of light-regulated c-di-GMP production or degradation have been reported (*5, 23, 41, 42*). To date two proteins have been described that combine BLUF light-sensing with EAL PDE activity, BlrP1 and PapB. Light-excitation of the BLUF-EAL hybrid, BlrP1, increased its PDE activity fourfold (*23*). By comparison the PapB-

PapA complex showed a 2.5 fold increase upon light excitation (*24*). PixD and Slr1692 could play a similar role. The importance of c-di-GMP for motility in *Synechocystis* was shown by recent work on the GGDEF domain containing protein Cph2 (*5*). Activity of the second GGDEF domain of Cph2 is regulated by an upstream cyanobacteriochrome domain. Blue light irradiation of a truncated Cph2 containing the CBCR and GGDEF motifs showed an increase in c-di-GMP levels and an inhibiting effect on motility (*5*). It is tempting to think that PixD-Slr1692 would act as a counterweight to the activity of Cph2. Our preliminary results suggested that deletion of *slr1692* does cause cells to be non-motile.

How direction of motion is changed in twitching motility is poorly understood. One of the best-studied systems is S-motility in *Myxococcus xanthus*. In this bacterium changes in direction are a result of reversals, during which the type IV pili switch polarity (*43*). Polarity switching is regulated by the Che-like Frz sytem. Phosphorylation of the CheY domain in the CheAY hybrid FrzE inhibits reversals. Similarly, the cyanobacterium *Synechococcus elongatus* did show bipolar localization of the light-sensitive MCP homolog PixJ (*44*). To our knowledge only one study describes localization of motility proteins (*45*). In this study the pilus-extending ATPase PilB1 co-localized with the RNA chaperone Hfq. In previous studies, it was shown that an absence of Hfq caused loss of motility (*6*). It will be interesting to see if other phototaxis proteins show a similar polarization. Besides affecting polarity, it is also not known whether *Synechocystis* shows the same reversal behavior as *M. xanthus* as reversals in individual *Synechocystis* cells was not observed when tracked over a 5 minute time period. *M. xanthus* reversals happen with a periodicity of approximately 5 – 10 minutes, although

the length of the periods are highly variable (*46*). Our observations may have therefore been too short to show reversals. It is also possible that *Synechocystis* uses a different mechanism to sample directions. The efficiency of displacement along the light axis compared to total distance traveled suggests that *Synechocystis* does not traveled in straight paths, but rather samples different directions as it moves towards or away from the light (Figure 4.9, (*8, 47*)).

PatA homologs play an important role in phototaxis and other processes in cyanobacteria. To date little is known about the signature PATAN motif, although our work shows that this domain constitutes the site of interaction between PixD and PixE. Structural information about the PATAN domain could be valuable in gaining more insight in the mechanism by which PixD transfers a signal to PixE. The value of a structure was shown by Ren *et al*. who reported in silico docking studies that suggested a different site than was previously proposed (*1, 48*). However, as structures of the PATAN domain are lacking it is hard to predict the structure of PixE using current methods. Truncated PixE appears to behave better than full-length PixE, making it a better candidate for crystallography. However, truncated PixE still suffers from low solubility (<1 mg/mL) and is therefore likely to yield small crystals at best. More PatA homologs should be tested for solubility.

The phenotype of a pixD deletion mutant was first reported a decade ago. To date we still know little about the mechanism behind the function of PixD. More detailed descriptions of the *ΔpixE* phenotype will help develop a better understanding of the role of the PixD-PixE interaction. Likewise the role of the Slr1692 phosphodiesterase needs to

be studied in more detail. The loss of motility and poor growth do suggest it could be part of the increasingly complicated phototaxis regulation system of *Synechocystis*.

References

1. H. Yuan, C. E. Bauer, PixE promotes dark oligomerization of the BLUF photoreceptor PixD. *Proceedings of the National Academy of Sciences* **105**, 11715-11719 (2008).
2. Y. Moon, Y. Park, Y. Chung, J. Choi, Calcium is involved in photomovement of cyanobacterium Synechocystis sp PCC 6803. *Photochemistry and Photobiology* **79**, 114-119 (2004).
3. D. Bhaya, K. Nakasugi, F. Fazeli, M. S. Burriesci, Phototaxis and impaired motility in adenylyl cyclase and cyclase receptor protein mutants of Synechocystis sp strain PCC 6803. *Journal of Bacteriology* **188**, 7306-7310 (2006).
4. K. Terauchi, M. Ohmori, Blue light stimulates cyanobacterial motility via a cAMP signal transduction system. *Molecular Microbiology* **52**, 303-309 (2004).
5. P. Savakis *et al.*, Light-induced alteration of c-di-GMP level controls motility of Synechocystis sp. PCC 6803. *Molecular Microbiology* **85**, 239-251 (2012).
6. D. Dienst *et al.*, The cyanobacterial homologue of the RNA chaperone Hfq is essential for motility of Synechocystis sp PCC 6803. *Microbiology-Sgm* **154**, 3134-3143 (2008).
7. J. Choi *et al.*, Photomovement of the gliding cyanobacterium Synechocystis sp PCC 6803. *Photochemistry and Photobiology* **70**, 95-102 (1999).

8. W. Ng, A. Grossman, D. Bhaya, Multiple light inputs control phototaxis in Synechocystis sp strain PCC6803. *Journal of Bacteriology* **185**, 1599-1607 (2003).

9. D. Trautmann, B. Voß, A. Wilde, S. Al-Babili, W. R. Hess, Microevolution in Cyanobacteria: Re-sequencing a Motile Substrain of Synechocystis sp. PCC 6803. *DNA Research* **19**, 435-448 (2012).

10. D. Bhaya, Light matters: phototaxis and signal transduction in unicellular cyanobacteria. *Molecular Microbiology* **53**, 745-754 (2004).

11. D. Bhaya, A. Takahashi, A. Grossman, Light regulation of type IV pilus-dependent motility by chemosensor-like elements in Synechocystis PCC6803. *Proceedings of the National Academy of Sciences of the United States of America* **98**, 7540-7545 (2001).

12. S. Yoshihara, F. Suzuki, H. Fujita, X. X. Geng, M. Ikeuchi, Novel putative photoreceptor and regulatory genes required for the positive phototactic movement of the unicellular motile cyanobacterium Synechocystis sp PCC 6803. *Plant and Cell Physiology* **41**, 1299-1304 (2000).

13. A. Wilde, B. Fiedler, T. Borner, The cyanobacterial phytochrome Cph2 inhibits phototaxis towards blue light. *Molecular Microbiology* **44**, 981-988 (2002).

14. R. Narikawa *et al.*, Novel Photosensory Two-Component System (PixA-NixB-NixC) Involved in the Regulation of Positive and Negative Phototaxis of Cyanobacterium Synechocystis sp. PCC 6803. *Plant and Cell Physiology*, (2011).

15. J.-Y. Song *et al.*, Near-UV cyanobacteriochrome signaling system elicits negative phototaxis in the cyanobacterium Synechocystis sp PCC 6803. *Proceedings of the National Academy of Sciences* **108**, 10780-10785 (2011).

16. K. Okajima *et al.*, Biochemical and functional characterization of BLUF-type flavin-binding proteins of two species of cyanobacteria. *Journal of Biochemistry* **137**, 741-750 (2005).

17. S. Sato *et al.*, A Large-scale Protein protein Interaction Analysis in Synechocystis sp. PCC6803. *DNA Research* **14**, 207 (2007).

18. S. Masuda, K. Hasegawa, H. Ohta, T. Ono, Crucial Role in Light Signal Transduction for the Conserved Met93 of the BLUF Protein PixD/Slr1694. *Plant and Cell Physiology* **49**, 1600-1606 (2008).

19. S. Yoshihara, X. Geng, M. Ikeuchi, pilG gene cluster and split pilL genes involved in pilus biogenesis, motility and genetic transformation in the cyanobacterium Synechocystis sp PCC 6803. *Plant and Cell Physiology* **43**, 513-521 (2002).

20. S. Yoshihara, M. Ikeuchi, Phototactic motility in the unicellular cyanobacterium Synechocystis sp PCC 6803. *Photochemical & photobiological sciences : Official journal of the European Photochemistry Association and the European Society for Photobiology* **3**, 512-518 (2004).

21. K. S. Makarova, E. V. Koonin, R. Haselkorn, M. Y. Galperin, Cyanobacterial response regulator PatA contains a conserved N-terminal domain (PATAN) with an alpha-helical insertion. *Bioinformatics (Oxford, England)* **22**, 1297-1301 (2006).

22. A. M. Stock, V. L. Robinson, P. N. Goudreau, Two-component signal transduction. *Annual Review Of Biochemistry* **69**, 183-215 (2000).

23. T. R. M. Barends *et al.*, Structure and mechanism of a bacterial light-regulated cyclic nucleotide phosphodiesterase. *Nature* **459**, 1015-1018 (2009).

24. T. Kanazawa *et al.*, Biochemical and Physiological Characterization of a BLUF Protein−EAL Protein Complex Involved in Blue Light-Dependent Degradation of Cyclic Diguanylate in the Purple Bacterium Rhodopseudomonas palustris. *Biochemistry* **49**, 10647-10655 (2010).

25. N. Tschowri, S. Busse, R. Hengge, The BLUF-EAL protein YcgF acts as a direct anti-repressor in a blue-light response of Escherichia coli. *Genes & Development* **23**, 522-534 (2009).

26. U. Jenal, J. Malone, Mechanisms of cyclic-di-GMP signaling in bacteria. *Annual review of genetics* **40**, 385-407 (2006).

27. U. Römling, Cyclic di-GMP, an established secondary messenger still speeding up. *Environmental Microbiology*, no-no (2011).

28. D. Lagarde, L. Beuf, M. Vermaas, Increased production of zeaxanthin and other pigments by application of genetic engineering techniques to Synechocystis sp strain PCC 6803. *Applied and Environmental Microbiology* **66**, 64-72 (2000).

29. G. Tang *et al.*, EMAN2: an extensible image processing suite for electron microscopy. *Journal of Structural Biology* **157**, 38-46 (2007).

30. F. Lopes Pinto, A. Thapper, W. Sontheim, P. Lindblad, Analysis of current and alternative phenol based RNA extraction methodologies for cyanobacteria. *BMC Molecular Biology* **10**, 79 (2009).

31. H. Yuan *et al.*, Crystal structures of the Synechocystis photoreceptor Slr1694 reveal distinct structural states related to signaling. *Biochemistry* **45**, 12687-12694 (2006).

32. H. Yuan, V. Dragnea, Q. Wu, K. H. Gardner, C. E. Bauer, Mutational And Structural Studies Of The PixD BLUF Output Signal That Affects Light-Regulated Interactions With PixE. *Biochemistry*, 110620194047052 (2011).

33. S. Masuda, T. Ono, Biochemical characterization of the major adenylyl cyclase, Cya1, in the cyanobacterium Synechocystis sp PCC 6803. *Febs Letters* **577**, 255-258 (2004).

34. J. Mitschke *et al.*, An experimentally anchored map of transcriptional start sites in the model cyanobacterium Synechocystis sp. PCC6803. *Proceedings of the National Academy of Sciences* **108**, 2124-2129 (2011).

35. V. Jakovljevic, S. Leonardy, M. Hoppert, L. Søgaard-Andersen, PilB and PilT Are ATPases Acting Antagonistically in Type IV Pilus Function in Myxococcus xanthus. *Journal of Bacteriology* **190**, 2411-2421 (2008).

36. J. Mattick, Type IV pili and twitching motility. *Annual Review of Microbiology* **56**, 289-314 (2002).

37. J. J. Bertrand, J. T. West, J. N. Engel, Genetic Analysis of the Regulation of Type IV Pilus Function by the Chp Chemosensory System of Pseudomonas aeruginosa. *Journal of Bacteriology* **192**, 994-1010 (2010).

38. A. Darzins, The *pilG* gene-product, required for *Pseudomonas aeruginosa* pilus production and twitching motility, is homologous to the enteric, single-domain response regulator CheY. *Journal of Bacteriology* **175**, 5934-5944 (1993).

39. A. Darzins, Characterization of a *Pseudomonas aeruginosa* gene-cluster involved in pilus biosynthesis and twitching motility - sequence similarity to the chemotaxis proteins of enterics and the gliding bacterium *Myxococcus xanthus*. *Molecular Microbiology* **11**, 137-153 (1994).

40. Y.-J. Moon *et al.*, The Role of Cyanopterin in UV/Blue Light Signal Transduction of Cyanobacterium Synechocystis sp PCC 6803 Phototaxis. *Plant and Cell Physiology* **51**, 969-980 (2010).

41. Z. Cao, E. Livoti, A. Losi, W. Gärtner, A blue light-inducible phosphodiesterase activity in the cyanobacterium Synechococcus elongatus. *Photochemistry and Photobiology* **86**, 606-611 (2010).

42. M. Tarutina, D. A. Ryjenkov, M. Gomelsky, An Unorthodox Bacteriophytochrome from Rhodobacter sphaeroides Involved in Turnover of the Second Messenger c-di-GMP. *Journal Of Biological Chemistry* **281**, 34751-34758 (2006).

43. S. Leonardy, I. Bulyha, L. Sogaard-Andersen, Reversing cells and oscillating motility proteins. *Molecular Biosystems* **4**, 1009-1014 (2008).

44. Y. Kondou *et al.*, Bipolar localization of putative photoreceptor protein for phototaxis in thermophilic cyanobacterium Synechococcus elongatus. *Plant and Cell Physiology* **43**, 1585-1588 (2002).

45. N. Schuergers *et al.*, Binding of the RNA chaperone Hfq to the type IV pilus base is crucial for its function in Synechocystis sp. PCC 6803. *Molecular Microbiology* **92**, 840-852 (2014).

46. B. D. Blackhart, D. R. Zusman, "Frizzy"; genes of *Myxococcus xanthus* are involved in control of frequency of reversal of gliding motility. *Proceedings of the National Academy of Sciences of the United States of America* **82**, 8767-8770 (1985).

47. M. Burriesci, D. Bhaya, Tracking phototactic responses and modeling motility of Synechocystis sp. strain PCC6803. *Journal of photochemistry and photobiology. B, Biology* **91**, 77-86 (2008).

48. S. Ren, R. Sato, K. Hasegawa, H. Ohta, S. Masuda, A Predicted Structure for the PixD–PixE Complex Determined by Homology Modeling, Docking Simulations, and a Mutagenesis Study. *Biochemistry* **52**, 1272-1279 (2013).

Curriculum vitae

Albertus Jan 'Arjan' Vermeulen

Education

January 2007 – February 2015
Ph.D. Biochemistry – Indiana University
September 1999 – September 2006
M.Sc. Biology – Wageningen University

Research

"Light-sensing in bacteria"
Advisor: Dr. Carl Bauer
(Indiana University)

"Survival of human pathogens in soil"
Advisors: Drs. Ariena van Bruggen and Eelco Franz
(Wageningen University)

"Biochemical properties of chlorite dismutase"
Advisors: Drs. Alfons J. M. Stams and Arthur F. M. Wolterink
(Wageningen University)

Publications

A.J. Vermeulen, and C.E. Bauer. 'Members of the PpaA family bind cobalamin' – in preparation

A.J.Vermeulen, K. He, and C.E. Bauer 'Exploring the role of BLUF, LOV, GAF and PYP-GAF photoreceptors in Rhodospirillum centenum with transcriptomics' – in preparation

Mehboob, F., A. F. M. Wolterink, A.J. Vermeulen, B. Jiang, P.-L. Hagedoorn, A. J. M. Stams, and S. W. M. Kengen. 2009. 'Purification and characterization of a chlorite dismutase from Pseudomonas chloritidismutans.' FEMS Microbiology Letters 293:115-121

Poster presentations

April 6 – 11, 2014
"Exploring the roles of BLUF, LOV, GAF and PYP-GAF photoreceptors in *Rhodospirillum centenum* with transcriptomics."
Gordon Conference – Photosensory Receptors and Signal Transduction (Lucca, Italy)

August, 2012
"Assaying the interactions of the PixD-PixE components of the *Synechocystis* sp. PCC6803 phototaxis signaling pathway with Slr1692"
International Symposium on Phototrophic Prokaryotes (Porto, Portugal)

Awards and Fellowships

May 2013
Outstanding Associate Instructor award
Department of Molecular and Cellular Biochemistry, Indiana University

Summer 2009
Floyd Microbiology Fellowship

Summer 2008
Floyd Microbiology Fellowship